Norwegian University
of Life Sciences

Master's Thesis 2019 30 STP
Faculty of Science and Technology

Monitoring of the Formation of Disinfection By-Products (DBPs) in a Large Drinking Water Distribution System

Kristine Sandaa
Industrial Economics and Technology Management

Master's thesis 2019

Monitoring of the Formation of Disinfection By-Products (DBPs) in a Large Drinking Water Distribution System

KRISTINE SANDAA

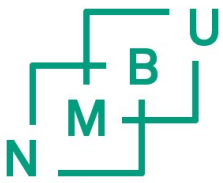

Faculty of Sciences and Technology
Norwegian University of Life Sciences
Ås, Norway 2019

Monitoring of the Formation of Disinfection By-Products (DBPs) in a Large Drinking Water Distribution System

Supervisors: Gregory V. Korshin, Professor in Physical Chemistry at the Department of Civil & Environmental Engineering, University of Washington (UW).
Harsha Ratnaweera, Professor in Civil Engineering at the Faculty of Sciences and Technology, Norwegian University of Life Sciences (NMBU).

Master's Thesis 2019
Faculty of Sciences and Technology
Norwegian University of Life Sciences
Drøbakveien 31, 1433 Ås
Telephone +47 67 23 00 00

Typeset in LaTeX
Ås, Norway 2019

Til min kjære farmor,

takk for at du alltid var der.

Acknowledgements

This thesis concludes a five-year Masters of Science in Industrial Economics and Technology Management at the Norwegian University of Life Sciences (NMBU). The thesis consists of 30 credits and was written the Spring and Summer quarter 2019 at University of Washington (UW), Seattle.

Firstly, I would like to express my sincere gratitude to my supervisors, Professor Gregory Korshin and Professor Harsha Ratnaweera, for their valuable guidance and feedback during this process. A special thanks to the Valle Scholarship and Scandinavian Exchange Program for giving me the opportunity to pursuit graduate research at UW and gain knowledge in my field of interest. Thanks to my beloved peer, Simen Lunderød Øverbø, for always smiling and spreading positive energy at the office.

I thank Lynn Kirby at Seattle Public Utilities (SPU) for good discussions and for always having the answers to my questions. Her knowledge about the Seattle area and drinking water treatment has been of great contribution to this thesis. Thanks to Daniel Acland at UC Berkeley for excessive guidance and inputs on the economic part of the thesis. In addition, I would like to thank Abhilash Muralidharan Nair and Nataly Sivchenko at NMBU for help with the ANN and Unscrambler analysis, and Vasilis Niaouris and Guarav Mahamuni at UW for help with the Python programming codes. Thanks to Surbhi Malik for proofreading.

Further, I would like to extend my thanks to Joel Palage for both great support throughout the process and LaTeXguidance, and for proving that smart Swedes do exist. I am grateful to my parents for being great role models and inspiring me to pursuit higher education. A special thank you to all my fellow Huskies at Allen library for good laughs and encouraging words during ups and downs.

At last, I would like to thank Collegium Alfa and Tekna NMBU for making my years as a student the most special and unforgettable time of my life. I am forever grateful for all the people I've met and the memories made at both NMBU and UW.

.....

Kristine Sandaa
Seattle, August 2019

Abstract

Disinfection By-Products (DBPs) are ubiquitous in chlorinated drinking water. US Environmental Protection Agency (EPA) has stated that DBPs formed in chlorinated drinking water is a potential health risk to the general public. Numerous studies have shown association with long-term DBP exposure and bladder, rectal and colon cancer, as well as reproductive and developmental health effects. This is a major public health issue and a cost to society due to required health treatment, loss of mobility and sickness days.

DBP levels vary as a function of water residence time, temperature, seasonal variations of the concentration and reactivity of Natural Organic Matter (NOM) and treatment methods at the Drinking Water Treatment Plant (DWTP). Due to climate change, more intense precipitation and higher average temperature, the surface waters' NOM content is expected to increase and thus, cause more frequent DBP spikes.

While periodic sampling and analysis of a limited number of drinking water samples are expensive, there is a need to develop online methods and predictive models to quantify DBP concentrations in real time in distribution systems. With a rapid development in the quality of online monitoring sensors, decrease in their costs, expansion of the set of water quality parameters that can be quantified, now it is time to pursue a consistent implementation of proactive monitoring of DBPs in drinking water systems.

This study examined DBP data of discrete sampling and online monitoring that have been generated over 10 years in the Seattle water distribution system. The main objectives with the data processing were to identify potential factors influencing high DBP concentration and map "hot spots" of the DBP formation in the Seattle Water Supply System. The results obtained were used to select optimal locations for implementation of online monitoring sensors in the distribution system. A Cost Benefit Analysis (CBA) was conducted to estimate the net benefits for the Seattle city to deploy a system of online monitoring sensors.

Sammendrag

Desinfeksjonsbiprodukter (DBPs) er en uønsket konsekvens ved desinfesering av drikkevann. US Environmental Protection Agency (EPA) har uttalt at klorert drikkevann er en potensiell helserisiko for allmennheten. Flere studier har påvist en sammenheng mellom langsiktig eksponering av DBP og blære-, tykktarms- og endetarmskreft, så vel som reproduktive og utviklingsmessige helseeffekter. Dette er en trussel for folkehelsen samt en stor samfunnskostnad på grunn av nødvendig helsebehandling, tap av mobilitet og sykefravær.

DBP varierer som en funksjon av oppholdstid, temperatur, behandlingsmetoder ved drikkevannsrenseanlegget og sesongvariasjoner av konsentrasjonen og reaktiviteten til Naturlig Organisk Materiale (NOM). Som en følge av klimaendringer vil det i fremtiden bli mer intens nedbør og høyere gjennomsnittstemperaturer, og overvannkilders NOM innhold forventes øke og dermed føre til hyppigere DBP episoder.

Det er i dag et behov for å utvikle online metoder og prediktive modeller for å kvantifisere DBP-konsentrasjoner i sanntid i distribusjonssystemer, da periodisk prøvetaking og analyse av et begrenset antall drikkevannsprøver er kostbart og ineffektivt. Per dags dato, pågår det en rask utvikling i kvaliteten på online overvåkningssensorer. Samtidig som online overvåkningssensorer blir rimeligere og mer robuste, utvides også av settet med vannkvalitetsparametere som kan kvantifiseres. Det er derfor påtide å implementere en proaktiv overvåking av DBP i drikkevannssystemer.

I denne studien ble DBP-data, som har blitt generert over en tiårsperiode basert på drikkevannsprøver og online overvåking fra Seattles drikkevannssystem, analysert. Hovedmålet med analysen var å identifisere potensielle faktorer som påvirker høy DBP-konsentrasjon og kartlegge "hot spots" av DBP-formasjonen i Seattles drikkevannssystem. Resultatene som ble oppnådd ble brukt til å velge optimale lokasjoner for implementering av online overvåkningssensorer i distribusjonssystemet. En kostnadsnytteanalyse (CBA) ble utført for å estimere nettofordelene for byen Seattle ved å implementere overvåkningssensorene i nettet.

Table of Contents

List of Figures

List of Tables

Acronyms

ANN Artificial Neural Networks. 48, 51, 59, 71, 87, 95

BDCM Bromodichloromethane. 13, 20

CBA Cost Benefit Analysis. 2, 3, 31–33, 35, 51–57, 59, 73, 74, 81, 88–93, 97

CPI Consumer Price Index. 56, 74, 89, 90

Ct Contact Time. 6–8, 10, 22

DAS Differential Absorbance Spectroscopy. 24, 25, 93, 94

DBA Dibromoacetic acid. 12

DBAC Dibromoacetone. 12

DBCM Dibromochloromethane. 13, 20

DBP Disinfection By-Product. 1–3, 5, 8–13, 15–25, 27, 28, 30, 35, 48–52, 54–56, 59–61, 65, 73, 74, 81–89, 92–95, 97, 98, 103

DOC Dissolved Organic Carbon. 22, 26, 29, 30

DWTP Drinking Water Treatment Plant. 1, 2, 6–8, 23, 35, 37, 45, 47, 49–51, 54, 55, 59–64, 67, 71, 73, 81–87, 93–95, 97, 98

ECD Electron Capture Detector. 104

EPA Environmental Protection Agency. 2, 14, 15, 18, 20, 21, 37, 52, 56, 82, 88–90

EU European Union. 20

GS Gas Chromatography. 104

HAA Haloacetic Acids. 1, 11–15, 17, 20–23, 47, 49, 50, 59–61, 63–68, 71, 72, 81–83, 86, 87, 89, 103, 104

HAN Haloacetonitriles. 15, 17

IAA Iodoacetic acid. 12, 13

LAE Life Average Exposure. 18

LECR Life Excess Cancer Risk. 18

MBA Mucobromic acid. 12

MCL Maximum Contaminant Levels. 20, 21, 54, 82

METB Marginal Excess Tax Burden. 57, 75, 77, 89

MLR Multiple Linear Regression. 50, 63, 85

MS Mass Spectrometer. 104

MVA Multivariate Analysis. 50, 86

NDMA N-nitrosodimethylamine. 10, 12

NOM Natural Organic Matter. 8, 10, 11, 13, 15, 21–24, 27, 54, 82–84, 86, 94, 97

NPDWR The National Primary Drinking Water Regulations. 20, 54

NPV Net Present Value. 31–33, 51, 53, 54, 57, 75–77, 79, 88, 90–92, 97

PAR Population Attributable Risk. 52, 89

PC Principal Component. 67, 68, 86

PCA Principal Component Analysis. 50, 66, 67, 86

PF Potency Factor. 18

PLS Partial Least Squares. 30

PLSR Partial Least Square Regression. 50, 66, 69

PV Present Value. 75, 76, 90

SDR Social Discount Rate. 31, 53, 57, 76, 77, 79, 89–92, 97

SOP Standard Operating Procedure. 104

SPU Seattle Public Utilities. 2, 3, 45–51, 54–56, 82–84, 92, 93

SUVA Specific Ultraviolet Absorbance. 24

THM Trihalomethanes. 1, 10–13, 15–17, 20–24, 30, 47, 49, 50, 59–61, 63, 65, 67–72, 81–83, 86, 87, 103

THMFP Trihalomethanes Formation Potential. 30

TIAA Triiodoacedic acid. 12, 13

TOC Total Organic Carbon. 21, 22, 26, 29, 30, 42, 43, 49, 64, 65, 68, 71, 82, 83, 85, 86

TOX Total Organic Halogen. 13, 24

TTHM Total Trihalomethanes. 13, 20, 23, 52, 89

UV Ultraviolet Light. 5, 8, 10, 12, 13, 22, 24–28, 39–41, 73, 93, 94

UV-Vis Ultraviolet-visible spectrophotometry. 27, 28

UVA Ultraviolet Light Absorbance. 3, 49, 50, 59, 62, 63, 65–68, 71, 85, 86

UVT Ultraviolet Light Transmittance. 8, 39, 41, 49, 62

WAC Washington Administration Code. 37

WHO World Health Organization. 5, 18–20, 95

WTP Willingness to Pay. 31, 56

1

Introduction

1.1 Background

Disinfection of drinking water causes ubiquitous organic compounds known as Disinfection By-Product (DBP) to be formed. DBPs are extremely hard to remove from drinking water once they have been formed. The most efficient way to reduce DBP formation, is to remove the DBP precursors and regulate the operational parameters at the Drinking Water Treatment Plant (DWTP).

Chlorine is the most commonly used disinfection method worldwide and is a cost-effective technique that efficiently inactivates most microorganisms. It is the only disinfectant, in addition to chloramine, that provides residual disinfection to drinking water in the distribution system, which is crucial to prevent waterborne diseases. However, chlorine also results in the highest formation of halogenated DBPs.

Previous research has demonstrated clear linkages between the consumption of DBPs present in drinking water and increased risks of cancer and chronic illness (Richardson et al., 2007). Increased levels of DBP groups such as Trihalomethanes (THM) and Haloacetic acids (HAA) have been specifically shown to be associated with higher cancer risks. This is a major, global public health issue and a financial burden on society due to required health treatment, loss of mobility and sickness days.

Spectroscopic online monitoring sensors and DBP predicting models can in principle be efficient tools to monitor and eventually decrease DBP formation. For the last few decades, there has been a rapid development in the quality of sensors that can be deployed for online monitoring of water quality. Technological development has decreased sensor costs and the quantification of related parameters has expanded with the help of online monitoring sensors. The development of new models relate these sensors' outputs with the formation and degradation of DBPs and other micro-pollutants.

1.2 Problem Statement

The City of Seattle, which uses chlorination in the water supply, has been mandated to monitor DBP concentrations four times a year at selected locations. There are two large watersheds in the Seattle area, Cedar and Tolt, supplying drinking water to 1.4 million people. For this thesis, DBP and water quality data from both Cedar and Tolt DWTP have been provided by the Seattle Public Utilities (SPU).

As several chlorinated DBPs have been linked to cancer and chronic illness, US Environmental Protection Agency (EPA) has stated that DBPs are a potential health risk to the general public (US EPA, 2005b). This problem is not only valid for Seattle, but is also a global issue that needs to be addressed. Worldwide, most countries use chlorination as a primary disinfectant, and incautious use of chlorination will lead to higher DBP concentrations.

It is therefore of utmost importance for water utilities to gain a complete and real-time picture of the DBP concentration in the drinking water. The goal is to reduce the overall DBP concentration and thus, decrease the number of cancer and chronic illness cases attributed to DBP exposure.

1.3 Objectives of Study

The ambition of the thesis research is to evaluate the potential for adequately time-resolved water quality monitoring. The monitoring takes advantage of online measured parameters that act as virtual sensors to predict DBP concentrations in a drinking water distribution system without taking actual samples therein. The first part of the research is to process the data and identify potential factors influencing DBP formation. The results from this will be used to select optimal locations for the online monitoring sensors in the distribution system.

The second part of the thesis is to investigate the City of Seattle's benefits and cost associated with the deployment of online monitoring sensors in the distribution system through a Cost Benefit Analysis (CBA). The main assumption in the CBA is that by decreasing the DBP concentration in the distribution system through implemention online monitoring sensors, the annual number of new bladder cancer cases in the city would decrease. The results for the analysis will be used to recommend the city's priority on the issue.

Based on the background and problem statement, the main objectives of the thesis study are:

1. Process multi-year DBP data available from SPU and identify potential "hot spots" of DBP formation.

2. Evaluate available DBP and water quality data and other operational conditions (e.g. pipe condition, re-chlorination) to identity potential factors influencing the occurrence of high DBP values.

3. Use the interpretation of the DBP and water quality data to select optimal locations for online monitoring sensors in the distribution system.

4. Estimate savings associated with the deployment of online monitoring versus society cost caused by the development of DBP-associated health problems.

5. Ascertain practical efforts needed to shift from the current paradigm of a post-factum reactive DBP monitoring to the new paradigm of proactive DBP monitoring.

1.4 Limitations

The thesis has the following limitations:

- Lack of water quality data from the samplings sites in the Seattle drinking water distribution system (pH, UV Absorbance (UVA), turbidity, chlorine concentration).

- Narrow DBP data at certain sampling sites and their locations mostly in the extremities of the Seattle drinking water distribution system.

- Limited epidemiological data to make assumptions for DBP exposure and risk of bladder cancer used in the CBA.

- Complex effects in a large distribution system having multiple factors influencing DBP formation.

2

Literature Review

The World Health Organization (WHO) states in its guidelines for drinking-water quality that the most common health risk associated with drinking water are infectious diseases caused by pathogenic bacteria, viruses and parasites (World Health Organization, 2011). To minimize the risk of these infectious diseases, it is essential to disinfect drinking water using one or more disinfection methods. The most common methods for drinking water disinfection are chlorination, while occasionally also ozonation and Ultraviolet Light (UV) radiation. When these methods are applied to drinking water, various chemical compounds known as DBPs are formed.

This Chapter contains discussion of DBPs and their health effects, DBP regulations, different disinfection methods, factors influencing DBP formation and the use of online monitoring sensors to predict DBP concentration in drinking water.

2.1 Disinfection Methods

More than one disinfection method is commonly used in drinking water treatment. The primary disinfectant inactivates the pathogens while the secondary disinfectant provides longer lasting disinfection as water flows through the pipes. All the disinfection methods have advantages and disadvantages, and they all produce some kind of DBPs. In the next subsections, the different disinfection methods and their respective advantages and disadvantages, are described and summarized in Table 2.1.

2.1.1 Chlorination

For more than a century, the use of chlorine in drinking water has been a practice and has eliminated a majority of waterborne diseases. Chlorination is effective for

inactivation of most microorganisms and is a highly cost-effective technique for drinking water disinfection. Chlorine is the most common primary disinfectant in the US.

In addition to its disinfectant characteristics, chlorine is useful for algal, bacterial and slime growth prevention both in drinking water treatment plans and pipeworks in the distribution system. Chlorine can also be used to control odour and taste in addition to provide iron, manganese and colour removal (White, 1986).

When free chlorine (Cl_2) is added to water, the following reaction occurs:

$$Cl_2 + H_2O \leftrightarrow HOCl + H^+ + Cl^- \tag{2.1}$$

As shown in Equation (2.1), chlorine added to water forms hypochlorous acid (HOCl), hydrogen ion and chlorine ion. HOCl is a weak acid and partially dissociates in water, forming hypochlorite ion (OCl^-). The pH determines which species dominates and thus, the efficiency of the chlorine disinfection. At a pH less than 7.5, HOCl dominates while at a higher pH OCl^- dominates. HOCl is a stronger oxidant than OCl^- and therefore disinfection using chlorine is more effective at a neutral to acidic pH (EPA, 2013).

The effect of chlorine depends in the on the Contact Time (Ct) shown in Equation (2.2):

$$Ct = \int_0^t C(t)dt \tag{2.2}$$

where Ct is contact time, C is concentration and dt is time.

The required chlorine contact time (Ct_{req}) for an efficient disinfection of bacteria and viruses, depends on the water source (surface water, groundwater etc.) and the inactivation requirements for the individual DWTP. The inactivation requirements are described as log reduction where 1 log = 90% removal, 2 log = 99% removal, 3 log = 99.9% removal etc. Other factors needed to determine Ct_{req} are minimum temperature, maximum pH and minimum chlorine residual.

Chloramine

Chloramine (NH_2Cl) is a weaker disinfectant than chlorine, requiring a greater contact time for disinfection at the DWTP. Because of its high Ct values, chloramine is a poor primary disinfectant. Chloramine is formed when ammonia (NH_3) is added to chlorine. Chloramine is used as a secondary disinfectant and provides a longer-lasting disinfection

to the drinking water.

Chlorine dioxide

Chlorine dioxide (ClO_2) is an explosive hazard and therefore it is synthesized at the point of use in a DWTP. It is a powerful oxidizing agent that can decompose into chlorite and chlorate. Chlorine dioxide is proven to be more effective in inactivation of *Giardia* than free chlorine, but less effective against *E. coli* and rotaviruses.

2.1.2 Ozone

Ozone (O_3) is one of the strongest oxidizing agents in water treatment and the most efficient disinfectant for all types of microorganisms. The main objective to use ozone as the first treatment step is the removal of taste and odor, colour and micropollutants from the water. Ozone is more effective than chlorine in inactivating all kinds of bacteria, viruses and the parasites *Giardia* and *Cryptosoridium* (WHO, 2004).

Ozonation has a higher cost than chlorination and does not provide residual disinfection as ozone rapidly decomposes in water. Ozone is generated on site, converted from liquid oxygen (O_2) to ozone gas (O_3) by using electrical plasma discharge. For disinfection requirements, Equation (2.2) is used for ozonation as well for chlorination. The Ct product for ozone is shorter than for chlorine, as ozone is more reactive than chlorine.

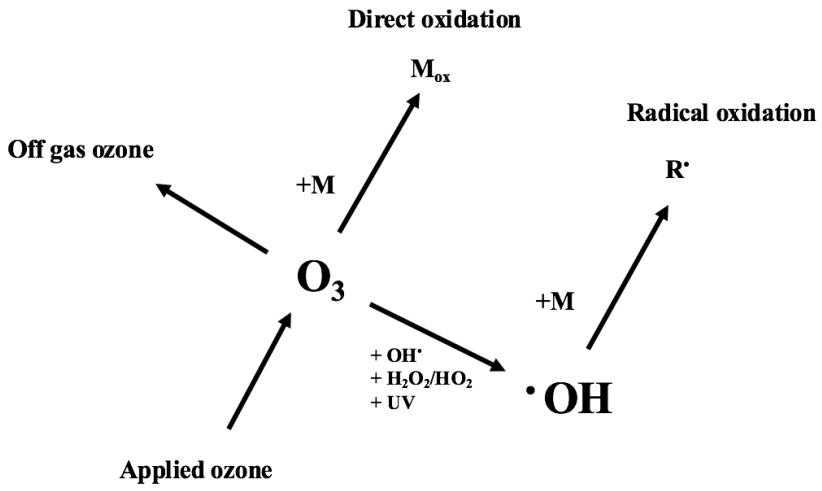

Figure 2.1: Ozone reaction mechanism as O_3 and °OH (Lenntech, 2019).

As shown in Figure 2.1, the oxidation of organic/inorganic compounds occur via O_3 or OH radicals, or a combination of both. When added to water, ozone can decompose into OH radicals (°OH) which are the strongest oxidants (Minakata et al., 2012). The OH radicals react fast with dissolved compounds. Due to its strong oxidizing characteristics, ozone reacts with Natural Organic Matter (NOM) splitting it into smaller molecules and also removing color from water.

2.1.3 UV radiation

UV radiation inactivates pathogenic microorganisms by denaturation of DNA, thus making the organism unable to replicate. UV is the primary disinfectant for *Cryptosoridium* and *Giardia* (Norsk Vann, 2009). Factors that effect the UV efficiency are turbidity, iron concentration and magnesium concentration. UV only disinfects water at the point of contact and it does not provide any residual disinfection to the water in the distribution system. For UV radiation, the Ct term is also used, but is expressed slightly differently as shown in Equation (2.3):

$$D = I \times t \tag{2.3}$$

where D is dosage (mJ/cm^2), I is the radiation intensity (mW/cm^2) and t is time (s).

It is the water's UV Transmittance (UVT) which determines the UV-plant disinfection efficiency. The required UVT efficiency for approved UV disinfection is individual for every DWTP. Using UV as a disinfectant requires continuous power supply. If the power at a DWTP fails, the UV light intensity fails and the system loses its efficiency to safely disinfect the water.

2.1.4 Coagulation and filtration

Coagulation and filtration are not disinfection methods per se, but they are very common water treatment techniques to remove particulates and turbidity from surface waters. Coagulation has been reported to remove substantial amounts of NOM from surface waters, which is the number one precursor for DBPs (Liang and Singer, 2003). Thus, using coagulation and filtration as a pre-treatment step to disinfection in drinking water can have a big impact on the DBP formation.

2.1.5 Comparing the disinfection methods

The disinfection methods have individual strengths and weaknesses which are described in this subsection. To provide an organized overview of the different disinfection methods, they are presented in Table 2.1.

To sum up the information presented in Table 2.1, chlorine is a cheap and effective disinfectant. Using chloramine, chlorine dioxide or ozone is generally more expensive than chlorine. In addition, ozone and chlorine dioxide do not provide adequate protection in the water distribution system due to their instability (Chowdhury et al., 2011). Alternate disinfection methods may lower the chlorinated DBP concentration, but can form other toxic byproducts, increase disinfection cost and lead to microbiological recontamination in the water distribution system (Sadiq and Rodriguez, 2004).

Table 2.1: Advantages and disadvantages for the disinfection methods.

Disinfection method	Advantages	Disadvantages
Chlorination	- Highly cost-effective disinfectant, by far the cheapest. - Effective against most viruses/bacteria. - Well known and developed disinfection method. - Provides residual disinfection in distribution system. - Prevents bacterial and algal growth on pipes.	- Forms the greatest amount of halogenated DBPs. - Does not inactivate protoza like *Giardia* and *Cryptosoridium*. - Gaseous form dangerous. - Poor biofilm penetration. - Can cause pipe corrosion. - Effectiveness reduced at higher temperatures; increasing pH decreases effectiveness. - Taste and odor.
Chloramine	- Forms lower DBPs concentrations than chlorine. - Longer residual disinfection in the distribution system. - Relatively inexpensive. - Effective against most viruses/bacteria. - Penetrates biofilm better than chlorine.	- Generated on site, might lead to complications. - Higher cost treatment than chlorination. - Weaker disinfectant than chlorine, require longer Ct. - Forms N-nitrosodimethylamine (NDMA) (more toxic than halogenated DBPs). - Relatively less effective than chlorine against protoza. - Nitrification potential. - Taste and odor. - Can cause pipe corrosion.
Chlorine dioxide	- Does not form any halogenated DBPs. - Longer residual disinfection in the distribution system. - Relatively unaffected by pH. - More effective against a broader range of microbes than chlorine. - Taste and odor control.	- Relatively expensive. - Greater skill level required to operate. - May be a challenge to maintain desired residuals.
Ozonation	- Most efficient disinfectant with regards to microorganisms. - Reacts with NOM which reduces the DBP formation potential by removing the precursors. - Minimal influence of pH. - Eliminates taste and odor.	- Lack of disinfection residual. - Biological regrowth in distribution system. - High cost treatment. - Limited information about its DBPs. - When ozonation is followed by chlorination, concentration of brominated THMs may increase.
UV	- No chemicals are required. - No DBPs are formed from UV radiation. - Normally effective against all viruses, bacteria and parasites. - Requires short contact time.	- Lower dosages may not be effective for some viruses and pathogens. - Dependent on access to stable power supply. - Lack of disinfection residual. - High turbidity and organic matter in water reduces the UV efficiency. - Requires frequent maintenance.

2.2 DBP Occurrence in Drinking Water

Historically, chlorination revolutionized drinking water treatment, reducing the incidence of waterborne diseases globally. Chlorination and filtration have been haled as a major public health achievement of the 20th century (Calderon, 2000). DBPs were initially discovered in 1974 by Rook who identified chloroform and other THMs in chlorinated water (Rook, 1974). Since then, over 600 individual DBPs have been found through laboratory research. Thus, the main focus in the drinking water research field is to document and understand the occurrence of DBPs and their effect on human health.

DBPs are an unintended consequence of disinfecting drinking water and are formed when disinfectant reacts with NOM and/or inorganic substances. The main factors affecting the amount of DBPs formed are pH, temperature, reaction time and chlorine dose. These parameters are further discussed in subsection 2.5.

Figure 2.2 illustrates the main groups of DBPs and their occurrence. The two main DBP groups are THM and HAA, when combined constitute about 40 percent of the mass of all DBPs. As shown in Figure 2.2, half of the existing DBP are unidentified and so are the toxicological health risks they pose to humans.

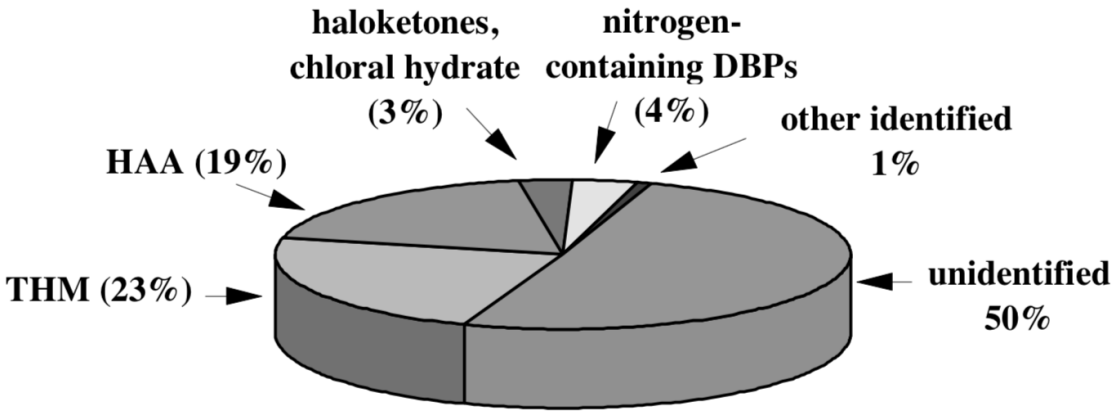

Figure 2.2: Representation of a typical DBP distribution. Figure adopted from Krasner et al., 1989.

The speciation of DBP depends on the type of disinfectant, dose, type of organic/inorganic matter and other precursors present in the drinking water. Table 2.2 shows the significant DBP species formed when using the different disinfection methods in drinking water treatment.

From Table 2.2, it is clear that chlorine is the disinfectant that is the source of highly significant halogenated organic products. The two main DBP groups, THMs and HAAs,

are both products of chlorine disinfection. Chlorine dioxide produces less halogened DBP products, and forms chlorite and chlorate which are inorganic DBP products. Chloramine causes both halogenated and inorganic DBPs to form. Ozone as a disinfectant forms brominated DBPs and bromate which are highly genotoxic and carcinogenic (Richardson et al., 2007). UV is the only disinfectant that does not produce any kind of DBPs.

Table 2.2: DBPs species present in disinfected waters (WHO, 2004).

Disinfectant	**Significant halogen products**	**Significant inorganic products**	**Significant non-halogen products**
Chlorine /Hypochlorous acid	- THMs - HAAs - Haloacetonitriles (HANs) - Chloral hydrate - Chloropicrin - Chlorophenols - N-chloramines - Halofuranones - Bromohydrins	- Chlorate (mostly from hypochlorite)	- Aldehydes - Cyanoalkanoic acids - Alkanoic acids - Benzene - Carboxylic acids
Chlorine dioxide	- Iodinated THMs, especially iodoform - Iodoacetic acid (IAA) - Triiodoacedic acid (TIAA)	- Chlorite - Chlorate	Unknown
Chloramine	- HANs - Cyanogen chloride - Organic chloramines - Chloramino acids - Chloral hydrate - Halokentones	- Nitrate - Chlorate - Hydrazine	- Aldehydes - Ketones
Ozone	- Bromoform - Mucobromic acid (MBA) - Dibromoacetic acid (DBA) - Dibromoacetone (DBAC) - Cyanogen bromide	- Chlorate - Iodate - Bromate - Hydrogen peroxide - Hypobromous acid - Epoxides - Ozonates	- Aldehydes - Ketoacids - Ketones - Carboxylic acids
UV	None	None	None

As shown in Table 2.2, chloramine produces similar DBPs as chlorine, but with lower concentrations. The use of chloramine can result in up to 90 percent reduction in the THM and HAA levels compared to chlorination (Thompson et al., 2016). One toxic DBP specifically associated with chloramine is NDMA which is more toxic than THM and HAA (Richardson, 2005, Ellington et al., 2008). NDMA is found to be a highly genotoxic

compound and a possible human carcinogen. Studies indicated that the formation of iodinated DBPs may be higher with chloramination than with chlorination (Ellington et al., 2008).

The halogen products formed by chlorine dioxide are iodinated THMs, IAA and TIAA (Ye et al., 2013, Zhang et al., 2015). For the iodinated THMs, iodoform is the major species formed when chlorine dioxide is used. As shown in Table 2.2, chlorine dioxide forms the inorganic DBPs chlorite and chlorate. Chlorine dioxide produces limited DBPs because it neither reacts with NOM to form THMs nor with ammonia to form levels of chloramines (WHO, 2004). However, traces of HClO can form upon the decay of Cl_2 in water.

In drinking water treatment, the use of ozone as a treatment step before chlorine creates a significantly smaller amount of chlorinated DBPs as ozonation decreases the ability of NOM to react with the chlorine (Norsk Vann, 2009). However, when using ozone as a disinfectant, bromated DBPs can form which are more genotoxic and carcinogenic than halogenated DBPs. The only DBP created by ozonation regulated in the US is bromate.

As presented in Table 2.2, UV radiation does not produce any known DBPs. Even though UV radiation as a disinfection method does not form DBPs, there have been studies conducted to investigate how UV influences DBP formation when combined with other disinfection methods. A study by Reckhow et al., 2010 revealed that UV treatment on two separate water sources did not substantially change the THM, HAA or Total Organic Halogen (TOX) concentrations of the two water sources. There was a small reduction in the formation of the DBP groups, but it did not exceed 10 percent.

2.2.1 Halogenated DBPs

Halogenated DBPs are formed when chlorine, chloramines or ozone react with NOM in the water. TOX is a collective parameter for all halogenated DBPs. In Table 2.3, the main halogenated DBPs classes and their chemical formulas are presented.

THM and HAA are regulated in two groups: Total Trihalomethanes (TTHM) and HAA5. TTHM comprise of four compounds: *chloroform*, *Bromodichloromethane (BDCM)*, *Dibromochloromethane (DBCM)* and *bromoform*. HAA5 comprise of five compunds: *monochloroacetic acid*, *dichloroacetic acid*, *trichloroacetic acid*, *bromoacetic acid* and *dribromoacetic acid*. Figure 2.3 and 2.4 show the chemical structure of the compounds.

HAA9 consists of the same compounds as HAA5 and also includes *bromochloroacetic*

acid, *bromodichloroacetic acid*, *bromodichloroacetic acid* and *tribromoacetic acid*. The HAA9 group is not regulated, but is on the US EPA's list of unregulated contaminants to be publicly monitored by water systems (US EPA, 2019).

Table 2.3: Main halogenated DBP classes (Korshin et al., 2002).

Chemical name	**Abbreviation**	**Chemical formula**
Trihalomethanes	THM	CCl_xBr_y, $x + y = 3$
Haloacetic acids	HAA	$CH_xCl_yBr_z$, $x + y + z = 3$
Haloacetonitriles	HAN	$CH_xCl_yBr_zCN$, $x + y + z = 3$
Haloketones	HK	$CH_xCl_yBr_zCOCH_3$,$x + y + z = 3$
Trihalonitromethane	THNM	$CCl_xBr_yNO_2$, $x + y = 3$
Cyanogen halide	CNH	Cl-CN, Br-CN
Chloral hydrate	CH	CCl_3-CHO

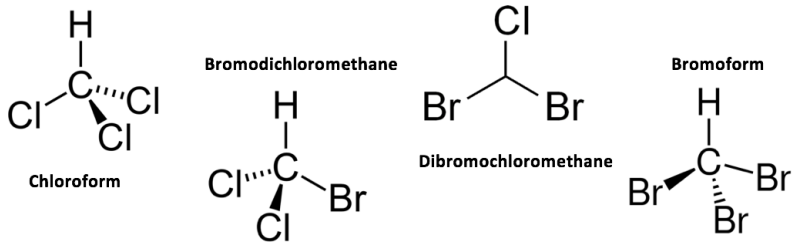

Figure 2.3: Chemical structure for TTHMs.

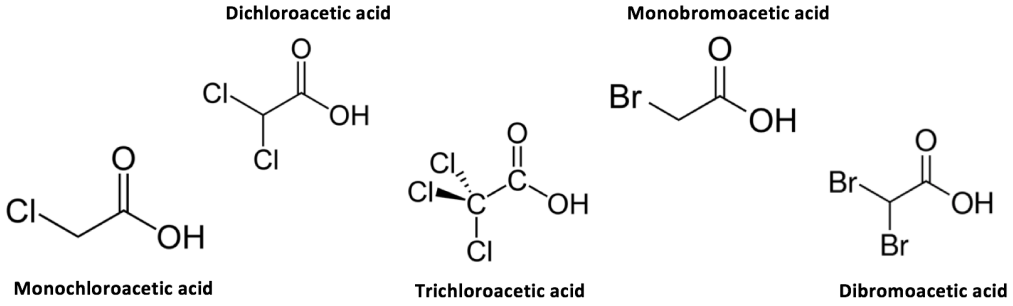

Figure 2.4: Chemical structure for HAA5.

2.2.2 Brominated and inorganic DBPs

In most water sources, bromide and iodide ions are naturally present. The bromide ions can react with either disinfectants - hypochlorite (HClO) or ozone. If bromide reacts with hypochlorite, it is oxidized to HBrO which then reacts with NOM to incorporate bromine into DBPs. Brominated DBPs are of greater health significance than chlorinated DBPs as they are found to be more genotoxic and carcinogenic (Richardson et al., 2007).

If the bromide reacts with ozone, then the inorganic compound bromate is formed. The formation of bromate is dependent on the presence of bromide and the ammonia concentration in the water (Sadiq and Rodriguez, 2004). Bromate is one of the eleven DBPs regulated in the US and is also a known carcinogen.

2.2.3 "New" and emerging DBPs

Today, there is an intensive, ongoing research to identify and understand emerging, unregulated DBPs. These DBPs include iodo-THMs, iodo-acids, haloamides, halonitromethanes, halofuranones, haloacetonitriles (HAN)s, haloacetaldehydes, nitrosamines and halobenzoquinones (Thompson et al., 2016).

Studies show that iodo-THMs tend to be more toxic than chlorinated and brominated THMs (Ellington et al., 2008). Iodo-acid is the most toxic DBP identified to this date and is estimated to be two times more genotoxic than bromoacetic acid. Recent research recognizes the DBPs not monitored regularly (in particular, iodinated, nitrogenous DBPs) have higher genotoxicities and cytotoxicities than commonly monitored DBPs, like THM and HAA (Richardson et al., 2007).

2.3 Health Effects of DBPs

As mentioned above, chlorinated drinking water is linked to over 600 individual DBPs and adverse health effects associated with them. However, the behavioral characteristics of only about 20 DBPs are known (Sadiq and Rodriguez, 2004). A research study by Lee et al., 2013 concluded that the cancer risk by overall exposure of THM in tap water was higher than 10^{-6}, which is a negligible risk level, as defined by the US EPA.

Humans are exposed to DBPs through ingestion, inhalation and dermal contact. The ingestion exposure is through drinking water and dermal contact through showering, bathing, swimming etc. It is of utmost importance to understand the linkage between long-term DBP exposure and possible risk to human health.

2.3.1 DBPs, cancer risk and chronic illness

Several studies have linked exposure to DBPs and increased risk of bladder cancer and colorectal cancer. A study conducted by Villanueva et al., 2004 concluded the risk of bladder cancer increases with long-term exposure to DBPs at levels observed in industrialized countries. The study used THM as a marker for DBPs and the primary data analyzed were from US, Canada, France, Italy and Finland. The DBP exposure associated with an increased risk of bladder cancer was found to be valid only for men. For women, no association was found between THM exposure and risk of bladder cancer in the study. Research shows that the risk of bladder cancer increases with both increase in concentration and duration of exposure to chlorinated DBPs (King and Marrett, 1996,Villanueva et al., 2007).

A study by King et al., 2000 in southern Ontario, Canada from 1992-94, investigated possible relations between rectal and colon cancer, and exposure to DBPs. They studied cases with a 40-year period exposure to THM, representing DBPs, estimating individual exposure to water source, chlorination status and DBP concentration. The study included more than 1,500 cases. The study showed that there is an increased risk of colon cancer among males with long-term exposure to chlorinated DBPs. However, there was no association with exposure to DBP and colon cancer for females, nor of rectal cancer for male or females. King et al., 2000 and his research group emphasize on the limited amount of literature addressing this issue and that the result are only partially fitting due to this reason. Research by Rahman et al., 2010 found a positive association between colorectal cancer and exposure to DBPs in drinking water.

In addition to cancer risks, DBPs have been associated with chronic and sub-chronic illness such as cardiac anomalies, stillbirth, miscarriage, low birth weight and preterm delivery (Chowdhury et al., 2011, Werler, 2011). Dodds et al., 2004 found evidence for an increased risk of stillbirth associated with exposure to chlorinated DBPs. The results from the study shows women with residual total THM level of 80 μg/L had twice the risk of a stillbirth compared to women with no exposure to THMs. Waller et al., 1998 and her research team examined the association between spontaneous abortion and exposure to THM in a study with over 5,000 pregnant women. The women their in

first trimester drinking more whan five glasses of tapwater containing an average THM concentration of 75 μg/L or more had an increased risk of spontenous abortion.

2.3.2 Toxicological table and life excess cancer risk

Table 2.4 presents the ratings of toxicological groups for the DBP classes.

Table 2.4: Summary of toxicological DBPs. Table adopted from Sadiq and Rodriguez, 2004.

Class DBP	Compound	Rating	Detrimental effects
THM	Chloroform	B2	Cancer, liver, kidney and reproductive effects.
	Dibromochloromethane	C	Nervous system, liver, kidney and reproductive effects.
	Bromodichloromethane	B2	Cancer, liver, kidney and reproductive effects
	Bromoform	C	Cancer, nervous system, liver and kidney effects.
HAA	Dichloroacetic acid	B2	Cancer, reproductive and developmental effects.
	Trichloroacetic acid	C	Liver, kidney, spleen, reproductive and developmental effects.
HAN	Trichloroacetonitrile	C	Cancer, mutagenic and clastogenic effects.
Halogenated aldehydes and ketones.	Formaldehyde	B1	Mutagenic (inhalation exposure).
Halophenol	2-Chlorophenol	D	Cancer, tumour promoter.
Inorganic compounds	Bromate	B2	Cancer.
	Chlorite	D	Developmental and reproductive effects.

The rating groups in Table 2.4 are from US EPA's Disinfection Profile and Benchmarking Guidance Manual and is defined as following: B1: Probable human carcinogen (with some epidemiological evidence), B2: Probable human carcinogen (sufficient laboratory evidence), C: Possible human carcinogen, D: Non classifiable.

Scientists and epidemiologists assess the threat the individual DBPs impose on public health by calculating applicable Potency Factors (PF) and categorizing the DBPs in rating groups. Equation (2.4) describes the Life Excess Cancer Risk (LECR) which is the lifetime probability of a typical individual developing a cancer. The LECR is calculated by summing up the products of exposure by each route by its potency factor using Life Average Exposure (LAE) and PF (Grellier et al., 2015):

$$LECR = \sum LAE_i \times PF_i \tag{2.4}$$

where LAE is in mg, PF is in $(\text{mg/kg-day})^{-1}$ and i is the exposure route (ingestion, inhalation or adsorption). The LECR is an upper bound estimate and considered a conservative overestimate that is protective of public health.

2.3.3 The effect of waterborne diseases

Chlorine, chlorine dioxide and chloramine are the only disinfectants that provide an acceptably stable residual disinfection in a water distribution system, preventing growth of bacteria and viruses in pipes. Even though chlorinated drinking water contains DBPs, the consequences of not disinfecting the drinking water adequately are dramatic and severe. In January 1991, a cholera epidemic broke out in Peru killing 3,100 inhabitants and sickening more than 400,000 people. The cause of the epidemic was the absence of safe drinking water and sanitation (Rice and Johnson, 1991).

Lack of proper disinfection of drinking water can also occur in countries with highly developed infrastructure. In May 2010, a large *E.coli* disease outbreak in Walkerton, Canada caused the death of seven people and 2,300 sickened. The reason was contamination of municipal drinking water sources by bacterial pathogens. The amount of chlorine in the system was lower than required by the utility protocol. Due to the low chlorine residual, the *E.coli* overwhelmed the system causing a break out (Salvadori et al., 2009). WHO states the following in the Guidelines for Drinking-water Quality: "in all circumstances, disinfection efficiency should not be compromised trying to meet the guidelines for DBPs, including chlorination by-products, or trying to reduce

concentrations of these substances" (World Health Organization, 2011). In other words, waterborne pathogens pose a real and immediate threat to human health and thus DBPs are the lesser of two evils.

2.4 DBP Monitoring and Regulations

Drinking water regulations worldwide are based on known DBPs, their toxicological information and analytics. This information is not available for most DBPs, due to incomplete data and research. This might result in possible severe health impacts due to unregulated DBPs. The WHO international guidelines are described as a minimum requirement for practice of safe drinking water.

2.4.1 WHO Guidelines

Table 2.5 presents the WHO Guidelines for DBPs in addition to those discussed in this subsection.

Table 2.5: WHO guidelines for DBPs (World Health Organization, 2011).

DBP	Guideline values (mg/L)
Dichloroacetic acid	0.05[a]
Trichloroacetic acid	0.2
Bromate	0.01[a]
Chlorite	0.7[a]
Chloral hydrate	0.01[a]
Dichloroacetonitrile	0.02[a]
Dibromoacetonitrile	0.07
Cyanogen chloride	0.07
2,4,6-Trichlorophenol	0.2
Formaldehyde	0.9

a: Provisional guideline value

The WHO Guidelines for TTHM is represented by Equation (2.5): the sum of the ratio of the concentration of each THM to its respected guideline value should not exceed 1.

$$\frac{C_{bromoform}}{GV_{bromoform}} + \frac{C_{BDCM}}{GV_{BDCM}} + \frac{C_{DBCM}}{GV_{DBCM}} + \frac{C_{chloroform}}{GV_{chloroform}} \leq 1 \tag{2.5}$$

In Equation (2.5), GV is guideline value and C is concentration. The WHO guideline values are 0.3 mg/L for chloroform, 0.06 mg/L for BDCM, 0.1 mg/L for DBCM and 0.1 mg/L for bromoform (World Health Organization, 2011). The WHO's remaining guideline values for DBPs are found in Table 2.5.

The European Union (EU) have standard values for TTHM and bromate where the regulated standards are 0.1 mg/L and 0.01 mg/L, respectively (ECHA, 2017). The EU standard values are implemented in the Norwegian drinking water regulation, *Drikkevannsforskriften*.

2.4.2 EPA Drinking Water Regulations

The US EPA sets the The National Primary Drinking Water Regulations (NPDWR). The NPDWR are the standards for the legally Maximum Contaminant Level (MCL) and treatments techniques that apply to public water systems. The objective of the standards is to protect the public health by limiting the level of contaminants in the drinking water. In the NPDWR, there are MCLs for microorganisms, disinfectants, DBPs, radionuclides and inorganic and organic chemicals.

The eleven DBPs currently regulated in the US are: TTHM, HAA5, bromate and chlorite. Table 2.6 shows the EPA regulations for the MCL for DBPs from the NPDWR.

Table 2.6: EPA regulations for MCLs for DBPs (USEPA, 2009).

DBP	MCL (mg/L)
Total trihalomethanes (TTHM)	0.080
Halo aceticacids (HAA5)	0.060
Bromate	0.010
Chlorite	1.0

The EPA has developed the regulations which each state has adopted and is responsible

to enforce. The state can choose to use the same regulations as the EPA, or set a more stringent standard if desired. The state utilities are required to examine a number of water quality samples at the treatment plants and in the distribution systems. The number of samples required are based on source water type, population and number of treatment plants. If a utility exceeds the MCL on a running annual average, the utility is required to give a public notification.

2.5 Factors Influencing DBP Formation

The formation of DBPs depend on source water quality characteristics, disinfection methods used and the location in the treatment process where the disinfection is added. The most important water quality factors are organic precursors materials, known as NOM, inorganic species (e.g. bromide ion), water temperature and pH. For the disinfectant, dose, contact time and residual disinfectant concentration are the most important factors. These factors are discussed in the following subsections.

2.5.1 NOM

NOM is one of the most important influence factor parameter in drinking water treatment and it is measured in Total Organic Carbon (TOC). NOM is the major precursor for DBPs, in particular of THM and HAA. NOM consists of both hydrophobic and hydrophilic organic material. Site-specific characteristics of NOM like molecule weight, structure and functionality affects the DBP formation. NOMs are a highly complex entity and researchers are still working on finding correlations between NOM fractions properties and DBP formation.

Both the hydrophobic and hydrophilic fractions of NOM influence the THM and HAA formation. Coagulation of water remove more hydrophobic than hydrophilic NOM fractions, resulting a shift in the THM and HAA distribution (Liang and Singer, 2003). NOM concentrations in water vary significantly in time and space. Surface water tends to contain higher concentration of NOM than groundwater and thus treated surface water also contains higher concentration of DBP.

Water sources with high concentrations of NOM present a severe challenge for water treatment operations. Not only is NOM the major precursor for DBPs, there are several other negative impacts caused by NOM. Firstly, NOM adds unwanted colour, taste and

odour to the water. In addition, NOM causes membrane fouling, blocks activated carbon filtration processes, influences corrosion on water pipes, leads to regrowth and biofilm formation in the distribution system and compete for adsorption sites. Eikebrokk et al., 2018 recently published a field study concluding that the first treatment step in drinking water treatment (coagulation or nanofiltration) is the most efficient method to remove NOM.

In their field study, Eikebrokk et al., 2018, pointed out the predicted effect climate change will have on NOM concentration. It is predicted to be a 15-20 percent increase in NOM concentration by 2100 in the Nordic countries where the field study was conducted. All the sites had a positive relationship between NOM concentration and precipitation amount. Therefore, all utilities participating in the study were recommended to install in-situ sensors for temperature and rainfall (along with weather forecast) to get an early warning of potential high NOM concentration episodes.

Established indicators for NOM are UV_{254}, TOC/Dissolved Organic Carbon (DOC) and fluorescence. UV_{254} is the absorbance of UV at wavelength 254 nm. UV_{254} absorbance also is a well established surrogate measurement for nitrate, turbidity, color, TOC and DOC (Chow et al., 2013). While TOC/DOC indicates the concentration of organic substances, UV_{254} accounts for specific structure and functional groups of NOM. UV_{254} is a frequently used surrogate parameter used in DBP prediction models, that are further described in subsection 2.6. Water with higher specific UV absorbance values is more responsive to removal of organic matter by coagulation than water with lower pecific UV. In general, coagulation remove more HAA precursors than THM precursors (Liang and Singer, 2003).

2.5.2 Temperature and pH

Temperature strongly affects the kinetics of chlorine consumption and DBP formation in a distribution system (Roccaro et al., 2008). The rates of decay of both chlorine and chloramine increase at higher temperature. Due to this, higher amounts of chlorine need to be added during warmer seasons to ensure adequate levels of residual disinfectant in the distribution system.

Generally, the Ct product required to inactivate microorganisms is lower at higher temperatures. The microbial activity is known to be higher in distribution systems with warmer water (Sadiq and Rodriguez, 2004). Thus, both chlorine consumption and DBP formation are affected by seasonal variations. In summer months both chlorine con-

sumption and DBP formation is expected to be higher than in winter months.

Another parameter influencing both the efficiency of disinfection and the formation of DBPs is pH. A higher concentration of THMs are formed at higher pH than HAAs and vice-versa (Liang and Singer, 2003, Sadiq and Rodriguez, 2004). In other words, at lower pH levels there is to be expected a higher HAA formation than for THM.

Most chlorine reactions are pH dependent, resulting in pH to have a significant effect on chlorinated DBPs. The pH of the water system also determines the type and amount of DBPs formed. For example, a lower, more acidic pH result in formation of less chloroform, one of the four TTHM (Hung et al., 2017).

2.5.3 Reaction time and chlorine dose

In general, longer reaction time leads to higher formation of DBPs. Studies also reveal higher disinfection dose yields higher DBP formation potential (Sadiq and Rodriguez, 2004). A study by Liang and Singer, 2003 shows, that with all other factors being stable, fewer DBPs are formed when the disinfectants are added later in the process.

Chlorination and chloramine are the only disinfectants used for residual disinfection in the distribution system. The excess chlorine residual increases the formation of DBP with increased chlorine dose, contact time and concentration of NOM (Norsk Vann, 2009).

An important note is that higher concentrations of DBPs are generally observed in the extremities of the water distribution system compared to the treated water at the DWTP. However, HAA may degrade in extremities of the distribution system according to newer research (Sadiq and Rodriguez, 2004).

2.6 Models to Predict DBP Formations

There are two ways to predict the DBP concentration in a water body: 1) direct analysis, or 2) modelling. Direct analysis requires skills and effort in sample collection and preservation, in addition to being very costly and having a significant turnaround time. On the other hand, the advantage of modelling is that one can have multiple modelling targets, use complex reaction mechanisms and have multiple fitting parameters. Modelling requires site specificity and the use of calibration.

Surrogate parameters are used to estimate the DBP formation in the models. The definition of a surrogate parameter is an intrinsic relationship with the parameter of interest and one that can be easily monitored and quantified (Korshin et al., 2002). In the following paragraphs, different models variations to predict DBP formation are discussed.

DBP prediction models are based on either field-scaled or laboratory data, and the majority of the models are empirically based. Since chlorine is the most popular and traditional disinfectant, the biggest modelling efforts have been based on THMs. Most models are based on multivariate regression analysis where the variables are subjected to a logarithmic transformation (Sadiq and Rodriguez, 2004).

Two commonly used variables in the DBP prediction models are UV_{254} and $SUVA_{254}$. These are the two variables with the strongest correlation with DBP formation. Specific Ultraviolet Absorbance (SUVA) is defined in Equation (2.6) and is a good predictor of the aromatic carbon content of NOM and the DBP formation potential in water.

$$SUVA_{254} = \frac{UV_{254}}{DOC} \times 100 \tag{2.6}$$

Studies by Korshin et al., 2002 have explored the use of Differential Absorbance Spectroscopy (DAS) to predict DBPs. DAS quantifies the change in UV absorbance induced by chlorine addition as presented in Equation (2.7):

$$\Delta A_\lambda = A_\lambda^{chl} - A_\lambda^{int} \tag{2.7}$$

DAS focuses on the change in UV absorbance resulting from halogenation. The change in absorbance (ΔA_λ) is almost entirely attributable to chlorination induced changes in NOM in a given water sample. Research shows that change in NOM is closely related to incorporation of chlorine into NOM. Thus, DAS can be used to monitor the halogenation of NOM, measured by TOX.

The result from the Korshin et al., 2002 shows that formation of individual DBP and TOX is strongly correlated with DAS. The correlation between ΔA_{272} and TOX was especially strong (R^2=0.99). This suggests that DAS can be used in simple and inexpensive tests which can further be used to quantify the formation of numerous DBPs. DAS can be used as both a monitoring tool in the treatment plant and distribution system or as an analytical tool in tests of alternative treatment processes.

The correlations between DAS and formation of individual DBPs have the potential to revolutionize drinking water utilities way of working. The knowledge of the differential absorbance at various points in the distribution system can help one predict the concentration of DBPs in a way that is both inexpensive and time saving. The differential absorbance can be measured by implementing UV absorbance/fluorescence online monitoring sensors and import the sensor readings automatically to a SCADA system. The following section discusses online monitoring sensors and how they can be used to predict DBP formation.

2.7 Use of Online Monitoring Sensors to Predict DBP Concentrations

With regards to the health effects of DBPs described in section 2.3, there is a need to develop a more accurate, continuous monitoring of the DBP concentration in drinking water. The first real-time monitoring was used in the 1980's to track the pollution levels in rivers in the industrial areas of Western Europe. The Meuse river in Netherlands and the Rhine river in Germany experienced pollution at alarming levels and thus, were the first places that installed in-situ online monitoring instruments (Callaghan et al., 2019).

Since then, the focus has increasingly shifted to obtaining a complete picture of water quality using a variety of technologies instead of grab sampling and analysis. Today, there is a number of reliable online/in-situ monitoring instruments on the commercial market. Online high-frequency monitoring provides insight into the dynamics of water quality - rapid and short variations in the water quality.

2.7.1 Definitions

Online monitoring is defined as unattended sampling, analysis and report of a chemical, physical and/or biological parameter (Callaghan et al., 2019). The frequencies of the online monitoring vary anything from seconds and minutes apart up to one or more hours.

There are two different online monitoring tools, sensors and analyzers. A sensor responds directly to a physical stimulus (e.g heat, light, sound, pressure etc.) and transmits the signal on a display to future monitoring. An analyzer performs an automated version of an analytical method. In general, online sensors are considered more robust than

analyzers. For this thesis, the focus is on online monitoring sensors as they best fit the objectives of the thesis.

Figure 2.5 illustrates the basis of spectroscopic methods used for online monitoring. Their purpose is to identify and quantify chemical compounds in a water body based on their unique spectra. As the illustration shows, the beam emits a wavelength adsorbed by the molecules in the water which re-emits a wavelength detected by a sensor. By reading the 'new' wavelength spectra, scientists can map the important drinking water parameters like TOC, DOC, turbidity, chlorine concentration etc. The use of UV and fluorescence spectroscopy is further discussed in subsection 2.7.3.

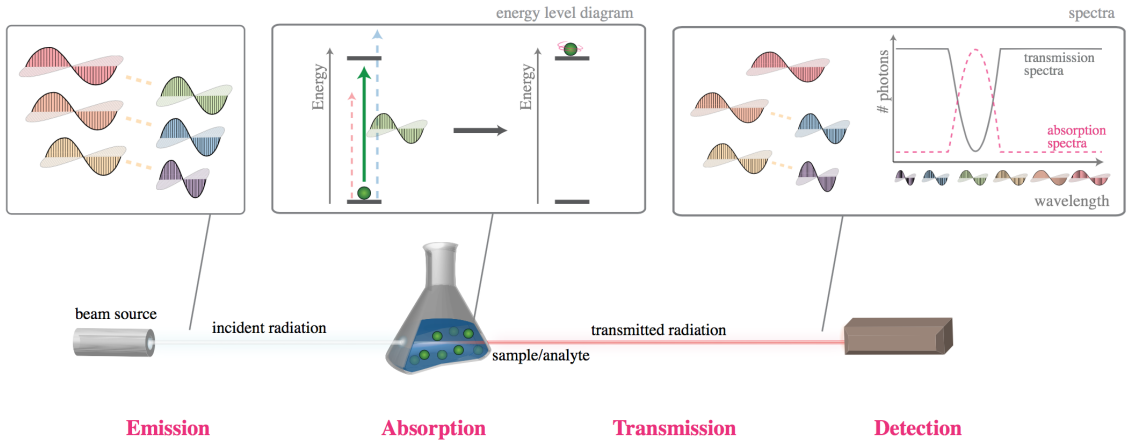

Figure 2.5: Illustration of spectroscopy. Figure by Chui, 2011.

2.7.2 BlueTech Insight Report

BlueTech Research published in 2019 an Insight Report on online water and wastewater sensors and analyzers (Callaghan et al., 2019). The key takeway from the report is the utilities' shift in focus from reliance on grab sampling/analysis to obtaining a complete picture of water quality by using a wider range of techniques.

The water quality industry is growing rapidly and the emphasis on continuous monitoring, online sensors and rapid testing become more profound. The report states that since the beginning of the 2000's, more than a 100 new manufacturing companies have been established commercially. These companies are specifically targeting the water market and it is estimated that the companies combined will introduce more than 100 new sensor technologies each year.

Today's global market for environmental monitoring sensor is large and the BlueTech report estimates an annual value of 2-3 billion US dollars. This estimate does not include the expected rapid growth of the industry. The cost of the sensors and analyzers has a wide range from $ 200 up to $ 50,000. A higher price can be expected for more complex systems.

According to BlueTech, there are five main factors contributing to growth in the water monitoring industry: 1) Development and growth of computer power, 2) More sophisticated wireless communication, 3) Affordability of remote power systems, 4) More sophisticated data analysis tools and 5) Development of drone technologies and satellite sensing. The most advanced online water sensors can measure multiple parameters at the same time.

In addition to the main factors contributing to growth, legislation and regulations also have important influence. A new EU Drinking Water Directive, likely to take effect in 2020, mandates utilities throughout the bloc to perform risk assessments both during the drinking water production and distribution process. This generates a legislative push towards more online monitoring and can rapidly increase the market size significantly. The new Drinking Water Directive is an important driver for both the development and the deployment of sensor technology.

In the next decade, a shift towards more robust online measurement equipment is expected. The sensors will be more reliable, transparent, intelligent and communicative. Big data management will play a key role in the infrastructure management.

2.7.3 UV absorbance and fluorescence spectrometers

It is a challenge to directly measure the concentration of DBPs in the background of various natural organic matter. As described in subsection 2.6, one can estimate the DBP concentration in water based on the changes of NOM and application of UV absorbance or fluorescence spectroscopy. The UV absorbance and fluorescence spectrometers are described in this subsection.

UV-Vis absorbance

Ultraviolet Light (UV-Vis) absorbance spectroscopy is now a frequently used tool for water utilities to optimize the water treatment process and manage the water quality. In UV-Vis absorption measurements, a spectrophotometer measures the amount of light

absorbed by the sample and the absorbance of the sample is determined based on the intensity of light. There are several types of spectrophotometers, single beam and double beam design, double beam being the most precise (Chow et al., 2013).

UV absorbance measurements can be used for process optimization, source water monitoring and determination of surrogate water quality parameters in treated water. As mentioned in subsection 2.5.1, UV absorbance is a well established surrogate measurement for a variety of water quality parameters. Further development to extend UV absorbance as a surrogate parameter to Cl demand and DBP formation have been carried out (Callaghan et al., 2019).

Fluorescence

Fluorescence is a complementary technique to the UV-Vis. Although it occurs in the same wavelength range as UV-Vis, the photon re-emits a longer wavelength than the one received when going from the excited to the ground state. Fluorescence spectroscopy is a potential monitoring tool because of its high sensitivity and selectivity. It is not as established a measurement method as is UV-Vis in the water industry, but many promising prototypes have been developed (Li et al., 2016, Tedetti et al., 2013, Ryškevič et al., 2010).

The sensitivity of fluorescence spectroscopy may be 10-1000 times higher than that of UV adsorption (Henderson et al., 2009). There are three generations of lamps used in UV and fluorescence spectrometer: low pressure mercury lamps (LP-Hg), Xenon lamps and deep UV LED lamps. The Deep UV LED lamp is the latest new-generation lamp and is small in size, with a low power demand, low cost and a fast on-off operation.

2.7.4 Online monitoring sensors on the market

Table 2.7 summarizes some of the most developed online monitoring sensors on the commercial market. Manufacturers often create a series of similar sensors with slightly different functions that can be customized to fit the customers needs. The cost of the individual sensors vary widely and companies are hesitant to publicly quote their prices on the products.

Table 2.7: Examples of online monitoring sensors available on the commercial market.

Company	Product	Function
RealTech	Real Spectrum P_L sensor	UV-Vis spectrometer providing real-time continuous monitoring for UV spectrum 190-750 nm. Multiparameter sensor in-situ with chemical cleaning.
Xylem	1. UV-VIS spectral sensors 2. YSI EXO2 Multiparameter Sonde	1. UV-Vis sensor best for measurement of TOC or DOC. Has a UV range of 200-720 nm and has integrated ultrasonic cleaning. 2. Multiparameter sonde with wireless communication and battery life of 90 days. Can be configurated with other sensors or used separately.
S::CAN	Spectro::lyser	UV-Vis spectrometer providing real-time continuous monitoring for UV spectrum 200-750 nm. Multiparameter probe in-situ with xenon flash lamp and automatic cleaning. Recommended by public authorities like the US EPA.

One of the most developed online monitoring sensors on the market right now are the sensors from S::CAN, which is discussed in the next subsection.

2.7.5 S::CAN online monitoring system

Chow et al., 2013 conducted a series of case studies using S::CAN online monitoring systems. The two major and five minor case studies evaluated the robustness of the S::CAN hardware and the surrogate parameter algorithm which is in-built in the hard-

ware. The study addressed different issues, the most relevant being development of the monitoring of new surrogate parameters such as real time monitoring/prediction of DBP formation.

The S::CAN Spectro::lyser is one of the online instruments on the commercial market using UV absorbance to predict TOC, DOC, THM/DBP and nitrate concentration. The sensor does not provide data on absolute concentration, but it can be used as an alarm tool targeting any sudden changes in the water quality. The sensor's algorithms are based on on-site experience instead of standard solutions created in laboratory. The S::CAN Spectro::lyser has an automatic hydraulic cleaning and can last weeks without maintenance.

Figure 2.6: The S::CAN Spectro::lyser. Picture from S::CAN, 2017.

The Chow et al., 2013 study compared the S::CAN sensors data predictions with grab samples from the same water analyzed in the laboratory. The parameters analyzed was DOC, TOC, UV_{254}, color and Trihalomethanes Formation Potential (THMFP). From this evaluation, the research team established that good prediction of concentration can only be obtained for well-characterised waters.

The analytical results from the standard laboratory methods and the S::CAN Spectro::lyser correlated very well using Partial Least Squares (PLS). For UV_{254}, color and DOC the correlations were R^2=0.98, R^2=0.96 and R^2=0.84, respectively. The overall conclusion from the case study is that UV absorbance is an applicable measurement that is convenient and technically achievable. In addition, the use of multiple wavelength sensors with PLS calibration can improve the reliability and accuracy of the measurement.

2.8 Cost Benefit Analysis

CBA is a method used to assess the economic efficiency of proposed public policies through the systematic prediction of social cost and social benefits. The purpose of the CBA is to find the most efficient solution by maximizing the social welfare. If the net positive social benefits outweigh the social cost, then the policy should be implemented (Boardman et al., 2006).

The alternatives in a CBA are ranked by valuing all the impacts over the lifetime of an alternative project in monetary units, discounted to a specific year. This unit is called Net Present Value (NPV) and is defined in Equation (2.8):

$$NPV = -I + \sum_{t=0}^{n} \frac{1}{(1+s)^t}(B_t - C_t) \tag{2.8}$$

where I is the investment, s is the Social Discount Rate (SDR) and B_t and C_t denotes benefit and cost in year t. The basic decision rule if the CBA has only one alternative, is to adopt the project if the NPV is positive. If the CBA has several alternatives, the alternative with the largest NPV should be selected.

The steps of a modern CBA is illustrated by Figure 2.7. The first step is to specify the set of alternatives for the defined problem. The counterfactual is the status quo, which means no change in government policy. Second step is to determine the standing. This includes choosing a perspective by deciding whose benefit and cost count. The third step is to identify the impact categories, catalogue them and select the appropriate measurement indicators.

Step four is to predict the impacts quantitatively over the life of the project. Further, in step five, all the impacts are to be monetized. Monetizing is attaching dollar value to an impact. The value of an output in a CBA is usually measured in terms of willingness to Pay (WTP). WTP is defined as the maximum price or below a person is willing to pay for a product. If a person is not willing to pay for an impact, then the impact has zero value in a CBA.

Step six is to discount benefits and costs to obtain present values. Future benefits and costs are discounted relative to present benefit and cost in order to obtain their present value. In step seven, the NPV is calculated for each alternative by using Equation (2.8). The general rule is to choose the alternative with the largest NPV.

To consider the uncertainties around the assumptions made in the CBA, a sensitivity

analysis is preformed which is step eight. Both the uncertainties about the predicted impacts and the monetary valuation of each unit in the impact are considered.

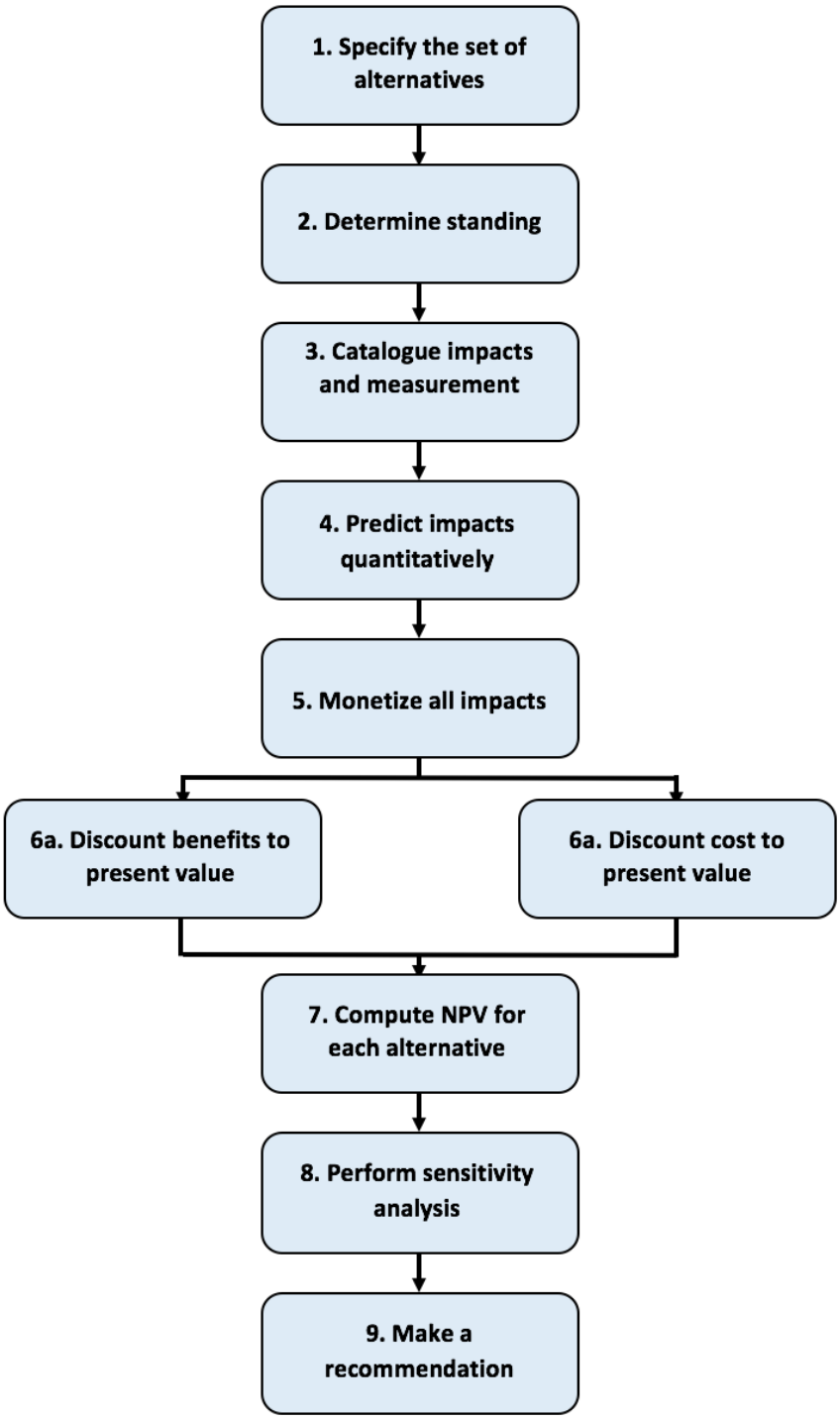

Figure 2.7: Steps for a modern CBA (Boardman et al., 2006).

The final step is to make a recommendation based on the CBA. Here, both the NPV of each alternative and the sensitivity analysis are considered before making the final recommendation. Generally, the analysts should recommend the alternative with the

largest NPV, but the sensitivity analysis might show that another alternative is preferable. It is important to remember the NPVs are predicted values and take that into account when making a comprehensive recommendation.

This CBA method was used for estimating cost savings and health benefits as a result of the implementation of a consistent and rigorous online monitoring program, described in section 3.6.

3

Methods

This Chapter describes the methods used for analyzing the DBP data from the water quality samples, and a thorough description of the Seattle DWTPs and the distribution system. The first part is an introduction to the Seattle Water System followed by a description of Cedar and Tolt Treatment Facilities and their treatment steps. Secondly, different aspects of the distribution system are described. Thirdly, the analytical methods for the data analysis are presented. At the end of the chapter is a description of the method and cost associations for the CBA.

3.1 Seattle Water System

Seattle is a coastal city in the Pacific Northwest region of the United States. The two DWTPs providing drinking water for Seattle are Cedar and Tolt Treatment Facilities. Combined they daily provide water to 1.4 million people in the Seattle area, including wholesale costumers. The city of Seattle owns the majority of both Cedar and Tolt watersheds which results in both watersheds being uninhabited and protected. The two facilities have different treatment methods to disinfect the drinking water. Cedar Treatment Facility has no filtration and uses ozonation, UV radiation and chlorination as disinfection methods. Tolt Treatment Facility uses coagulation/filtration to filter the water and, ozonation and chlorination as disinfection methods. The water treatment steps for the two facilities are described in detail in the next to subsections.

Figure 3.1 is an illustration of the the water system in Seattle. Tolt watershed is located east of Seattle while Cedar watershed is located southeast. The area marked yellow in the illustration is the Seattle Retail Service Area and where the water quality sampling sites are located. There are five sampling sites in the distribution system for the Cedar water and seven sampling sites for the Tolt water.

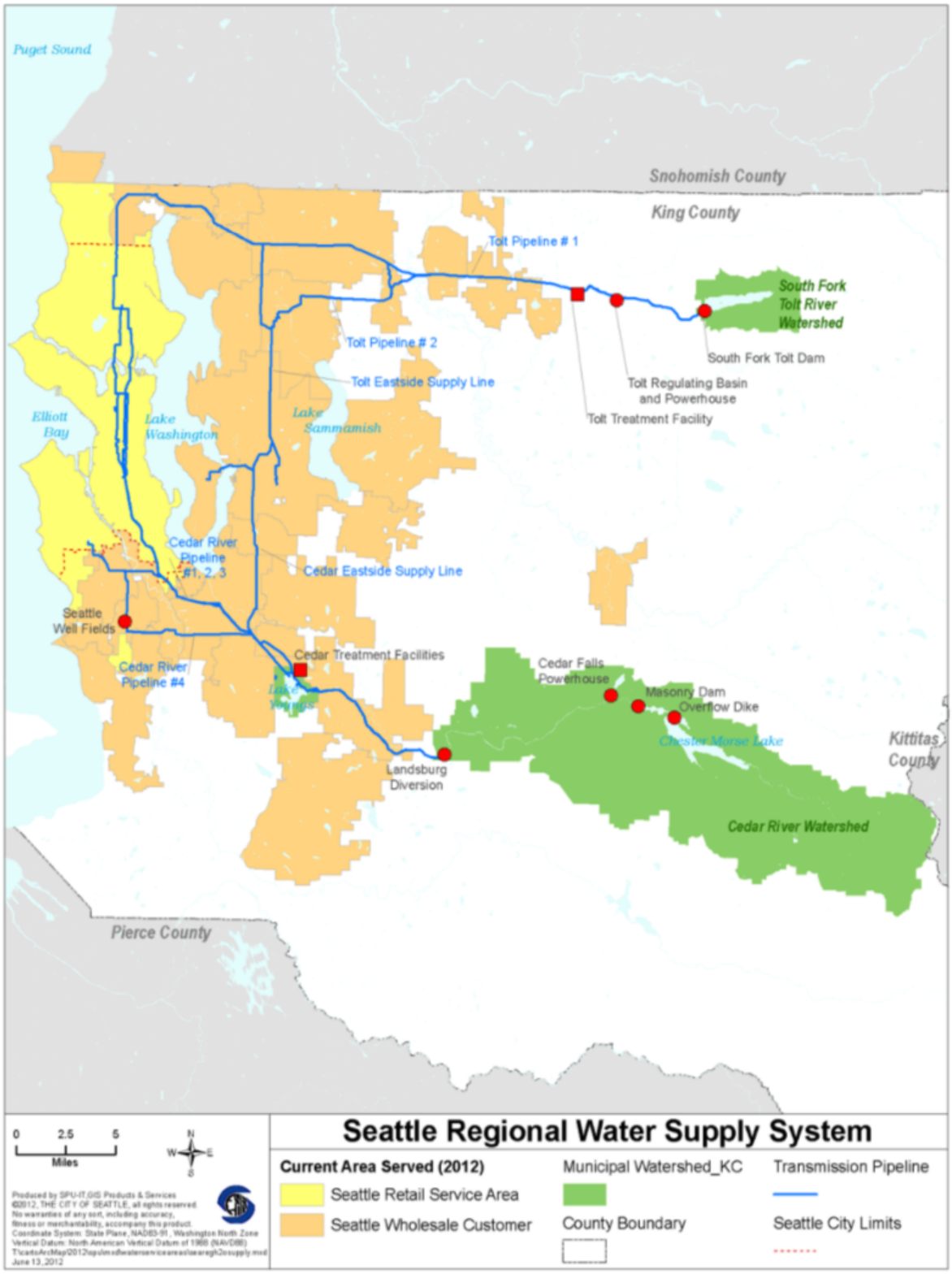

Figure 3.1: Seattle Regional Water Supply System (Seattle Public Utilites, 2019a)

Seattle is a rapidly expanding city. Since the 1980's, Seattle's population has increased with over 50 percent while the total water consumption has decreased with 26 percent

(Seattle Public Utilites, 2019a). Figure 3.2 shows the development of the annual water demand versus population growth for Seattle from 1930 to 2015. Due to utility and consumer awareness, water consumption has decreased despite the rapid increase in population. Summer droughts in the Seattle area in the late 80's and early 90's made the Seattle citizens more aware of water consumption. To decrease the total water consumption, a series of measures were implemented: installation of low pressure shower heads, low flow toilets and, less water used on lawns and gardens. The measures were successful; in the mid 1980's the annual demand in Seattle region per day was about 640 million liters of water per day (ML/d) (170 MGD) while in 2015 it was about 455 ML/d (120 MGD) (Seattle Public Utilites, 2019a).

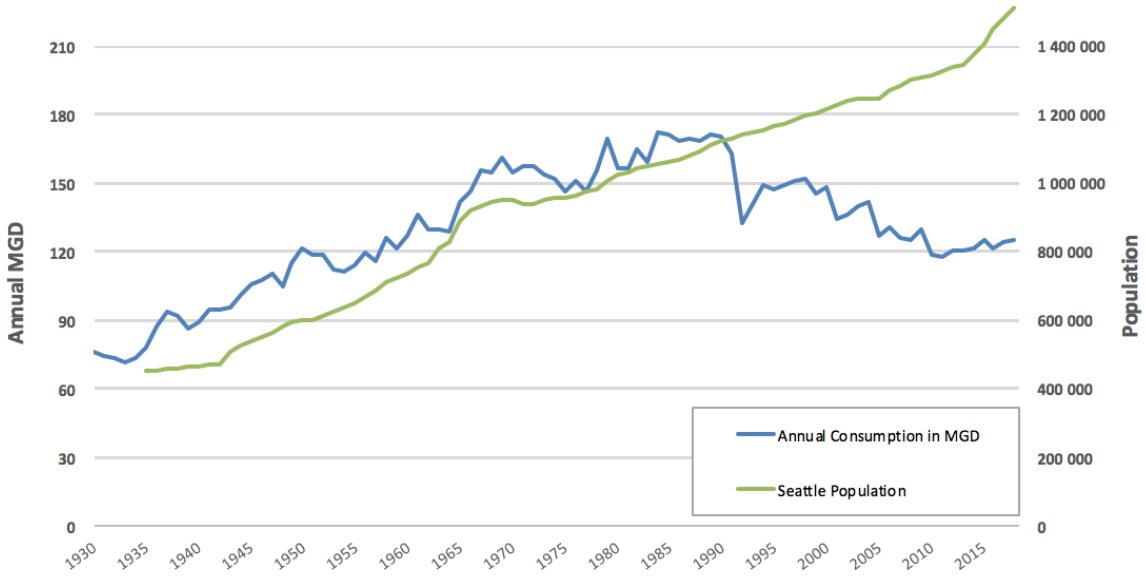

Figure 3.2: Total Seattle Regional Water System Demand in Million of Gallons per Day (MGD) from 1930-2015 (Seattle Public Utilites, 2019a).

3.2 Washington State Disinfection Requirements

For disinfection requirements in Washington state, the EPA has delegated the primary enforcement of authority to Washington State Department of Health. The State Drinking Water Regulations set the requirements for the disinfection of the drinking water. The requirements are found in the Washington Administration Code (WAC). Table 3.1 shows the disinfection requirements for Cedar and Tolt DWTP set by WAC 246-290-630.

As shown in Table 3.1, the disinfectant requirements in terms of log removal for Cedar is higher than Tolt for all the contaminants. The treatment plants use different disinfectant for each contaminant. Cedar uses ozone for *Giardia* disinfection while Tolt uses ozone

and filtration. To disinfect *Cryptosoridium*, Cedar uses UV radiation while Tolt uses filtration. As for virus disinfection, both Cedar and Tolt use chlorination.

Table 3.1: Disinfection Requirements for Cedar and Tolt in log removal.

	Cedar	**Tolt**
Giardia	4	3
Cryptosoridium	3	2
Viruses	5	4

3.3 The Treatment Facilities

The two treatment facilities, Cedar Treatment Facility and Tolt Treatment Facility, are discussed in this section.

3.3.1 Cedar Treatment Facility

Cedar River Watershed has been a drinking water source for the Seattle area for over a hundred years. The new Cedar Treatment Facility started operation in 2004. It supports about 60-70 percent of Seattle's drinking water with up to 680 ML/d. The Cedar River Watershed consists of 90,500 acres of land and is a highly protected mountain watershed. No commercial activities are allowed within the watershed to minimize the risk of spreading contaminants and diseases. A distinct object regarding the Cedar Treatment Facility is the absence of filtration before initiating disinfection. The main reason for this is the protection of the watershed and the glacial moraine in the watershed which provides a natural filtration to the water.

The daily average of water treated per day at Cedar Treatment Facility varies with season. In the warmest months in summer, July and August, the daily average is about 400 ML/d. From November-March, the winter season, the daily average is between 240-250 ML/d.

The raw water from the Cedar Watershed travels through three locations before it gets transferred to the distribution system:

1. *Landsburg Diversion and Treatment*

2. *Lake Youngs reservoir*

3. *Cedar Treatment Facility*

At Landsburg Diversion and Treatment, the raw water is dosed with 1 mg/L free chlorine (Cl_2) to keep the transmission pipes clear. However, when the water enters Lake Youngs, the chlorine concentration is less than 0.2 mg/L which means the water is still considered raw water. At Landsburg, the UVT of the water is measured continuously every 15 minutes by a online monitoring sensor.

Further, the water flows from Landsburg to Lake Youngs reservoir where it has a six months detention time. At Lake Youngs, 3-4 mg/L calcium carbonate ($CaCO_3$) is added to the water to raise the pH. Next, the water is pumped out of Lake Youngs and flows to the Cedar Treatment Facility. The treatments steps at the Cedar Treatment Facility are ozonation, UV radiation and chlorination, respectively. The primary disinfectants are ozonation and UV, while the secondary disinfectant is chlorination.

Lake Youngs

Lake Youngs serves as the transmission reservoir for the Cedar river water prior to treatment and has a volume of 42 billion liters. The pumping station at Lake Youngs is 122 meters offshore water and 12 meters deep to ensure good water quality. Table 3.2 provides information on the raw water quality in Lake Young. On a regular basis, the water in Lake Youngs can be describes as soft with high transmittance (UVT), low turbidity, low organics and for the most of the time low in iron.

Table 3.2: Raw Water Quality in Lake Youngs (Seattle Public Utilites, 2014).

Parameter	**Unit**	**Average**	**Range**
Turbidity	NTU	0.4	0.2 - 1.6
Temperature	°C	12	2 - 24
pH		7.6	6.9 - 8.6
Alkalinity	mg/L as $CaCO_3$	17	12 - 22
Hardness	mg/L as $CaCO_3$	24	18 - 28
Iron	mg/L	0.04	<0.01 - 0.15
TOC	mg/L	0.8	0.3 - 1.7
Transmittance	%	96	93 - 98

The water quality in Lake Youngs vary due to seasonal changes. In the spring (from March to June) algae bloom occurs in the lake and causes management problems for the utility. In 2008-2019, the genus *Lindavia* caused algae bloom in Lake Youngs. This

was an algae species never seen in Lake Young before and had a pronounced negative impact on both the treatment plant and the distribution system. At Cedar Treatment Facility, screens, monitors, pumps and pipes were clogged by the algae. There were additional impacts to the wholesale and residential costumers who had clogging and loss of pressure in the distribution system.

To prevent the physical changes to the treatment plant and distribution system caused by the seasonal algae bloom, a change in the water flow got implemented. When there is algae blooming in Lake Youngs, the raw water is bypassed from the lake. In other words, the raw water travels directly from Landsburg Diversion to Cedar Treatment Facility. When bypassed from Landsburg to Cedar, the water travels through a cement tunnel of 3 meters in diameter, before transferred to two steel pipes which are 1.5 meters in diameter. Since 2008, Lake Youngs has been bypassed for a time period in the spring, with the exception of the year 2015. The bypass information was an important factor when analyzing the raw water data.

Treatment step 1: Ozonation disinfection

The first disinfection treatment step at Cedar Treatment Facility is ozonation. Figure 3.3 illustrates the treatment process of ozonation and UV at Cedar Treatment Facility. The raw water is pumped out of Lake Young and transferred to the ozone injection chamber.

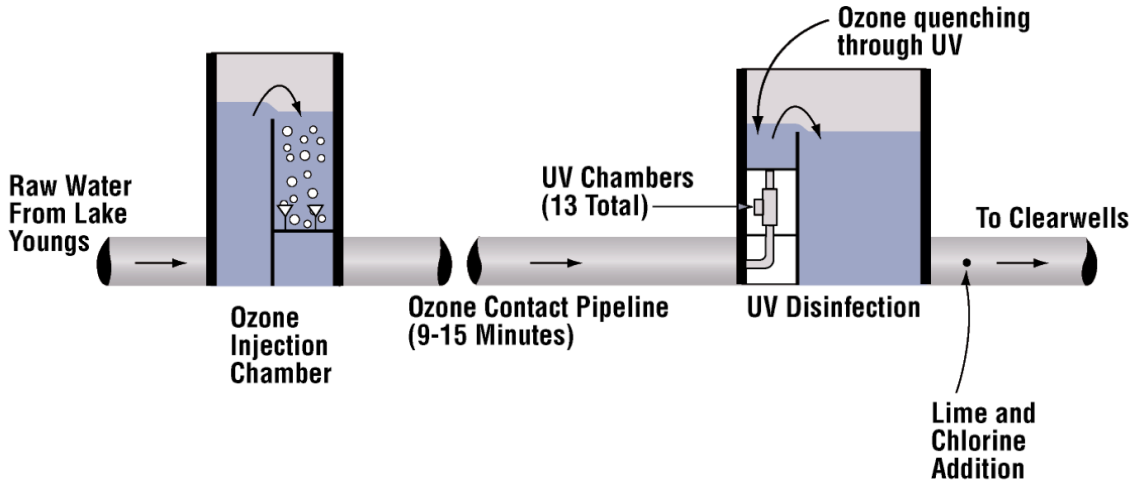

Figure 3.3: Illustration of ozonation and UV at Cedar Treatment Facility (Seattle Public Utilites, 2014).

In the injection chamber, liquid oxygen (O_2) is converted to ozone gas (O_3) using electrical plasma discharge. The ozone reacts with the water by diffusing the gas into the

injection chamber where the water remains for less then a minute. The average ozone dosage is 0.3-0.6 mg/L. The water stays in contact with the ozone while it travels from the injection facility to the UV disinfection facility. The diameter of the pipes are 2 meters and the contact time is estimated to be 9-15 minutes, depending on the flow rate.

Treatment step 2: Ultraviolet light (UV) disinfection

Before the UV disinfection, any ozone left in the water is removed by adding sodium bisulfite ($NaHSO_3$) to protect the glass in the UV chamber. At the same location, the second monitoring of the water's UVT is measured continuously by an online monitoring sensor.

In the UV chamber, the contact time of the water being treated is less than a second. The target minimal dose for UV is 40 mJ/cm^2. The UVT of the water needs to be over 90 percent for the utility to get approval for the UV disinfection. Factors that affect the transmittance of the water are turbidity, iron concentration and magnesium concentration. These factors are present during a lake turnover. After the water has been disinfected using UV, an average of 3-5 mg/L $CaCO_3$ is added to raise the pH to 8.2 for corrosion control.

Treatment step 3: Chlorination disinfection

The last disinfection step at Cedar Treatment Facility is chlorination. The water enters two big circular concrete tanks, called clearwells, that have a combined volume of 75 million liters. The clearwells act as temporary storage reservoirs where the chlorination disinfection is completed. The contact time in the clearwells vary widely from thirty minutes and up to two hours.

The disinfectant used is gas chlorine (Cl_2) and the target dose for the drinking water varies with season. In winter months, the target residual dose for Cedar is 1.5 mg/L while in the summer months it varies between 1.6 mg/L and 1.7 mg/L. The dose of chlorine added to water varies seasonally between 2.0-2.56 mg/L. There is need for a higher Cl_2 dose in summer than in winter. In summer, the daily average Cl_2 used is between 800-890 kg. To compare, in winter the daily average Cl_2 used is 550-600 kg.

After the clearwells, residual chlorine is added at the outlet where water is transferred to the distribution system. This is an important safeguard to prevent microbial con-

tamination after treatment.

3.3.2 Tolt Treatment Facility

Tolt watershed has been a drinking water source since 1964 and South Fork Tolt River is the surface water source. The size of Tolt watershed is about 10,000 acres. The new Tolt Treatment Facility finished its construction in 2001 and it supports 30-40 percent of Seattle's drinking water needs. Tolt Treatment Facility provides up to 455 million liters drinking water per day. Like the Cedar watershed, the Tolt watershed is closed to the public, making sure that the water is protected from agricultural, recreational and residential pollution.

The Tolt water characteristics have some differences from the Cedar water which are important to take notice of. Table 3.3 provides information on the raw water in Tolt. First of all, the Tolt water has a lower average temperature than Cedar. The temperature in the Tolt water has an average at 9 °C and with a range of 2-15 °C. In Cedar, the water temperature average is 12 °C with a range between 2-24 °C. This is because the Tolt water is at a higher altitude up in the mountains where the air temperature is cooler.

Table 3.3: Raw Water Quality in Tolt (Seattle Public Utilites, 2019b).

Parameter	Unit	Average	Range
Turbidity	NTU	0.5	0.2 - 1.5
Temperature	°C	9	2 - 15
pH		6.9	6.6 - 7.3
Alkalinity	mg/L as $CaCO_3$	5.7	5.3 - 6.5
TOC	mg/L	1.3	1.2 - 1.6
Transmittance	%	87	82 - 90

The pH of the water in Tolt is slightly lower than the Cedar water. The average pH in Tolt is 6.9 while the average pH in Cedar is 7.6. In other words, the water in Tolt is slightly more acidic than in Cedar. The average TOC concentration in the Tolt water is 1.3 mg/L while in the Cedar water the average is 0.8 mg/L. Therefore, the NOM concentration in the Tolt watershed will generally be higher than Cedar watershed.

The daily average of water treated per day at Tolt Treatment Facility varies with season due to higher consumer demand in summer than winter. In the warmest summer months, July and August, the daily average of water treated at Tolt is between 260-270 ML/d.

In the winter months, from November-March, the daily average of water treated is about 140-145 ML/d.

The treatment steps in Tolt Treatment Facility are ozonation, coagulation/filtration and chlorination, respectively. The primary disinfectant is ozonation and the secondary disinfectant is chlorination. The treatment process for Tolt is illustrated in Figure 3.4. The only data used from Tolt Treatment Facility are generated from grab samples. The treatments steps at Tolt are described in detail in the next subsections.

Treatment step 1: Ozonation disinfection

Like in the Cedar Treatment Facility, the first step in Tolt Treatment Facility is ozonation. The raw water flows into the concrete injection chamber where the liquid oxygen (O_2) is converted to ozone (O_3) when passing through an electric field. The contact time remains as the water flows to the coagulation and flocculation treatment, as illustrated in Figure 3.4.

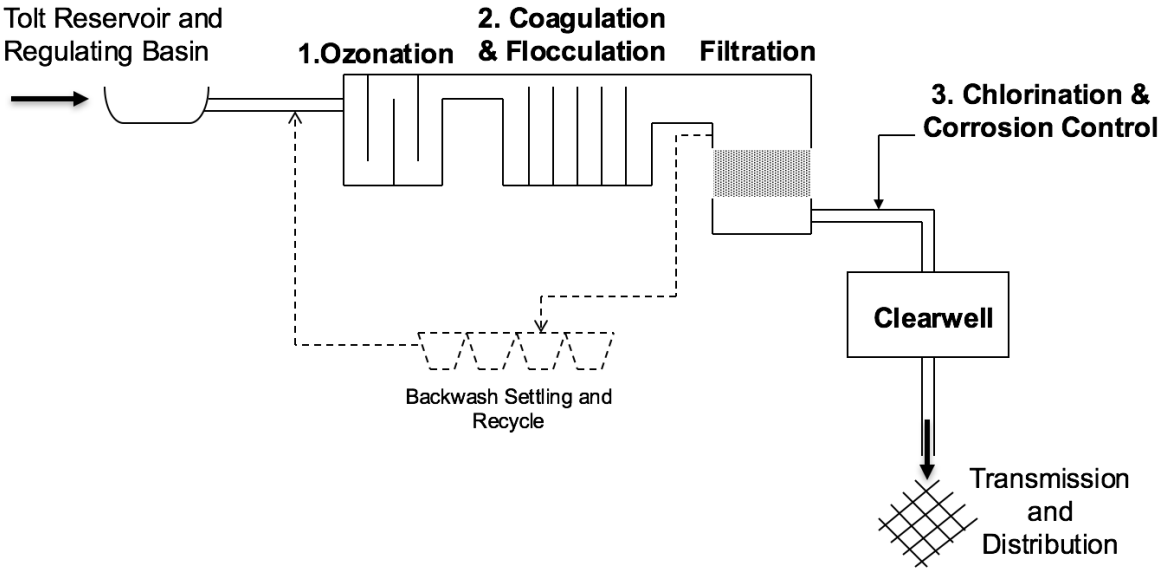

Figure 3.4: Illustration of the treatment process at Tolt Treatment Facility (Seattle Public Utilites, 2019b).

The ozone dose for Tolt is higher than Cedar because of lower temperatures and higher TOC concentration. The average ozone dose is 2.9 mg/L and the max ozone dose is 4.8 mg/L for the Tolt water.

Treatment step 2: Coagulation/Filtration

The primary coagulant used in Tolt Treatment Facility is ferric chloride ($FeCl_3$) and the coagulant aid is a cationic polymer. The average concentration for both the ferric chloride and the cationic polymer is 1-2 mg/L. During coagulation, the ferric chloride neutralizes the negative charge of the suspended particles in the water. The particles then bind together into heavier *flocs* that are easier to filter. The flocculation occurs in the chamber, before entering the filtration system.

For the filtration, the filter bed is a 1.8 meter deep, anthracite coal filter media removing particulates and pathogens as the water flows through the filter. At Tolt, there are six installed filters with a capacity each of 90 million liters. The filter is cleaned regularly by backwashing (reversing the water flow through the filter).

At peak flow (227 ML/d), the hydraulic detention time for the water to go through both the ozone and flocculation basins is 31.6 minutes. However, in reality the flow of the water is often a third of that. This often results in a detention time of more than one hour for the water.

Treatment step 3: Chlorination disinfection

The final treatment step is chlorination. The disinfectant used is chlorine gas (Cl_2) and the calculated dose is between 1.9 mg/L and 2.25 mg/L depending on the season. In winter months, the daily average chlorine used is about 300 kg, while in summer months the daily average can be as high as 550 kg. The target residual dose for chlorine at Tolt is constant at 1.5 mg/L regardless the season.

The clearwells reservoirs at Tolt have a combined storage of 28 million liters. The contact time varies from one to four hours depending on the water demand of the city. At the clearwells, an average of 10 mg/L $CaCO_3$ is added to raise the pH to 8.2 and to raise the alkalinity to 19 mg/L. Residual chlorine is added at the outlet where water is transferred to the distribution system.

3.4 Seattle Water Distribution System

The distribution system is described in this section. The first subsections describe the structure and function of the distribution system, followed by a description of the water quality sampling sites.

3.4.1 Reservoirs, transmission and distribution pipes

The distribution system consists of transmission pipes and distribution pipes transporting the water, and the reservoirs storing it. In addition, there are also local standpipes and elevated tanks storing a small portion of the water. The transmission pipes are the main structure of the distribution system and are depicted by the blue lines illustrated in Figure 3.1. The main transmission pipes' objective is to transport the water from the DWTP to the suburban areas marked yellow in Figure 3.1.

The transmission pipes consist of 340 km of large-diameter pipeline. The diameter of the pipes vary from 0.4 to 2.4 meters. The materials of the pipes are either steel, ductile iron or concrete. The main transmission pipelines transport the water from Cedar and Tolt to the reservoirs and standpipes, and sometimes directly to the distribution system. The distribution system contains about 2720 km of pipelines. The diameter of the pipes vary from 10 cm to 75 cm and the material is unlined or mortar-lined cast iron, ductile iron or steel-pipe (Seattle Public Utilites, 2018).

There are nine active reservoirs in the distribution system that SPU operates and maintains. The smallest reservoir has a capacity of 28 million liters while the biggest has a capacity of 230 million liters. Seven of the reservoirs store Cedar water and the remaining two store Tolt water. The size and location of the reservoir is important for determination of water detention time in the distribution system. For the smaller reservoirs close to dense populated areas (e.g. Seattle downtown), the detention time of the water is significantly shorter.

3.4.2 Pipe materials and condition

The age of the transmission lines varies from 20 to 100 years. About 2/3 of the material in the transmission pipes is steel and most of them have cement lining. The pipes in the distribution system are of various material and quality. Figure shows 3.5 that 41

percent of the distribution pipes are old unlined iron pipes and 38 percent is lined with cast. Most of the unlined cast iron pipes were installed in between the beginning of 1900's and 1930's. The oldest pipes in the distribution system are from the 1890's and new pipes are installed every year.

Unlined pipelines and bacteriological re-growth are two main factors affecting the water quality. The pipes made of unlined iron and steel are prone to react with the chlorine and therefore may be exposed to be damaged by corrosion. The rate of corrosion depends on the corrosivity of the environment (in most cases soil or water). If no protective system is installed, bare metal steel or ductile iron will rust when exposed to soil or water. Internal corrosion is managed by chemical adjustments and the use of internal linings. Around 40 percent of the pipelines in the distribution system do not have corrosion control (Seattle Public Utilites, 2019a).

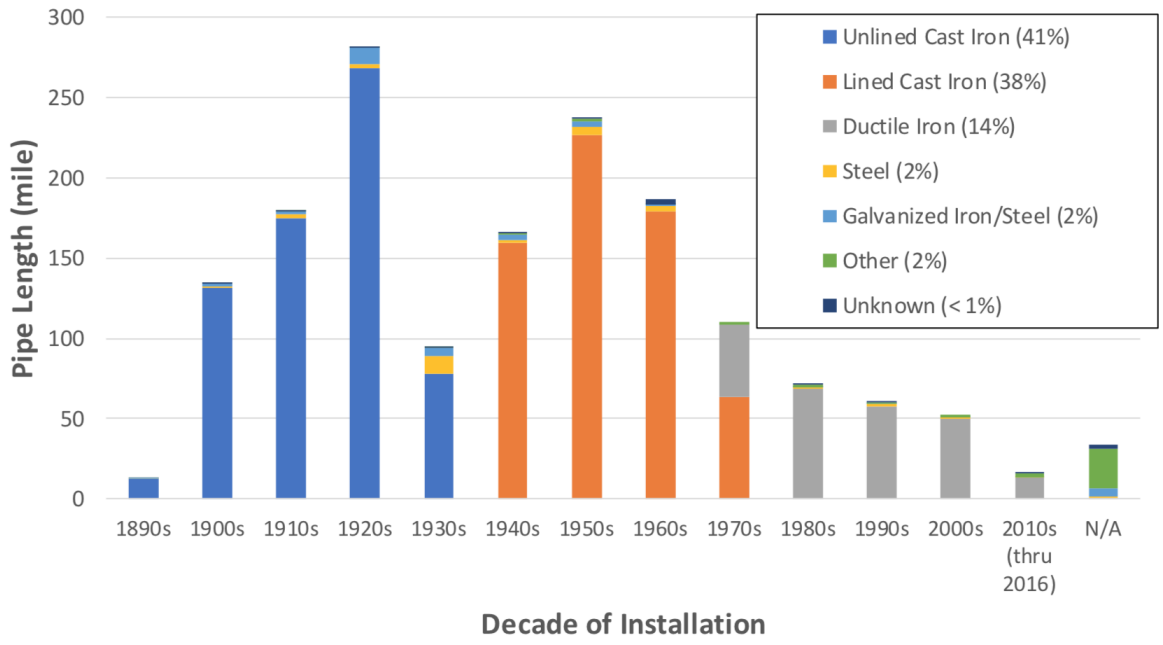

Figure 3.5: Pipe material and decade of installation for the distribution pipes (Seattle Public Utilites, 2019a).

In addition to being prone to corrosion, the unlined cast iron pipes have higher a potential for microbial biofilm growth. A biofilm is a layer of microorganisms which forms a matrix on the interior of the water pipeline. The biofilms may play a role in corrosion, function as a reservoir for pathogens and affect the aesthetics of the water (Chan et al., 2019). To prevent microbial biofilms, SPU re-chlorinate the transmission and distribution pipes.

3.4.3 Residual chlorine and re-chlorination

The residual chlorine in the distribution system is one important factor to take into account when analyzing the data. The target residual dose for Tolt is constant at 1.5 mg/L, while for Cedar the residual chlorine ranges from 1.5-1.7 mg/L due to seasonal changes. The residual chlorine is monitored continuously when the water leaves the treatment plant and is measured once every week at the distribution sites. A chlorine sample is taken daily at several locations along the transmission sites.

If the concentration of the residual chlorine measured is less than 0.2 mg/L at one of the distribution sites, the utility takes action by either adding more chlorine at the DWTP or in the distribution system. All re-chlorination in the distribution system happens in the reservoirs. The chlorine concentration is measured continuously at all the active reservoirs by an online monitoring senor. If the chlorine dose at a reservoir borderlines to the minimum target dose (e.g. 1 mg/L), the sensor detects it and chlorine is automatically added to the water.

Chlorine dosage depends on water temperature and season. If the detention time in the distribution system is low, the water might be re-chlorinated up to three times before being used.

3.4.4 Sampling sites

SPU is required to collect water quality samples quarterly in the distribution system at the twelve locations with the highest THM and HAA concentrations based on the initial distribution system evaluation. Table 3.4 contains information about the twelve sampling sites. The sampling and lab procedures at SPU are found in Appendix A.

As presented in Table 3.4, five of the sampling sites are supplied by Cedar water and the remaining seven of the sampling sites are supplied by Tolt water. All the distribution pipes transporting the Cedar water mainly consist of unlined cast iron (U) while the distribution pipes for Tolt mainly are lined cast iron (L). This piece of information is important for the analysis.

The number of reservoirs column indicates the number of reservoirs the water passes through before entering the sampling site. The last column states the estimated detention time spent in total in all the reservoirs. The information in Table 3.4 is of great significance for the analytical part.

Table 3.4: The water quality sampling sites in the distribution system.

Sampling site	Water source	Pipe material	Number of reservoirs	Est. detention time in reservoirs
C-1	Cedar	U	2	7 to 14
C-2	Cedar	U	3	8 to 18
C-3	Cedar	U	1	7 to 14
C-4	Cedar	U	1	7 to 14
C-5	Cedar	U	1	7 to 14
T-1	Tolt	L	1	7 to 21
T-2	Tolt	L	1	7 to 14
T-3	Tolt	L	1	7 to 14
T-4	Tolt	L	2	7 to 28
T-5	Tolt	L	2	7 to 28
T-6	Tolt	L	2	7 to 28
T-7	Tolt	L	1	7 to 28

3.5 Data Processing Methods

One of the main objectives of the thesis is to process the multi-year DBP and water quality data, and evaluate the factors influencing the occurrence of high DBP values. This subsection describes the methods used when analyzing the data provided by SPU. First is a presentation of the data sets followed by the methods used in Python, Unscrambler and the Artificial Neural Networks (ANN) model.

3.5.1 Description of the data

The entire data set presented in this thesis were provided by SPU. During the research study, several meetings were conducted with SPU personnel at which the details of the distribution system and water treatment process were discussed.

The raw data from SPU included:

1. DBP (THM and HAA) data at sampling sites in the distribution system from 2007-2018 (both Tolt and Cedar).

2. TOC data at DWTP from 2007-2018 (both Tolt and Cedar).

3. Online monitoring UVT data from Cedar before and after ozonation from 2008-2018.

4. Daily averages of chlorine concentration, pH, temperature and turbidity at the inlet of Cedar and Tolt DWTP from 2010-2018.

5. Daily averages of chlorine concentration, pH and turbidity at the outlet of Cedar and Tolt DWTP from 2010-2018.

The DBP data consists of quarterly samples from the twelve sampling sites presented in Table 3.4. The DBP samples are usually taken in the first week of February, May, August and November. The TOC data are grab samples taken every other week at the inlet of Cedar and Tolt DWTP. The online monitoring UVT data set from Cedar before and after ozonation was the most comprehensive data set as it had measurements at every 15 minute intervals for a decade.

The daily average data at the inlet at Cedar and Tolt DWTP are chlorine concentration, pH, temperature and turbidity. The same data sets were available for the outlet at Cedar and Tolt, except for temperature.

3.5.2 Data analysis using Python

The results were processed using Python 3.7.3 software to make graphical representation of the data. The raw data in the Excel files were uploaded to Pandas library in Python and transferred into numeric tables. Further, the selection of site in distribution system, time frame and parameter were conducted and put into a graphical representation using matplotlib.

In assessment of the online monitoring data from Cedar DWTP, some additional detailed coding had to be prepared considering the grand size of the raw data. The UVA of the water was calculated using the following Equation (3.1):

$$UVA = log(\frac{100}{UVT}) \tag{3.1}$$

The time resolution was matched by averaging the larger online monitoring data set to the smaller data set of DBPs. The online monitoring UVA data and the DBP data were compared of the using longitudinal graphs and scatterplots.

To check for correlation of the UVA at Cedar DWTP and the DBP concentration at the sampling sites, a N days iteration model based on summer or winter season was created in Python. The model is based on the date of the DBP measurement at the sampling site and goes back N number of days to in the UVA data measured at Cedar DWTP to check for correlation. Initially the UVA data has a data point every 15 minutes, but this was made to daily averages.

The inputs in the N days iteration model are the sampling site, Summer or Winter months, the N number of days and THM or HAA. The output from the model is a list of the R^2 value from Train 1 and Train 2 for the N number of days chosen and the DBP value at the sampling site.

For the linear regression models, the ordinary least square method in the scikit-learn library in Python was used to perform Multiple Linear Regression (MLR) to fit the two linear models. The same tool was used to make graphical representation of the data.

3.5.3 Data analysis using Unscrambler

Unscrambler is an analytical tool frequently used in advanced statistical analysis in various industrial segments, while also increasingly used in the water industry for modelling and prediction of water quality. For the data given by SPU, Unscrambler was used to conduct a Multivariate Analysis (MVA) to investigate potential correlation between THM/HAA formation and the water quality parameters.

A MVA is based on indirect measurements (in this case, pH, Cl measurement, temperature etc.) and empirical data form the basis for the analysis. The MVA consists of two main parts, the Principal Component Analysis (PCA) and the Partial Least Square Regression (PLSR). The PCA is a qualitative analysis that characterizes the structure of the data, while the PLSR relates the sets of variables to each other through regression and prediction graphs.

3.5.4 Data analysis using the ANN model

ANN are biologically-inspired computer programs which gather knowledge by detecting the patterns and relationship in data and are trained through experience, not from programming. As ANNs are well suited to perform pattern recognition, they can be used to perform time-series prediction and modelling.

The ANN models are created using MATLABs ANN Toolbox. The ANN models were tested for the data from Cedar DWTP only. The input and output data from Cedar DWTP was uploaded in the ANN model to train the model using different algorithms.

In the ANN model, the number of samples are randomly divided into the model's three steps: training, validation and testing. In training, the fraction of samples are used to train the model and the network is adjusted according to it's error. For validation, the fraction of samples are used to train algorithms to prevent overfitting. In testing, the fraction of samples are used for an independent test of the ANN network and measure performance. When creating the model, one has to decide a division of the samples between the training, validation and testing.

3.6 Cost Benefit Analysis

The main objective with the CBA is to estimate the society's benefits and costs associated with the deployment of online monitoring sensors in the distribution system. For simplicity and due to limited epidemiological data, the only health risk from DBP exposure considered in this analysis is bladder cancer. In the first subsection, the number of new annual bladder cancer cases in the Seattle Water System attributed to DBP exposure is estimated. Then the appropriate assumptions for each step in the CBA are made. The results from calculating the NPV and sensitivity analysis are to be used to recommend the city's priorities on the issue.

3.6.1 Bladder cancer and DBP exposure

To calculate the society's benefits from installing online monitoring sensors, it is important to target the number of new cases of bladder cancer that can be attributed to DBP exposure. The American Cancer Society, 2019 estimates 1,910 new bladder cancer cases in Washington state in 2019. SPU provides drinking water to 1.4 million people, which

is about 19 percent of the Washington state citizens. Assuming equal distribution, that yields 363 annual new bladder cancer cases in 2019.

The US EPA published in 2005 *Economic Analysis for the Final Stage 2 Disinfectants and Disinfection Byproducts Rule* (US EPA, 2005a, US EPA, 2005b). In the economic analysis, quantification of bladder cancer risk for individuals exposed to DBPs was calculated using Population Attributable Risk (PAR). Equation (3.2) defines PAR as:

$$PAR = \frac{\text{Attributable cancer cases}}{\text{Total cancer cases}} \tag{3.2}$$

The US EPA analysis used the Villanueva et al., 2004 pooled data analysis as an approach to quantify estimates for bladder cancer risk. In the Villanueva et al., 2004 study, the PAR for an average TTHM level >25-50 μg/L is found to be 17.1 percent (US EPA, 2005a). This is the TTHM level for the Seattle system and is used to estimate the annual new bladder cancer cases attributed to DBP exposure (defined as x in Equation (3.3)):

$$PAR = \frac{x}{363} \tag{3.3}$$

$$0.171 = \frac{x}{363} \tag{3.4}$$

$$x = 0.171 \times 363 \tag{3.5}$$

$$x = 62 \tag{3.6}$$

From Equation (3.6), the estimated annual new bladder cancer cases attributed to DBP exposure in the Seattle Water System is 62.

In this CBA, a linear relationship is assumed between the average DBP concentration and the number of bladder cancer cases attributable to DBPs. This implies if the average DBP concentration decreases by 10 percent, there will be a similar reduction in the annual cases of bladder cancer attributable to the DBP exposure. The same linear relationship assumption was made in the US EPA's economic analysis (US EPA, 2005b).

3.6.2 The CBA steps

The steps of a modern CBA is presented in Figure 2.7 and the following assumptions are made for each step in this analysis:

1. **Specify the set of alternatives.**
   This analysis has two alternatives:

   (a) Implementing the online monitoring sensors in the distribution system.

   (b) Keeping today's status quo, i.e. not implementing the online monitoring sensors.

   Because the analysis includes both an infrastructure project and public health policy, the time period for the analysis is 10 years.

2. **Determine standing.**
   By determining standing one decide whose benefit and cost count. This analysis has a a provincial perspective meaning the only cost and benefits accounted for are the Seattle residents, including the cost and benefits for the Washington state.

3. **Catalogue impacts and select measurement indicators.**
   Impacts are defined as the anticipated benefits and cost from of the alternatives. The choice of measurement indicators depend on data availability and ease of monetization. The impacts and measurement indicators for this analysis are further discussed in subsection 3.6.3.

4. **Predict the impacts quantitatively over project lifetime.**
   By predicting the impacts for each alternative one quantifies all impacts for each alternative for the chosen time horizon. The predicted impacts are further discussed in subsection 3.6.4.

5. **Monetize all impacts to present value.**
   The monetized impacts are further discussed in subsection 3.6.5.

6. **Discount benefits and costs to obtain present value.**
   The SDR used for this CBA is 3 % and 7 % for comparison reasons.

7. **Compute the NPV of each alternative.**
   The NPV computed for each alternative are discussed in the result subsection 4.3 and the calculation for scenario 2 is presented in Appendix E.1.

8. **Perform a sensitivity analysis.**
   Python 3.7.3 was used as a tool to perform the sensitivity analysis. The sensitivity analysis is further discussed in subsection 3.6.6.

9. **Make a recommendation.**
   The recommendation for the city of Seattle is based on the NPV for each alternative and the sensitivity analysis.

Because alternative b) is maintaining the status quo, only alternative a), implementation of the online monitoring sensors, is discussed in the following subsections.

3.6.3 Step 3: Catalogue impacts and select measurement indicators

Step 1 and step 2 in the CBA are defined in subsection 3.6.2. This subsection discusses step 3, the impacts the alternative a) is expected to have on the utility and society. The measurement indicator for this CBA is the number of new annual bladder cancer cases.

Impact on the utility

When cataloguing impacts, the first subject to evaluate is the link between the information the online monitoring sensors provide and the response of the utility. In this analysis it is assumed that the sensors are 100 percent accurate for simplicity, even though this is not always the case.

Based on the DBP analysis, it is expected to have excessive DBP levels twice a year, one DBP spike event at each DWTP. The Cedar DWTP usually experiences a high DBP spike every spring while Tolt experience a high DBP spike every fall. If the DBP concentration in the system exceeds 75 percent of the MCL set by the NPDWR, SPU start making changes to the operation at the DWTP and pay close attention to the DBP development.

Table 3.5 and 3.6 present the probability of cause for the DBP spike at each DWTP. The probabilities are estimated based on SPU's experience with DBP spikes (L Kirby 2019, personal communication, 18 June). When the sensors notify the utility of the problematically large DBP concentrations in the distribution system, there are several actions the SPU can take to lower the DBP concentration. The easiest action to carry out is to lower the detention time of the water in the reservoir by pushing more water though the system. A second action is lowering the chlorine dose. A third action for Cedar DWTP is to switch the water source from Lake Youngs to the river or vice versa. For Tolt DWTP, a third action is to optimize coagulation to remove NOM. The last

action is to reduce drinking water production at one DWTP and rely on the other DWTP.

Table 3.5: Probability for DBP spike causes at Cedar DWTP.

Cause of DBP spike	Probability of cause
Change of water source	0.8
Algae	0.1
Unknown	0.1

Table 3.6: Probability for DBP spike causes at Tolt DWTP.

Cause of DBP spike	Probability of cause
Drought followed by heavy rainfall	0.5
Landslides in watershed	0.3
Coagulation not optimized	0.1
Unknown	0.1

Which action(s) SPU chooses to carry out to reduce the DBP concentration depends on the cause and feasibility of the action to be carried out. Due to the complexity of the distribution system and uncertainties around the cost for each action, the cost for implementation for each action is not considered in the CBA.

Impact on the society

The predicted impacts from implementing alternative a) for the society is a lower risk of getting cancer or other chronic illnesses from decreased DBP exposure. This leads to saved cost for the society for cancer and/or other medical treatment. In addition, the business hours and tax money saved from people not getting sick-leave from work. As mentioned, bladder cancer is the only health risk considered in this analysis.

3.6.4 Step 4: Predict impacts quantitatively over project lifetime

By implementing the online monitoring sensors in the distribution system, it is expected that SPU can detect higher DBP concentrations earlier in the distribution system and therefore decrease the overall DBP concentration over time.

Three possible scenarios are considered when predicting the online monitoring sensors impact quantitatively over the project lifetime. The implementation of sensors are assumed to result in the following scenarios:

- *Scenario 1: 10 percent reduction in the overall DBP concentration.*
- *Scenario 2: 20 percent reduction in the overall DBP concentration.*
- *Scenario 3: 30 percent reduction in the overall DBP concentration.*

The effect of the individual three scenarios will be further considered in the CBA.

3.6.5 Step 5: Monetize all impacts to present value

Cost associated with bladder cancer risk

The US EPA's Cost of Illness Handbook defines society's total WTP to avoid an illness as the best evaluation measurement for a CBA. This includes all societal costs associated with avoiding an individual's illness: medical cost, work-related cost, educational cost, cost of support services required by people needing medical attention and the willingness of individuals to pay to avoid the health risk (Office of Pollution Prevention and Toxins, 2007).

However, it is difficult to make realistic estimate for many of these categories. Therefore, analysts use alternative measures to calculate the cost saved. Direct medical cost is the most used measure for lower-bound estimate of avoiding illness. The monetary information for bladder cancer used in the CBA is adapted from the Cost of Illness Handbook and only provides the lower-bound estimate for society's WTP. To convert the 1996 dollar value given in the Cost of Illness Handbook, the Consumer Price Index (CPI) Table from US Bureau of Labor Statistics was used to calculate the CPI multiplier (Bureau of Labor Statistics, 2015).

Cost associated with online monitoring sensors

The sensors evaluated in this analysis are spectroscopic UV absorbance sensors. There are four main expenses to consider when evaluating the cost of the online monitoring sensors: the cost of the sensors themselves, the implementation and IT integration cost (using the SCATA system), the cost of cabinet installation and the cost of maintenance.

Even though the time period of the analysis is 10 years, the online monitoring sensors sensors are still of value at the end of this analytical period. However, compared to the value of reducing the bladder cancer rate, the value of the sensors are negligible.

The last cost to consider is the excess burden of taxation, also known as the opportunity cost of public funds. Local government projects funded through taxes will have increased dead-weight loss, called Marginal Excess Tax Burden (METB). METB is the change in dead-weight loss resulting from raising an additional dollar of tax revenue and is the dead-weight caused by how taxes distort the market they are levied on. With respect to local government projects, the marginal tax source is viewed as the property tax. For this CBA, it is assumed that the whole project is funded by local tax revenue.

3.6.6 Step 8: Perform a sensitivity analysis

The last analytical step of the CBA is to conduct a sensitivity analysis to test the monetary value of the impacts. The sensitivity analysis was conducted in Python 3.7.3 by three main functions: the variable distribution function, the NPV distribution function and the p-value function. The sensitivity analysis was conducted for a SDR of 3 % and a SDR of 7 %.

The variables are presented by either a Poisson, triangular or normal distribution, depending on their lower and upper bounds. The NPV distribution calculated is based on the variable distribution. The number of iterations for the variable distribution function were 10,000 and 100,000 for the NPV distribution function. The p-value function calculates the probability that the NPV is less than zero and prints histogram distributions for the p-value, NPV mean and the NPV standard deviation.

The results from the CBA is presented in section 4.3.

4

Results

In this Chapter, the results from the data processing methods described in section 3.5 are presented, based on which the placement of the online monitoring sensors in the distribution system is decided. At the end of the Chapter, the results and sensitivity analysis from the CBA are presented.

4.1 Data Analysis of Seattle Water Distribution System

The following section includes the results obtained from the application of data processing methods. The first subsection presents the minimum, maximum and average concentration of THM and HAA at the sampling sites. In the following subsection, the online monitoring UVA data is presented, followed by the outcomes from Python, Unscrambler and the ANN model.

4.1.1 DBP concentration at sampling sites

Figure 4.1 presents the DBP concentration at each individual sampling site from 2008-2018. The green and blue lines represent the THM and HAA concentrations respectively. The sampling sites C-3, C-5, T-1, T-3, T-6 and T-7 are missing data from 2008-2011. As observed in Table 4.1-4.4, the Cedar sampling sites have the highest HAA peaks as compared to the Tolt sampling sites with highest THM peaks.

Table 4.1-4.4 present the minimum, maximum and average THM and HAA concentrations for Tolt and Cedar DWTP. Figure 4.1 show longitudial graphs for the data presented in Table 4.1-4.4.

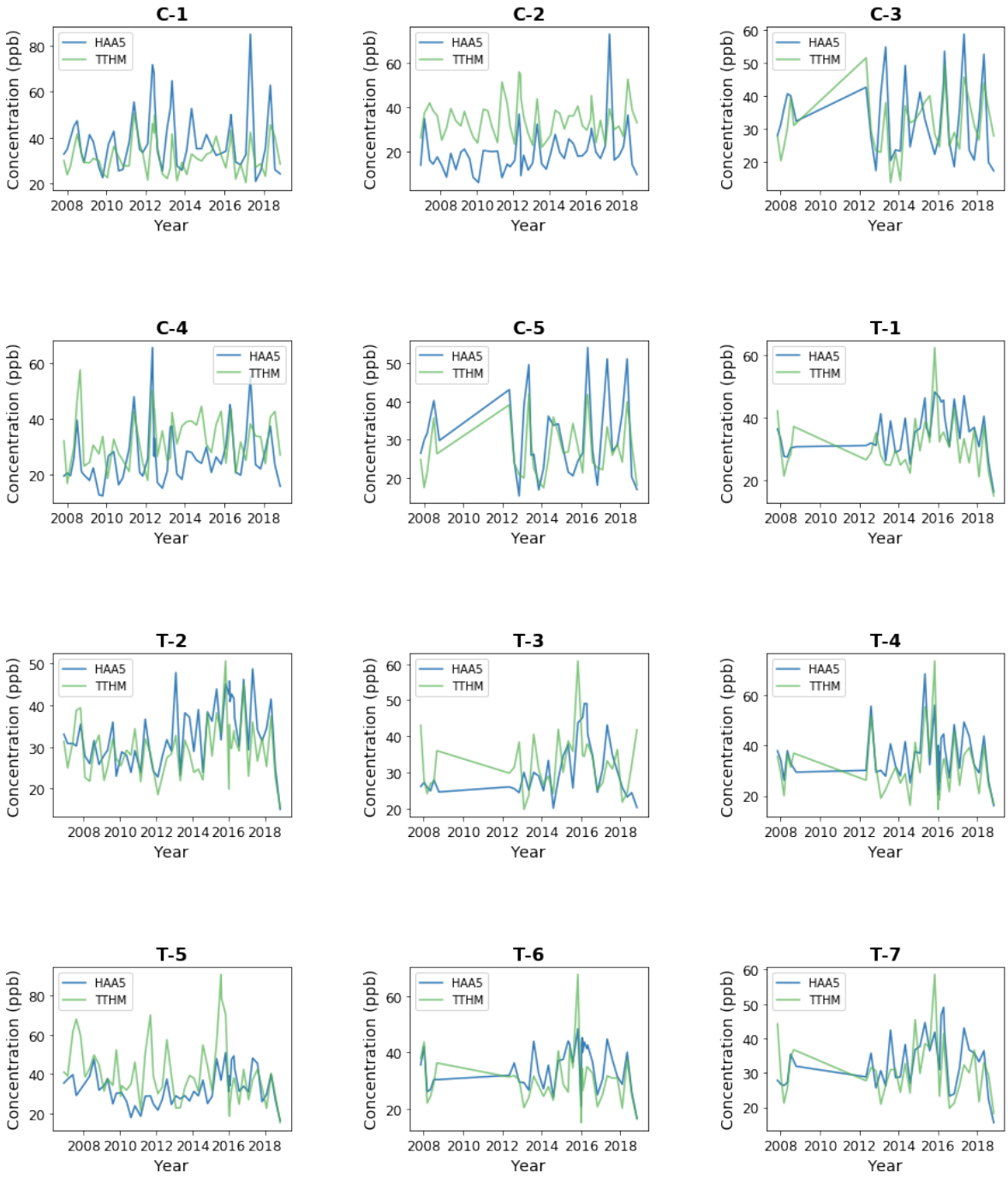

Figure 4.1: DBP concentration at the sampling sites from 2008-2018.

Table 4.1 and 4.2 present the min, max and average DBP concentration at Tolt DWTP. From the two tables, one can observe that the average HAA concentration is a bit higher than the average THM concentration at the sampling sites. However, the maximum concentration for THM is higher than for HAA, the THM peaks at T-4, T-5 and T-6 being particularly high.

Table 4.3 and 4.4 present the minimum, maximum and average DBP concentration at Cedar DWTP. The THM average for sampling site C-1 to C-5 is approximately 30 μg/L. The HAA average for sampling site C-1 to C-5 varies from around 20 μg/L to 40 μg/L. On the other hand, at the Tolt sampling sites, the maximum concentration for HAA is higher than for THM for Cedar. The sampling sites C-1 and C-2 have the highest measured HAA peaks at 85.2 μg/L and 72.8 μg/L, respectively.

Table 4.1: Minimum, maximum and average HAA concentration (in μg/L) for Tolt DWTP from 2008-2018.

HAA concentration	Sampling site						
	T-1	**T-2**	**T-3**	**T-4**	**T-5**	**T-6**	**T-7**
Max	48.3	48.6	49	68.2	50.8	48.4	49
Min	16.1	15.1	20.1	16	16.2	16.5	15.5
Average	35	33	30.6	36	32.8	34.8	33

Table 4.2: Minimum, maximum and average THM concentration (in μg/L) for Tolt DWTP from 2008-2018.

THM concentration	Sampling site						
	T-1	**T-2**	**T-3**	**T-4**	**T-5**	**T-6**	**T-7**
Max	62.6	50.5	60.8	73.3	90.7	67.8	58.6
Min	14.9	15.6	19.8	14.6	15.1	14.9	18.2
Average	31	29	32.5	31.4	39.9	30	30.9

Table 4.3: Minimum, maximum and average HAA concentration (in μg/L) for Cedar DWTP from 2008-2018.

HAA concentration	Sampling site				
	C-1	**C-2**	**C-3**	**C-4**	**C-5**
Max	85.2	72.8	58.1	65.8	54.2
Min	20.8	6.2	17.1	12.1	15.1
Average	39	19.8	32.8	26.4	31.3

Table 4.4: Minimum, maximum and average THM concentration (in μg/L) for Cedar DWTP from 2008-2018.

THM concentration	Sampling site				
	C-1	**C-2**	**C-3**	**C-4**	**C-5**
Max	50.4	55.8	51.4	57.7	42
Min	20.3	22	13.1	16.6	17.2
Average	31.8	34.4	31.5	32.5	27.6

4.1.2 The online monitoring at Cedar DWTP

The use of the online monitoring sensors are described in subsection 3.3.1 and the assessment of the data from the sensors are described in subsection 3.5.2. The UVT of the water is measured at Landsburg before it flows to Lake Youngs reservoir where it has a detention time of six months. Further, the water is transferred in two trains, Train 1 and Train 2 at Cedar DWTP, where the UVT is measured at both trains after ozonation. Figure 4.2 shows the UVA at Landsburg and the UVA at treatment Train 1 and 2 at Cedar DWTP from 2012-2014.

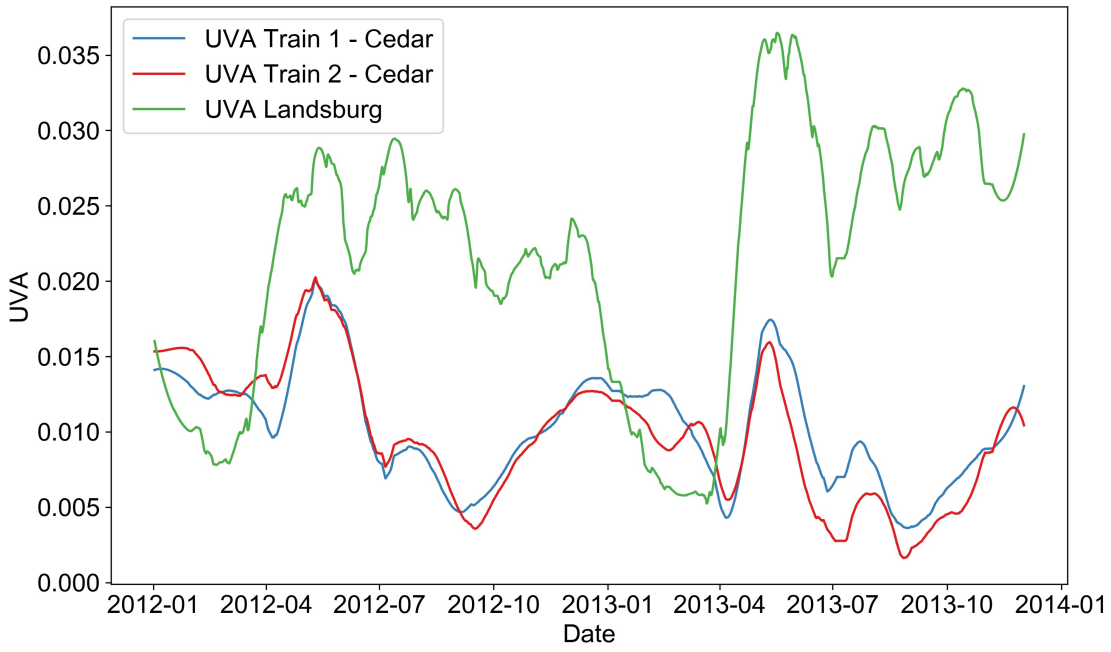

Figure 4.2: Online monitoring UVA data from Landsburg, Train 1 and Train 2 at Cedar DWTP from 2012-2014.

As shown in Figure 4.2, the drinking water measured at Landsburg has a higher UVA value than Train 1 and 2. The UVA fluctuates and is highest in spring for Train 1 and 2. Figure B.1 in Appendix B.1 presents the online monitoring UVA data from Landsburg and Train 1 and 2 at Cedar DWTP from 2015-2017. Figure B.1 illustrates that the sensors can be prone to failure over a longer time period, as the graphs from April to June 2015 and October to December 2015 are horizontal.

4.1.3 Data analysis using Python

The following subsection presents the results from the MLR graphical representation conducted in Python. The graphs presented in this subsection uses site C-1 and HAA prediction as an example. In Appendix B.2, the same graphs for site C-1 and THM prediction are presented.

pH

Figure 4.3 represents a scatterplot of pH and HAA concentration (parts per billion) from 2008-2018. The pH is measured at the sampling site on the same date as the HAA measurement, and ranges from 7.5 to 8.5. As seen in Figure 4.3, the scatterplot shows no clear relationship between the HAA concentration and pH at site C-1.

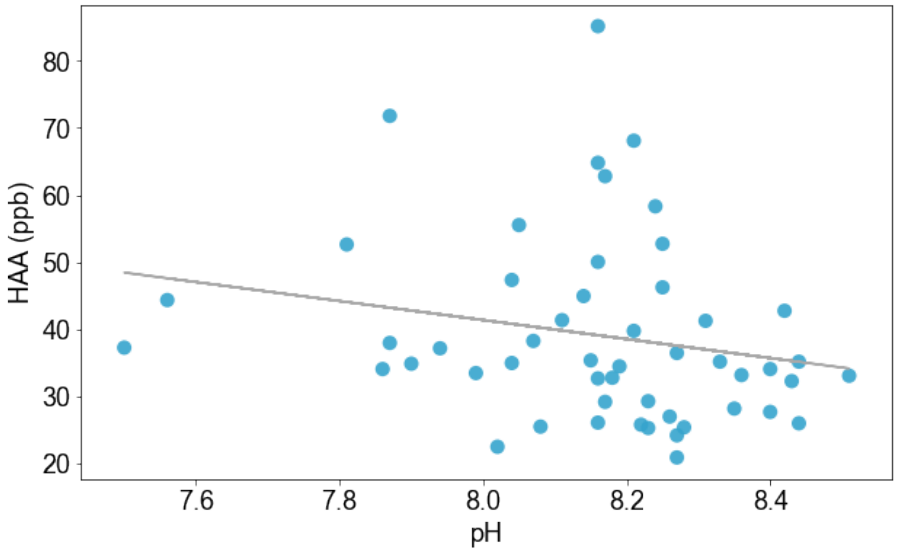

Figure 4.3: Scatterplot pH and HAA at sampling site C-1 from 2008-2018.

Temperature

Figure 4.4 represents a scatterplot of temperature and HAA concentration from 2008-2018. Similarly, the temperature is measured at the sampling site on the same date as the HAA measurement, and the temperature ranges from around 6.5 to 22.5 ° C. Synonymous to Figure 4.3, Figure 4.4 also depicts no clear relationship between HAA concentration and temperature at site C-1.

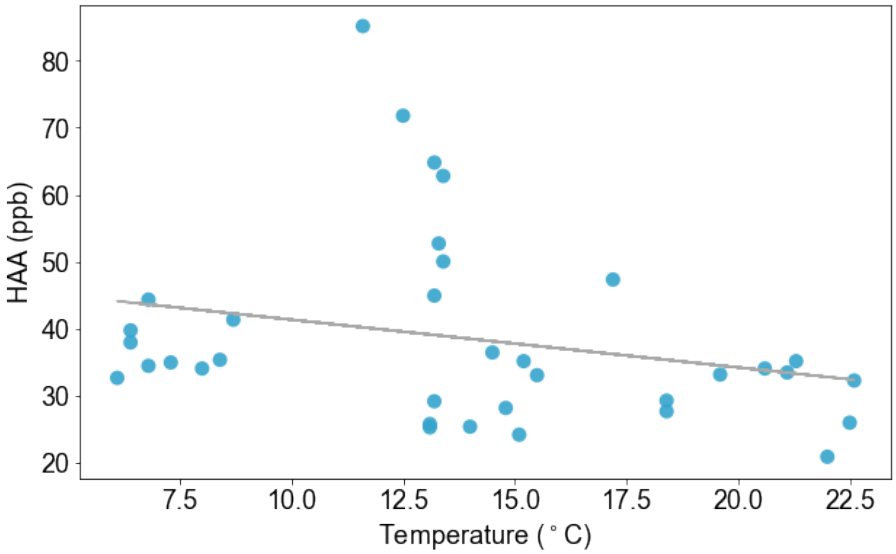

Figure 4.4: Scatterplot temperature and HAA at sampling site C-1 from 2008-2018.

TOC

Figure 4.5 represents a scatterplot of TOC and HAA concentration from 2008-2018. The TOC is measured at Cedar DWTP while the HAA is measured at sampling site C-1. To develop a reasonable analysis with the data available, the closest sampling date for HAA was matched with the closest sampling date for TOC. The TOC concentration ranges from around 0.65 to 1.1 mg/L. In Figure 4.5, one can see a trend for higher HAA concentrations proportional to higher TOC concentrations, but the relationship is not significant.

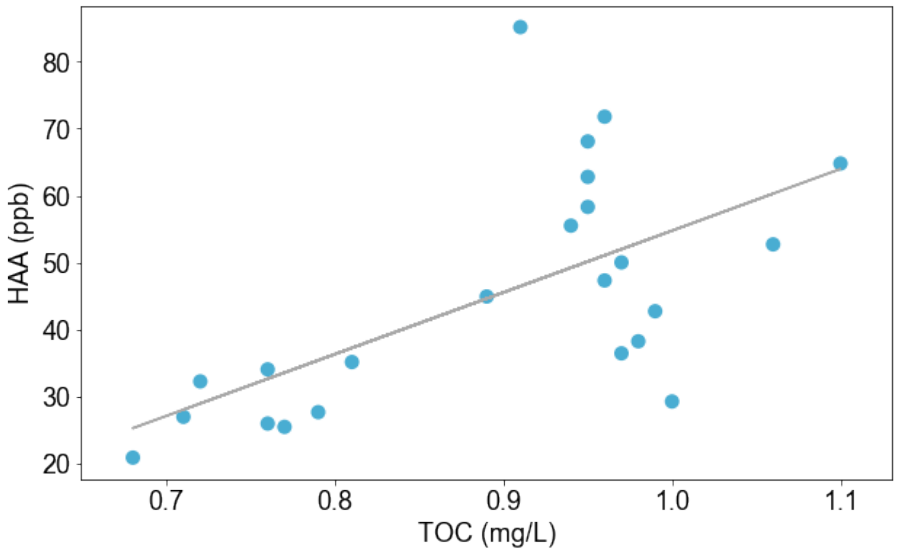

Figure 4.5: Scatterplot TOC and HAA at sampling site C-1 from 2008-2018.

The figures in Appendix B.3 contain the scatterplots for THM/HAA and TOC for all the sampling sites in the distribution system. For the Tolt data T-4 to T-8 in Figure B.6 and B.7, there is no clear relationship between DBP concentration and TOC concentration. For the Cedar and the remaining Tolt data (T-1 to T-3), the trend line shows a tendency for higher DBP levels at a higher TOC level. From Figure B.6 and B.7, it is clear that the TOC concentration in Tolt water is higher than that in Cedar.

UVA

For the N-days iteration model described in subsection 3.5.2, the summer months are defined as May, June, July and August and the winter months are November, December, January and February. The objective with the N-days iteration model is to check for correlation between 'n' number of preceding days from the date of DBP measurement and UVA.

The 'n' number of days tested in the model was 30. Figure 4.6 and 4.7 show the best result for the N-days iteration model for sampling site C-1. In Figure 4.6, which represents UVA and HAA in summer months, the best correlation obtained was R^2= 0.81, at n=6. The UVA ranges from around 0.006 to 0.02, while the HAA concentration ranges from around 20 μg/L to 85 μg/L.

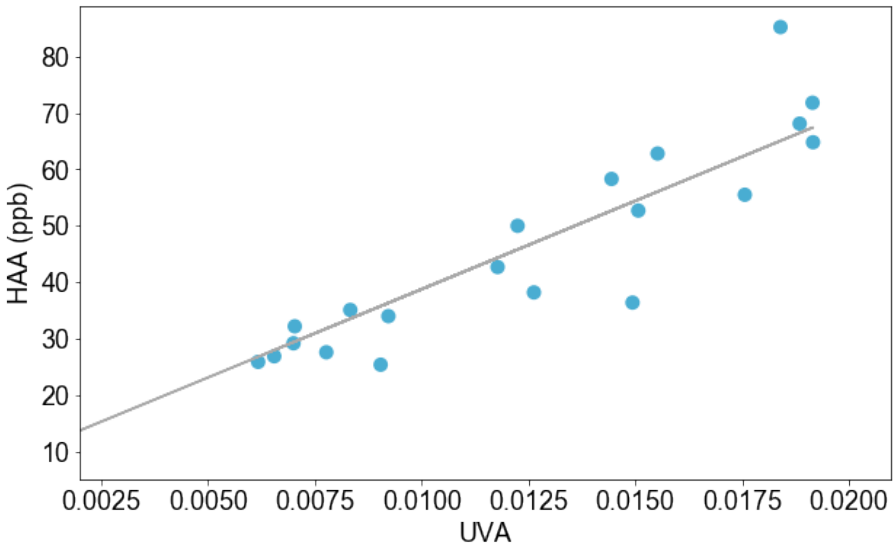

Figure 4.6: Scatterplot of UVA and HAA data for summer months at sampling site C-1 from 2008-2018.

In Figure 4.7, which represents UVA and HAA in winter months, the best correlation obtained was R^2= 0.55, at n=4. The UVA ranges from around 0.005 to 0.02 while the HAA concentration ranges from around 25 μg/L to 45 μg/L.

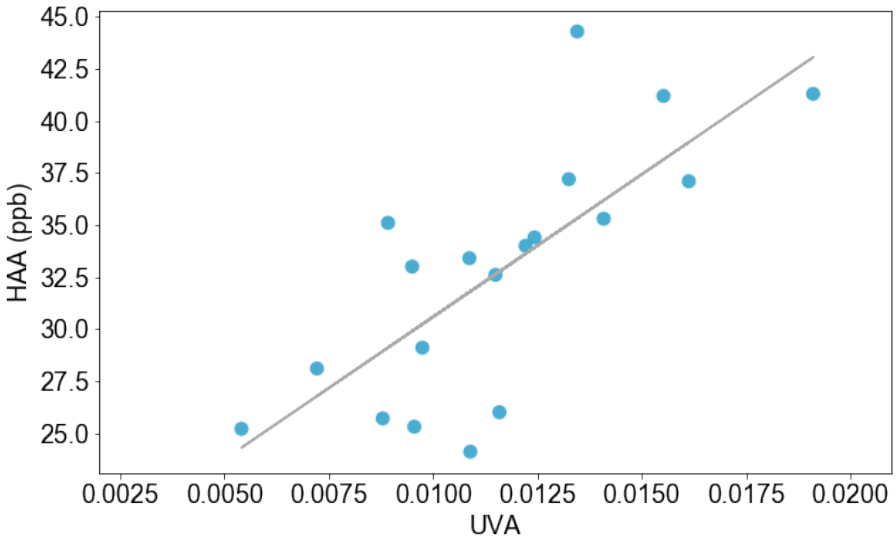

Figure 4.7: Scatterplot of UVA and HAA data for winter months at sampling site C-1 from 2008-2018.

4.1.4 Data analysis using Unscrambler

The following subsection presents the result from the Unscrambler analysis. The analysis covers qualitative PCA followed by quantitative PLSR. This analysis was applied to the

Cedar DWTP data only. Firstly, the entire data set (sampling sites C-1 to C-5) was modelled, which produced a poor result with a calibrated R^2 around 0.4 and 0.47 for THM and HAA, respectively.

To improve the outcome of the model, separate models were created for each site. The graphs presented in this subsection use site C-1 and THM prediction. Appendix C.1 contains the graphs for site C-1 and HAA prediction.

PCA

The data was first analyzed with the PCA. Figure 4.8 represents the total loading mean variables in a loading plot. The loading plot is useful to understand the correlations between the variables.

The variance in the data is explained by the Principal Component (PC). In this analysis, PC1 is based on the variances of water quality parameters. PC2 is mostly based on the variances of dimensions like plant-site distance and number for reservoirs. As shown in Figure 4.8, the variance in the data is described by 24 % with PC1 and 18 % with PC2. In total, with two PCs, the variance is described by 42 % for this model.

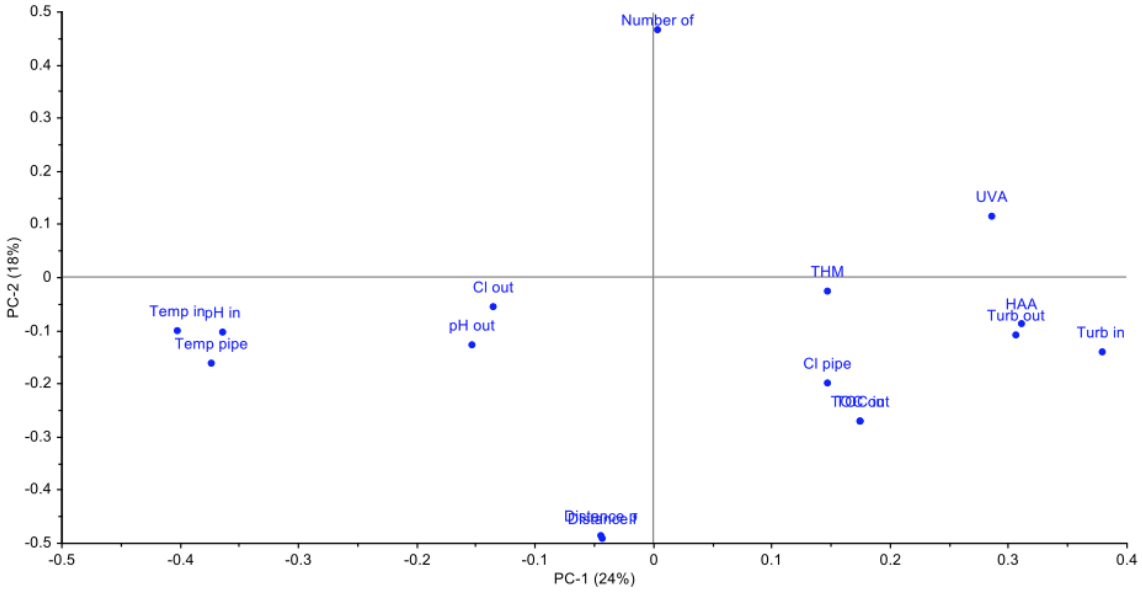

Figure 4.8: Loading plot for the PCA.

From Figure 4.8, one can observe that some loadings tend to correlate. The loadings UVA, HAA, turb in and turb out are located on the far right for the PC1 axis which

indicates correlation. Located on the far left on PC1, temp in, temp pipe and pH in indicate a correlation on the other side of the scale. For PC2, number of reservoirs is the most important loading.

Table C.1 represents the loadings for the two PCs. PC1 shows the covariance between HAA, turb in, turb out, UVA, TOC, THM, Cl pipe and is negatively associated with Cl out, pH out, pH in, temp in and temp pipe.

Figure 4.9 is a bioplot graph where variables (red) and samples (blue) are represented in the same plot. The bioplot shows the relationship between the variables and samples. For instance, samples R21, R25, R11 and R12 have the highest values of turb in, turb out, TOC in and Cl pipe, but lower values of temperature and pH. While R26 and R35 have high values of temperature and pH, but low values for turb in, turb out, TOC in and Cl pipe.

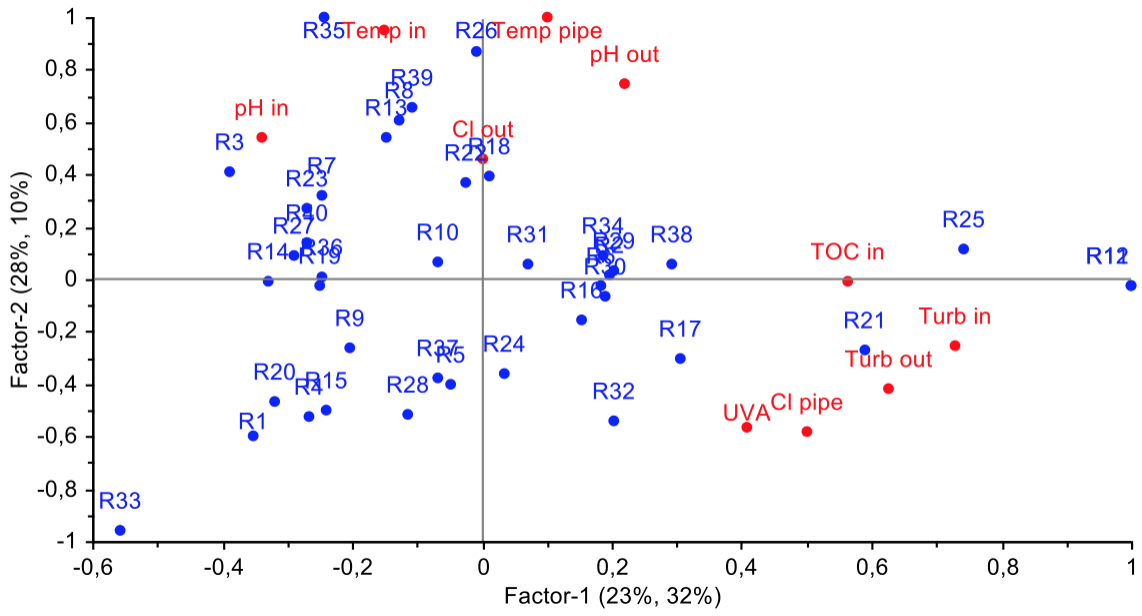

Figure 4.9: Bioplot for site C-1 and THM prediction.

In Figure 4.9, most of the samples are clustered around the center of the graphs, indicating a weak relationship between the variables and the samples.

The loading plot presented in Figure 4.10, plots both predictors (X) and response (Y). In this case, the predictors are the variables and the response is the THM concentration. Based on the results from Figure 4.10, THM has the highest correlation with TOC in for site C-1.

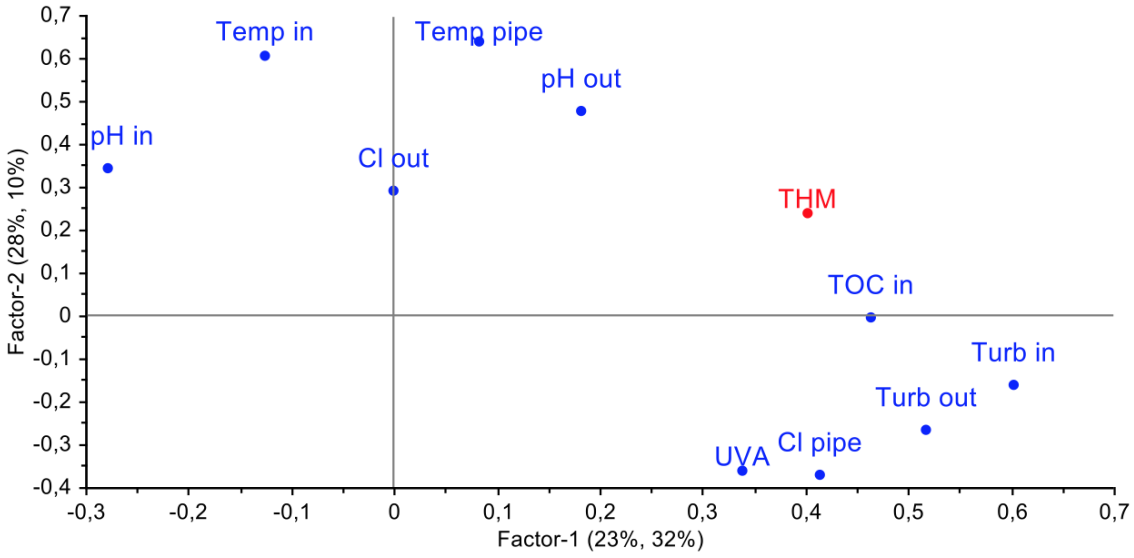

Figure 4.10: Loading plot for site C-1 and THM prediction.

PLSR

The second part of the Unscrambler analysis is the PLSR. In the PLSR, the R^2 value is applied to all prediction versus reference plots.

Figure 4.11 shows the prediction versus reference plot. The blue line is the predicted calibration and the red line is the cross-validation. The target line is marked in black which depicts a 100 % correlation. Ideally, all dots should fall on this line. However, the predicted R^2 for calibration with 4 factors is 0.55 for the data in Figure 4.11. The cross-validation R^2 is even lower at a 0.23.

If one would attempt to predict the THM concentration from the model presented in Figure 4.11, it would be a very rough estimation. For instance, if one were to predict a THM concentration of 22 μg/L (Reference Y axis), the predicted value would be roughly 27 μg/L (Predicted Y axis). On the other side, if one were to predict a THM concentration of 51 μg/L (Reference Y axis), the model would predict a THM concentration of 35 μg/L. Both examples are marked with green circles in Figure 4.11.

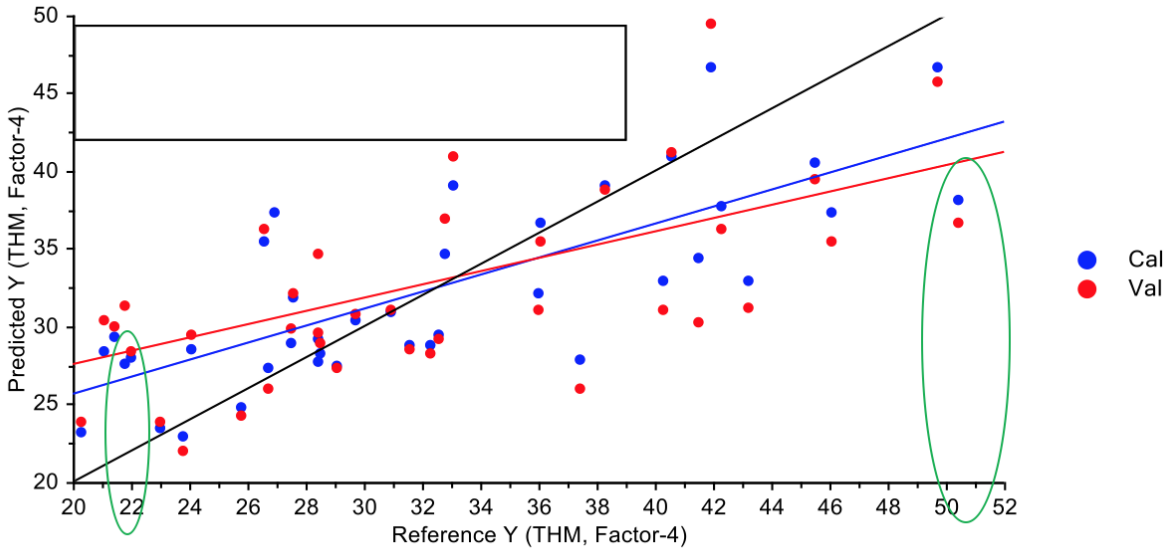

Figure 4.11: Prediction versus reference plot for site C-1 and THM prediction.

Figure 4.12 represents the prediction versus reference plot by samples. The blue line is the predicted calibration, the red line is the cross-validation and the green lines are the reference (real measured) values. The figure indicates the samples that are failed to be predicted by the model and the degree of that failure. For instance, for sample R6 the model predicts a THM concentration of roughly 35 μg/L, while the real samples measured a THM concentration of over 50 μg/L.

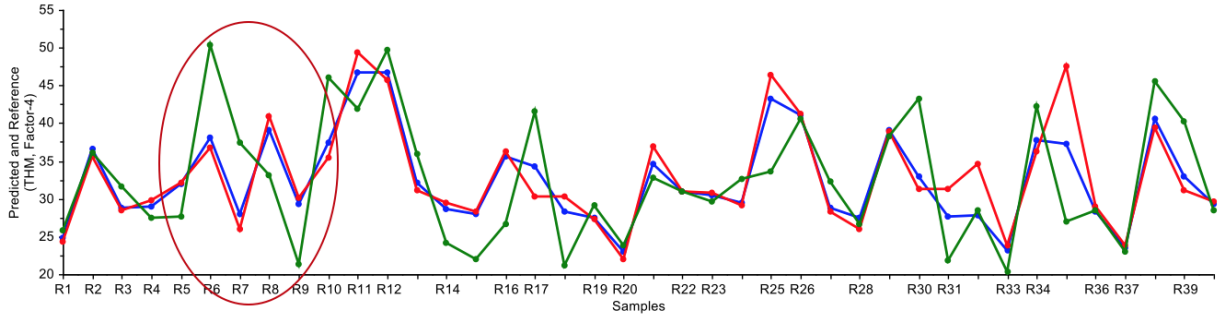

Figure 4.12: Prediction vs reference plot by samples for site C-1 and THM prediction.

As one can observe from Figure 4.12, the prediction follows a trend, but multiple samples are predicted with a high error (e.g. as marked by the red circle). The model is decent at predicting the trends, but fails to predict the THM peaks.

4.1.5 Data analysis using the ANN model

The ANN model was only tested for Cedar DWTP. The data parameters from the inlet of the DWTP were daily averages of UVA, TOC, pH, temperature, turbidity and chlorine concentration. For the outlet of the DWTP, the daily averages of TOC, pH, turbidity and chlorine concentration were used in the ANN model. The other data parameters added were THM and HAA concentration at the five sampling sites for Cedar water (and their site specific chlorine concentration and temperature).

Additional information added to the model were distance from DWTP to sampling site, distance from the last re-chlorination reservoir to sampling site, the number of reservoirs involved from DWTP to the sampling site and the estimated detention time in the reservoirs.

In the ANN model, 'n' is the number of neurons in the hidden layer of the ANN model. Increasing 'n' adds more mathematical functions in the network which improves the chances of fitting more complex data into the model. The target is the real values of THM or HAA used while creating the model, shown on the x-axis. The output refers to the THM or HAA values predicted by using the ANN model. The output in Equation (4.1) is defined as:

$$Output = Slope \times Target + Intercept \tag{4.1}$$

To use as a reference point, a perfect model is obtained with a slope = 1 and an intercept = 0 (See dashed lines in figures). However, this is never achieved.

For this model, the division for Training:Validation:Testing was 75%:15%:10%. The number of samples from Cedar DWTP were 176. Appendix D.1 contains the graphs for THM and HAA for n=2 and n=6. From the figures in Appendix D.1 and below, one can observe an interesting development in the All R^2 value for THM and HAA. For THM, the All R^2 value for n=2, n=6, n=10, is 0.59, 0.84 and 0.86, respectively. For HAA, the All R^2 value for n=2, n=6, n=10, is 0.81, 0.86 and 0.85, respectively.

For using the model on THM, the All R^2 value increased with the number of neurons while for HAA All R^2 was quite precise at n=2 and actually lower for n=10 than n=6.

Figure 4.13 and 4.14 presents the result from the ANN model using n = 10. As seen in the figures, there is a R^2 for training, validation, testing and All. The R^2 for All is a combination of training, validation and test. This value provides a composite measurement for the model which includes the model fit, overfitting avoidance and

repeatability of the model. Figure 4.13 and 4.14 have similar R^2 values with All R^2 =0.86 for THM and All R^2 = 0.85 for HAA. A R^2 value above 0.8 in this case, is considered a good model fit.

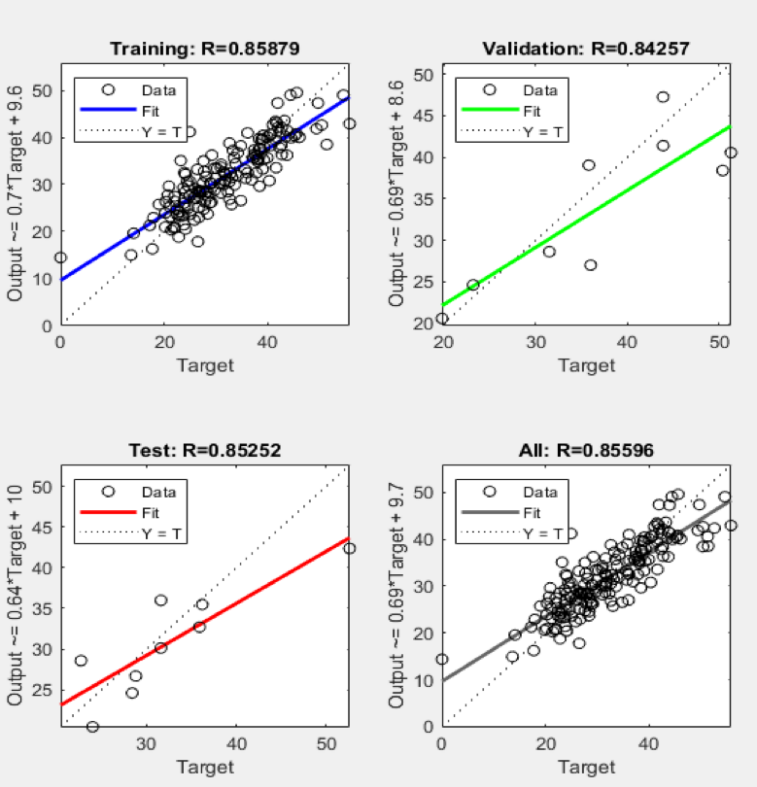

Figure 4.13: ANN model for THM with n=10.

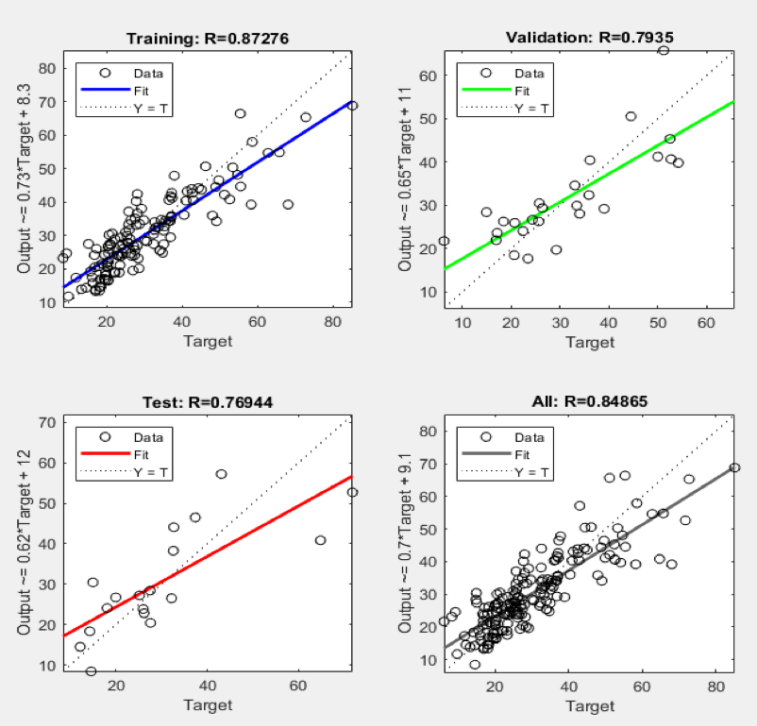

Figure 4.14: ANN model for HAA with n=10.

4.2 Implementation of Online Monitoring Sensors

Based on the DBP concentrations presented in subsection 4.1.1 and the distribution system described in Chapter 3, the following proposal is made for the implementation of online monitoring sensors. The proposal is primarily for the Seattle Regional Water Supply System, but can be used as a template for other water utilities.

The sensors recommended for implementation are spectroscopic UV absorbance sensors. The sensors are mainly employed to acquire data for DBP predicting models which are described in section 2.6. The most critical point to implement sensors are in the DWTP. Three sensors should be implemented at each DWTP: one at the inlet of the DWTP (before ozonation), one sensor post ozonation and the last sensor in the clearwells after chlorination.

For a distribution system, it is suggested to implement three sensors per DWTP. The first sensor is to be placed to the nearest site sampling point to the DWTP. The other two sensors should be placed at to different points in the extremities of the distribution system where the DBP concentration tends to be the highest.

In total, there is a need for 12 online monitoring sensors to provide a full image for the DBP formation both at the DWTP and the distribution system. It is critical that the UV absorbance sensors have an extremely high precision to ensure a good fitting DBP prediction modelling.

4.3 Cost Benefit Analysis

This section describes the results and the sensitivity analysis from the CBA. The main assumption in the CBA is that the implementation of online monitoring sensors will reduce the overall DBP concentration and thus, reduce the number of new annual bladder cancer cases. For each scenario, the following reduction in bladder cancer cases are estimated based on the methods and assumptions discussed in subsection 3.6.1:

- *Scenario 1: 10 percent reduction in the overall DBP concentration.*
  This constitutes a reduction in 6 new bladder cancer cases, ending up with a total of 56 new annual bladder cancer cases.

- *Scenario 2: 20 percent reduction in the overall DBP concentration.*

This constitutes a reduction in 12 new bladder cancer cases, ending up with a total of 50 new annual bladder cancer cases.

- *Scenario 3: 30 percent reduction in the overall DBP concentration.*
  This constitutes a reduction in 19 new bladder cancer cases, ending up with a total of 43 new annual bladder cancer cases.

4.3.1 Monetization of benefits

The CPI multiplier used in the CBA is 1.63 and was calculated using the CPI Table (Bureau of Labor Statistics, 2015). Table 4.5 represents the cost of bladder cancer treatment in 1996 US dollar value (from Office of Pollution Prevention and Toxins, 2007) and the calculated cost in 2019 dollar for survivors, non-survivors and the average bladder cancer patient. The bladder cancer cost for each patient group is considered a "life-time" cost and therefore has a time horizon of 20 years.

Table 4.5: The medical cost in 1996 and 2019 dollar for bladder cancer for survivor, non-survivor and average patient at a SDR of 3 % and 7 %. Table adapted from Office of Pollution Prevention and Toxins, 2007.

Patient group	**SDR 3 % ($ 1996)**	**SDR 7 % ($ 1996)**	**SDR 3 % ($ 2019)**	**SDR 7 % ($ 2019)**
Survivors	148,149	120,132	241,483	195,815
Non-survivors	77,983	73,424	127,112	119,681
Average patient	131,081	107,811	213,662	175,732

As seen in Table 4.5, survivors of bladder cancer undergo more expensive treatment than non-survivors due to their ongoing maintenance and care. The cost of the average patient is estimated based on age of diagnosis, survival and mortality probabilities for each year post-diagnosis. For benefits in the CBA, the medical cost of the average patient is considered, and survivor and non-survivor costs are considered the upper and lower limits, respectively.

4.3.2 Monetization of cost

Table 4.6 presents the total cost for the online monitoring sensors over a 10-year lifetime. As discussed in section 4.2, there is a need for a total of 12 sensors in the Seattle water system. The cost for each sensor is set to be approximately $ 50,000 based on the online monitoring sensor market. For each sensor, implementation and IT integration cost is estimated to be $ 8,000 while the cabinet installation is $ 50,000 per sensor. These two costs are only valid for the sensors implemented in the distribution system, which includes a total of six sensors.

The maintenance cost was the only cost that needs to be discounted to Present Value (PV). The estimated monthly cost for maintenance of the sensors is $ 2,000, which constitutes a yearly cost of $ 24,000. To calculate the excess burden of taxation, a METB of $ 0.17 per dollar of revenue was multiplied with the total cost of the projects.

Table 4.6: Total cost for the online monitoring sensors over a 10-year lifetime with a SDR of 3 % and 7 %.

Cost	**SDR 3 % ($)**	**SDR 7 % ($)**
Purchase	600,000	600,000
Implementation + IT integration	96,000	96,000
Cabinet installation	300,000	300,000
Maintenance	228,725	192,566
Excess burden of taxation	208,203	202,056

4.3.3 Calculation of the NPV

Appendix E.1 provides further insight for the calculation of the NPV for a SDR of 3 % and 7 % for scenario 2. Table 4.7 and 4.8 presents the PV benefits, PV costs and the calculated NPV for each scenario.

Table 4.7: NPV for each scenario with a SDR of 3 %.

Scenario	PV benefits ($)	PV costs ($)	NPV ($)
1	1,281,972	1,432,928	-150,956
2	2,563,944	1,432,928	1,131,016
3	4,059,579	1,432,928	2,626,650

As shown in Table 4.7 and 4.8, the PV cost for each scenarios is constant regardless the benefits provided. The PV cost is the sum of all the costs presented in Table 4.6. The PV benefits increase for each scenario and are calculated using the cost for the average bladder cancer patient multiplied with the reduction of new bladder cancer cases for each scenario.

Table 4.8: NPV for each scenario with a SDR of 7 %.

Scenario	PV benefits ($)	PV costs ($)	NPV ($)
1	1,054,392	1,390,622	-336,231
2	2,108,783	1,390,622	718,161
3	3,338,907	1,390,622	1,948,285

The NPV equals the difference between the PV benefits and PV costs. The NPVs in Table 4.7 and 4.8 for scenario 1 are negative, while the NPVs for scenario 2 and 3 are positive. The basic decision rule for an alternative relative to the status quo, is to adopt the project if the NPV is positive (Boardman et al., 2006). Nonetheless, before making a final recommendation a sensitivity analysis has to be conducted.

4.3.4 Sensitivity analysis

This subsection presents the result of the sensitivity analysis which is described in subsection 3.6.6. The sensitivity analysis was conducted for all scenarios with a SDR

of 3 % and 7 %. The distribution for each variable tested in the sensitivity analysis is presented in Appendix E.3.

There are seven variables tested in the sensitivity analysis: the number of cancer cases avoided (n), the cost of cancer treatment (cc), the cost of investment sensors (cs), the cost of cabinet installation (cci), the cost of implementation and IT integration (cii), the cost of maintenance (cm) and the METB.

In addition to the traditional sensitivity analysis, the break-even for the number (n) of new cancer cases annual bladder cancer cases avoided was predicted using the same Python function. The break-even number represents the breaking point of the minimal amount of new annual bladder cancer cases avoided, where the NPV is negative more than 50 percent of the times when running the functions in Python.

Sensitivity analysis for SDR of 3 %

Figure 4.15 presents the results from the sensitivity analysis for scenario 2 with a SDR of 3 %. Histogram a) shows the distribution of the NPV, histogram b) shows the mean of the NPV, histogram c) shows the p-value for the mean, which is less than zero and histrogram d) shows the standard deviation of the NPV. The mean NPV in histogram b) in Figure 4.15 is around $ 700,000. The mean of the p-value, observed in histogram c), is 0.176. The standard deviation of the NPV, from historgram d), is $ 1,020,000.

The results for the sensitivity analysis for scenario 1 and 3 are presented in Appendix E.4. For scenario 1 (see Figure E.11), the mean of the NPV and p-value are -$ 470,000 and 0.825, respectively. The standard deviation of the NPV is $ 695,000. The results for scenario 3 are presented in Figure E.12. For scenario 3, the mean of the NPV and p-value are $ 2,060,000 and 0.007, respectively. The standard deviation of the NPV is $ 2,280,000.

Sensitivity analysis for SDR of 7 %

Figure 4.16 presents the results from the sensitivity analysis for scenario 2 with a SDR of 7 %. The mean NPV in histogram b) in Figure 4.16 is around $ 380,000. The mean of the p-value, observed in histogram c), is 0.281. The standard deviation of the NPV, from histogram d), is $ 720,000.

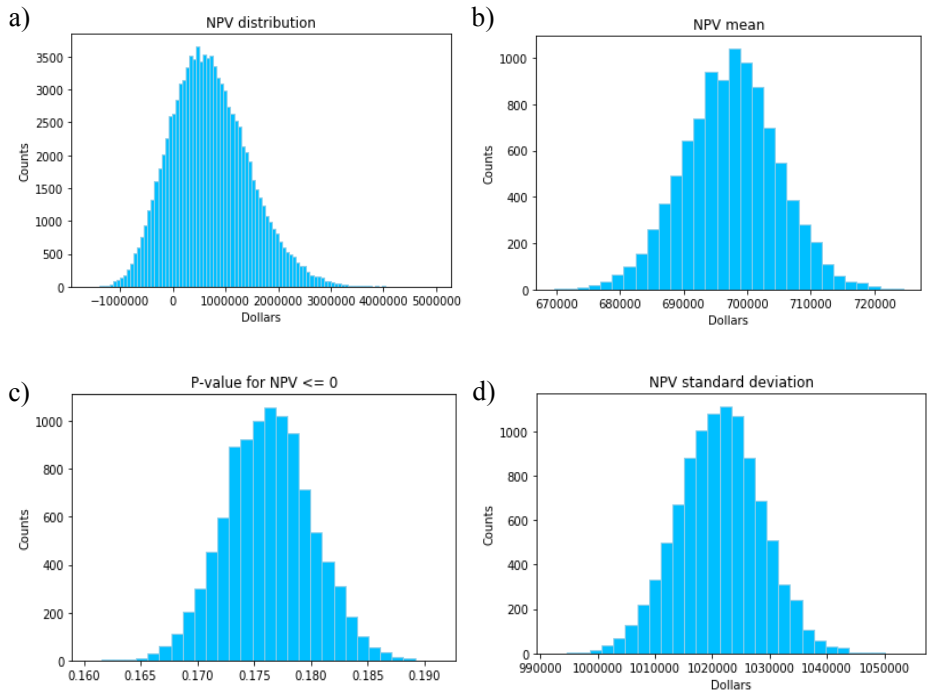

Figure 4.15: Results from the sensitivity analysis for scenario 2 with a SDR of 3 %. Histogram a): the NPV distribution, b) the NPV mean, c) the p-value for NPV<=0, d) the standard deviation for NPV.

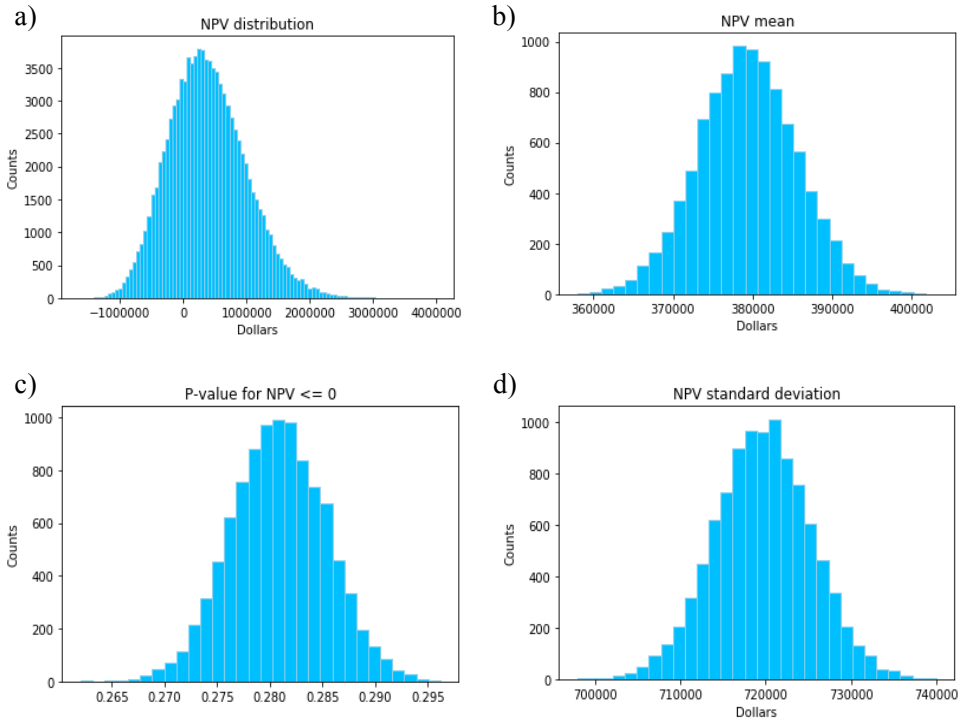

Figure 4.16: Results from the sensitivity analysis for scenario 2 with a SDR of 7 %. Histogram a): the NPV distribution, b) the NPV mean, c) the p-value for NPV<=0, d) the standard deviation for NPV.

The results for scenario 1 and 3 are presented in Figure E.13 and E.14, respectively. Figure E.13 shows that the mean of the NPV is -$ 605,000, the mean of the p-value is 0.91 and the standard deviation of the NPV is $ 740,000 for scenario 1. For scenario 3, presented in E.14, the mean NPV is $ 1,530,000, the mean of the p-value is 0.015 and the standard deviation of the NPV is $ 1,720,000.

Break-even number (n) of new annual bladder cancer cases avoided

The figures from testing the break-even number (n) of new annual bladder cancer cases avoided are presented in Appendix E.5. The break-even number represents the n that makes the p-value higher than 0.5, which indicates that the NPV is less than zero for more than 50 % of the cases.

The break-even number n for a SDR of 3 % is 8. The results from the break-even test is presented in Figure E.15. When n=8, the NPV mean is -$ 80,000, the p-value mean is 0.59 and the standard deviation of NPV is around $ 600,000. For a n=9, the NPV mean is $ 120,000, the p-value mean is 0.46 and the standard deviation of NPV is $ 650,000.

For a SDR of 7 %, the break-even number n is 9. Figure E.16 presents the result for the break-even test where the NPV mean is -$ 110,000, the p-value mean is 0.61 and the standard deviation of NPV is around $ 535,000. When n=10, the NPV mean is $ 50,000, the p-value mean is 0.49 and the standard deviation of NPV is $ 550,000.

4.3.5 Final recommendation

Based on the NPV and sensitivity analysis, the recommendation for the Seattle city is to chose alternative a), implementation of the online monitoring sensors, and implement the 12 online monitoring sensors in the Seattle Water System. The net social benefits exceeds the costs for scenario 2 and 3, and the same conclusion can be made from the uncertainties tested in the sensitivity analysis.

5

Discussion

This Chapter refers to the results presented in Chapter 4. The following sections discuss DBP spikes and causes, challenges and limitations in the data processing and, the strengths and weaknesses of the CBA. The last section is an overall consideration of online monitoring sensors and DBP monitoring.

5.1 DBP Spikes and Causes

The major challenge with drinking water treatment is that the conditions leading to better disinfection efficiency also lead to higher occurrence of DBPs. The following subsections discuss the DBP causes and the sampling sites in the distribution system. The first and second main objective in the thesis, process multi-year DBP data and identifying potential "hot spots" of DBP formation and identifying potential factors influencing the occurrence of high DBP values, will be addressed in this subsection. Once the water has left the treatment plant, there are many factors that can affect the water quality in the distribution system which isn't documented in the data set analyzed.

5.1.1 Potential DBP "hot-spots"

The twelve sampling sites and their properties were presented the methods chapter, in Table 3.4. The sampling sites are in general, the sites furthest away from the DWTP. As discussed in subsection 2.5.3, higher DBP concentrations are generally observed in the extremities of the distribution system.

Table 4.1-4.4 present the minimum, maximum and average DBP concentrations at the sampling sites from 2008-2018. Looking at the average THM and HAA concentration,

SPU is well below the EPA regulations for MCL presented in Table 2.6. However, the past recent years SPU has experienced high DBP spikes at sampling sites in the extremities of the distribution system.

As observed in Table 4.3, the HAA concentration peaked at 85.2 μg/L and 72.8 μg/L for sampling site C-1 and C-2, respectively. The THM concentration at sampling site T-5, T-6 and T-6, presented in Table 4.1, ranges from 58.6 μg/L to 90.7 μg/L, at maximum.

From an analytical standpoint, the sampling sites in the extremities of the distribution system are the hardest to analyze. Most of the water quality data from SPU are from the inlet and outlet at the DWTP and not from the actual sampling sites. The detention time from the drinking water leaving the treatment plant is significant and several factors change the water characteristics initially measured at the inlet and outlet of the DWTP that are presented in the next subsection.

5.1.2 Factors influencing high DBP values

From section 2.5 in literature review, one can make some assumptions on what can be expected to be found in the given data. A higher formation of THM can be observed at a higher pH and vice-versa for HAA formation. A higher chlorine concentration used at the DWTP can cause a higher DBP formation. A higher temperature could result in a higher DBP formation. Unlined cast iron pipes are prone to corrosion and microbial biofilms, which can also contribute to a higher DBP formation potential.

Higher concentrations of re-chlorination and a longer reaction time with chlorine leads to higher formation of DBPs. However, chlorine is needed for residual disinfection and is critical to avoid waterborne diseases.

Many of the components controlling DBP formation change with season: temperature, TOC/NOM, microbial activity, and the kinetics controlling chlorination/re-chlorination. All these factors contribute to a change in DBP formation. Seasonal variations affect both drinking water consumption and quality in a distribution system. The maximum DBP values are measured in spring and summer months, while minimum values are measured in winter. In summer months, the detention time can be as short as two weeks while in winter months it can be up to four weeks. The detention time is one of the largest uncertainties within the distribution system.

Table 3.5 and 3.6 map the most common events causing a DBP spike in the distribution system. For Cedar DWTP, change of water source from Lake Youngs to the river or vice

versa and algal bloom in Lake Youngs are the most common events observed. For Tolt DWTP, drought followed by heavy rainfall, landslide in the watershed or unoptimized coagulation are the main reasons for a potential DBP spike.

NOM is by far, the most important influence factor and the major precursor for DBPs. Seasonality factors that can lead to increased NOM concentration are heavy rainfalls, drought, the detention time in the distribution system, the pipe material and the pipe quality (e.g. leaky pikes) in the distribution system. Based on discussions with and data provided by SPU, it is observed that the tendency of spikes in DBP concentration do coincide with high precipitation and storm events.

Table 3.4 presents the sampling site characteristics. For sampling sites C-1 to C-5, the pipe material is unlined cast iron. For sampling site C-1 and C-2, the drinking water goes through two or three reservoirs where site C-2 has a high estimated detention time of 8 to 18 days. For the Tolt water sampling sites, T-4 to T-7 have the highest estimated detention in the which is 7 to 28 days. The pipe material for all Tolt sampling sites are lined cast iron and the number of reservoirs range from one to two. The biggest water quality difference for Cedar and Tolt, is the higher TOC content in the Tolt water, even after being treated at Tolt DWTP.

When comparing DBP concentrations presented in Table 4.1-4.4 and the information in Table 3.4, one can find some tendencies for the Cedar and Tolt drinking water. The Tolt water tends to have THM spikes while the Cedar water tends HAA spikes. The biggest differences with the Cedar and Tolt water as mentioned above are the TOC concentration, pipe material and detention time in distribution system, which might affect the distribution of THM and HAA formation.

5.1.3 Climate change and future water supply

In the *SPU 2019 Water System Plan*, the future impact of climate change and climate variability on the Seattle Water Supply System are investigated (Seattle Public Utilites, 2019a). The impacts of climate change are various, affecting air temperature, humidity, evaporation, rainfall, showfall, snowpack and runoff in terms of averages, extremes, timing and distribution.

The timing and magnitude of climate changes and its effect on water supply and demand are uncertain. In their Water System Plan, SPU conducted a climate analysis with projection from year 2000 to 2050. The results show an increasing trend in average temperature across all seasons. This causes an amplification of current seasonal patterns;

winter precipitation may increase and summer precipitation may decrease in the future. The expected warmer winter temperature result in less snow and more precipitation and longer droughts in the summer season.

The climate analysis concludes that SPU's water supply system will be increasingly vulnerable to the seasonal shift associated with climate change. More frequent and severe high flow events will effect the water quality causing high turbidity events and algal blooms that can be disruptive to supply operations.

The Eikebrokk et al., 2018 study concluded that summer droughts and heavy winter rain cause more frequent and higher NOM concentration in water sources, causing more frequent DBP events and an overall higher DBP concentration. To better track the effect of high NOM concentration episodes, the implementation of online monitoring sensors in the distribution system and sensors for temperature and rainfall (along with weather forecast) is recommended.

To understand how the high NOM concentrations affect the DBP concentration in the distribution system, it is recommended to increase the DBP sampling frequency in addition to implementation of the online monitoring sensors. It is especially important to take DBP samples after significant and acute NOM events, to better model and understand how NOM and turbidity affect the DBP concentration.

5.2 Challenges and Limitations in Data Processing

The main goal of the data processing is to gain a better understanding on how DBPs are related to water quality parameters in a real treatment system. Because of the grand size and the dynamics of the distribution system, there are several limitations to this study.

The main challenge with the processed data set in this thesis is the lack of DBP data and the fact that the DBP data is obtained from the sampling sites furthest away from the DWTP. Another main challenge is the fact that most of the water quality data is from the DWTP and not from the sampling points in the distribution system. Lastly, the long detention time of the drinking water in the distribution system is also a serious challenge.

Because of the long detention time, there are several factors influencing the water quality from when measured at DWTP to reaching the sampling site. The main factors are pipe

condition and material, bacteriological re-growth in pipe system, water age, sediments and detention time of water to mention a few. The following subsections discuss the strength and weaknesses with the data processing methods used in the study.

5.2.1 Data analysis using Python

To study the relationship between water quality parameters and DBP formation, MLR models were used. In general, regression models provide an efficient statistical approach to isolate and quantify effects on DBP formation. The coefficient of determination, R^2, explains the strength of the relationship between an independent and dependent variable, referred to as correlation.

When conducting the MLR models on the data set described in subsection 3.5.1, it quickly became apparent that the MLR modelling would not give any proficient results due to the data limitations discussed previously. Therefore, no further statistical analysis (e.g. removal of outliers, boxplots etc.) were conducted on the data set. Sampling site C-1 was used as an example for the data representation, and all the results from the other sites were more and less the same as for C-1.

The figures presented for sampling site C-1 in subsection 4.1.3 and Appendix B.2, show no clear relationship between pH and temperature and DBP formation. Site C-1 is the site furthest away from the DWTP and by the time the water reaches the sampling site, most of the DBP is already formed. If the same analysis was done for sampling sites closer to the DWTP, the MLR would give a better result.

The scatterplots of TOC and DBP at the sampling sites presented in Appendix B.3 show a positive relationship for some of the sampling sites (e.g. C-3 and C-5) while for other sites the results were inconclusive (e.g. T-4 and T-7). The TOC samples taken at the Cedar and Tolt TOC and the DBP samples at the treatment site were taken on separate days. This is an another reason due to which a clear relationship was not observed.

The purpose of dividing the N-days iteration model into summer and winter months is the fact that seasonal changes have major impact on the water quality parameters. The model was first made without considering the seasonal changes and did not give any clear results.

The N-days iteration model would have given better results if there was more DBP data for summer and winter months and if the UVA was measured closer to the the sampling

sites (e.g. if there was an online monitoring sensor in the distribution system). An other alternative that would provide better results would be if the DBP data was from sampling sites closer to the DWTP.

5.2.2 Data analysis using Unscrambler

Unscrambler was used to perform a MVA for the Cedar DWTP data. Due to the lack of water quality data in the distribution system, the calibrated R^2 for all the Cedar sampling sites were 0.4 and 0.47 for THM and HAA, respectively. For a MVA, a calibrated R^2 has to be 0.8-0.9 or above to conclude a correlation between the variables and sampling data. Because of the low R^2, any patterns found in the MVA were described as a casualty when interpreting the data.

For the PCA, the variance in the data is explained by 42 % for the model which is quite low. This implies that the variance THM and THM concentrations measured in the distribution system only can be described by around 40 % of the variables. For a MVA, a good data variance explain about 80-90 % for the model. The two PCs are variance of water quality parameters and variance of dimensions. From the loadings plot in Figure 4.8, one can observe the loadings UVA, HAA, turb in and turb out have the biggest impact on PC1. From what is discussed in section 2.5, this is plausible as UVA and turbidity are solid NOM indicators, and NOM is the the major precursor for DBPs.

Sampling site C-1 is used as an example for the THM and HAA predictions. The graphs for THM predictions are presented in subsection 4.1.4 while the HAA predictions graphs are presented in Appendix C.1. The bioplot for THM, presented in Figure 4.9 is inconclusive as the samples are clustered around the center of the graph. The HAA bioplot, presented in Figure C.1, has two more well-defined clusters. From Figure C.1, one can observe that one sample cluster seems to correlate with the loadings TOC in, turb in, turb out and UVA.

The loading plot for HAA, presented in Figure C.2, shows that HAA has the strongest correlation with TOC in, turb in, turb out and UVA. This verifies the tendency observed in Figure C.1. For the THM loadings plot, in Figure 4.10, one can observe that THM has the highest correlation with TOC.

The prediction versus reference for both THM and HAA show a low correlation. The best measured R^2 value was 0.55 for the THM prediction. Both models poorly predict the THM and HAA concentrations based on the reference data. In the prediction versus reference plot by samples, presented in Figure 4.12 and C.4, the green line represents the

real event while the blue and red line are prediction and cross-validation respectively. Figure 4.12 and C.4 show that the model is decent at predicting the seasonal changes. However, the model fails at prediction the DBP peak events, which is for sample R34 and R35 in Figure C.4 is significant.

5.2.3 Data analysis using the ANN model

The ANN model was only used on Cedar DWTP because of the lack of water quality data from Tolt DWTP. For future research, it is recommended to test the ANN model on the data from Tolt DWTP as well. The number of samples from Cedar DWTP used in the ANN model is 176. The usual number of samples for an ANN model is 200 or more. To be more confident about the result, more data from the treatment plant would be needed.

A perfect model in ANN has an All R^2 value that equals 1. However, in real life modelling, this can never be achieved. A value about 0.9 is considered very good correlation between the independent and dependent variable. For the ANN model for Cedar DWTP, the R^2 value was about 0.85 for both THM and HAA which is considered a satisfactory fit.

In ANN modelling, increasing the number of neurons makes the model complicated to fit the type of data which usually fails to obtain a correlation using a classical multiple regression. From the THM graphs in Appendix D.1, one can observe the difference in the All R^2 value for two neurons (n=2) and ten neurons (n=10) in the ANN model. For the HAA, there was not any significant difference in the All R^2 value for n=2 and n=10.

The biggest weakness with the ANN model is that outliers and other bias errors in the data are not considered. To get a better fit for the R^2 value one can change the division for Training:Validation:Testing to train the model to create a better fit. However, this was not done due to lack of time and resources.

From the data analysis, the ANN model was best fit for the DBP data analyzed with a R^2 of 0.85. Both Unscrambler and the ANN model show promising potential to use in corporation with spectroscopic online monitoring sensors to gain a real-time picture of the DBP concentration in a drinking water distribution system.

5.3 Strengths and Weaknesses of the CBA

The main objective of a CBA is to improve the quality of public decision making by investigating if a public policy provides the public a good. For this CBA, the main objective was to investigate if the implementation of online monitoring sensors would result in cost savings and health benefits for the city of Seattle. The benefits from implementation of the project is the number of annual new bladder cancer cases avoided per year due to implementation of online monitoring sensors in the distribution system.

As presented in section 4.3, the NPV for scenario 1 was negative while the NPV for scenario 2 and 3 were both positive. However, it is important to be aware of that the final NPV is a product of multiple assumptions and estimates. The following subsections discuss the weaknesses and strengths with the CBA method, the assumptions made and the sensitivity analysis.

5.3.1 Assumptions

The main assumptions with the biggest impact for the result of the CBA are the effectiveness of the sensors, relationship between DBP exposure and bladder cancer rate, the project's time peroid and the discount rate.

Because of the complexity of the system, it is hard to predict the impact of installing the online monitoring sensors in the distribution system will have on the average DBP concentration. The uncertainty of this made it reasonable to create different scenarios to look into what impact reducing the average DBP concentration would have on the city of Seattle. It has been found that reduction of the overall DBP concentration of 20 percent or more can have significant cost savings for the city.

DBP exposure and cancer risk

The EPA states that uncertainty remains around the estimates of quantifying annual new bladder cancer cases that can be attributed to DBP exposure. It is important to consider other factors that contributes to the risk of bladder cancer: age, sex, smoking history, occupation and socioeconomic status. These confounding factors independently affect the risk of developing bladder cancer. Hence, this is a very rough estimate at best of annual bladder cancer attributed to DBP exposure.

Another weakness in the CBA, is the assumption of a linear relationship between bladder cancer cases and DBP exposure. There is limited epidemiological data to establish a true linear relationship and evaluate this relationship in detail. The same assumption was made in EPA's *Economic Analysis for the Final Stage 2 Disinfectants and Disinfection Byproducts Rule* report and their key source of supporting data is Villanueva et al., 2004 (US EPA, 2005a, US EPA, 2005b).

Even thought the Villanueva et al., 2004 study supports a potential association between exposure to chlorinated drinking water and cancer, evidence is insufficient to establish a casual relationship (US EPA, 2005b). The epidemiology and toxicology literature provides important information that contributes to the weight of evidence for health risks from DBP exposure. But more research is required to confirm and target the health risks. Weaknesses with the Villanueva et al., 2004 study is that it only considers the exposure to TTHM and not HAA. In addition, the estimate of PAR $\sim$ 17.1 % represents the population in the whole US and not Washington state.

The biggest weakness to this CBA is the lack of consideration of the cessation lag period. The cessation lag is defined as the anticipated delay between the reduction of DBP occurrence and the exposure levels following implementation of a new measure (US EPA, 2005a). In other words, the cessation lag period is the amount of time it takes to achieve full reduction in the number of attributable bladder cancer cases due to the reduced DBP concentration.

The cessation lag period is not considered in this CBA because the calculation requires advanced model fitting and skills that is outside the scope of this thesis. Moreover, it is recognized that for a more advanced CBA the cessation lag period is essential to consider.

Monetization and time horizon

For this CBA, the project lifetime was set as 10 years. The CBA was conducted for a SDR of 3 % and 7 %. The METB used to calculate the excess burden of taxation was \$ 0.17 per dollar of tax revenue. The CPI multiplier used to convert the dollar value is 1.63. The impact of these parameters are discussed below.

After the project time period of 10 years, it is assumed that the online monitoring sensors have no real value due to rapid technology development and potential change of DBP regulations. During this 10 year period, many factors can effect the function of the sensors: the IT integration system can become outdated, the sensors might fail or need

to be replaced, or more advanced and robust multi-parameter sensors are introduced to the market. Possible scenarios like these are important to be considered in the CBA.

Even though the project's lifetime is 10 years, the "life-time" cost for bladder cancer treatment has a time horizon of 20 years. Optimally, the bladder cancer treatment should be considered over a 10-year time peroid as well. There are two main reasons for why it is not considered as such - firstly, to find the cost for an average bladder cancer patient, statistical models are required based on relative survival rates, historical data and probability calculations. These models are advanced and outside the scope of this thesis. Secondly, the cost of cancer treatment based on weighted average from year 10 to 20 is negligible compared to the cost from year 1 to 10.

The calculations made in the EPA's Cost of Illness Handbook for "life-time" cost for bladder cancer treatment was adapted to the CBA. Because the PV "life-time" cost was obtained in 1996 dollar value, a CPI multiplier of 1.63 was used to convert the cost to 2019 dollar value. There are several limitations with the 1996 data. Since 1996, cancer treatment methods have been developed and might be more efficient today. Due to technology development, it might be possible to diagnose bladder cancer treatment at an earlier stage to improve changes of survival. The market value of cancer treatment might exceed the inflation measured by the CPI, causing cancer treatment to be more expensive in 2019 than in 1996. All these factors need to be accounted for when examining the CBA results.

Due to the big difference between PV benefits and PV costs when 'n' is higher than the break-even number, the SDR does not affect the NPV as much as it usually does in a CBA. However, the sensitivity analysis is still conducted for both a SDR of 3 % and 7 %.

The real value of avoiding bladder cancer is much greater than the benefits calculated in the CBA. For the CBA, the only benefit considered was the direct medical cost associated with bladder cancer treatment. In addition to this, one has to consider life quality, family members involved in the treatment, pain and suffering. Inferring from this, it is clear that the benefits of installing the sensors outweigh the cost of the project.

Social discount rate (SDR)

The objective with the SDR is to weigh costs and benefits in the future compared to costs and benefits realized by society today. SDR is used when calculating NPV which is the single measure of the project's value. The choice of SDR might effect the outcome

of the CBA and result in a different policy recommendation.

Economists argue for what the most suitable SDR is. The US government have a prescribed SDR of 7 % while the British Treasury recommend using a SDR of 3.5 % (Boardman et al., 2006). For this CBA, the NPV was calculated using a SDR of 3 % and 7 %.

As presented in subsection 4.3.3, scenario 2 and 3 have a positive NPV with a SDR of 3 % and 7 %. The SDR had a small effect on costs as most of the expenses were at year 0 in the project. For benefits, the choice of SDR has a much greater impact as the medical costs are discounted over a 20-year time period. This effects the NPV which is considerably lower at a SDR of 7 % than for the NPV at a SDR of 3%.

5.3.2 Sensitivity analysis

The objective of the sensitivity analysis is to investigate how the NPV changes on adjusting the assumptions made in the CBA. If the NPV is still positive after running the analysis for the worst case scenarios, the analyst can with confidence make a recommendation to implement the project investigated.

The sensitivity analysis tests the uncertainties around the assumptions, the social discount rate and predicted number of new annual bladder cancer cases avoided. From the sensitivity analysis, one can conclude the NPV for scenario 1 (n=6) will be negative in more than 80 percent of all cases with a SDR of 3 % or 7 %. For a SDR of 3 %, the mean NPV was -$ 470,000 and the p-value was 0.825 while for a SDR of 7 % the mean NPV was -$ 605,000 and the p-value was 0.91. However, for scenario 2 and 3, it is very likely that the NPV will be positive.

The sensitivity analysis results for scenario 2 (n=12) show a positive NPV for a SDR of 3 % or 7 %. For a SDR of 3 %, the mean NPV was $ 700,000 and the p-value was 0.176 while for a SDR of 7 % the mean NPV was $ 380,000 and the p-value was 0.281. The results for the sensitivity analysis for scenario 3 (n=19) were satisfactory. For a SDR of 3 %, the mean NPV was $ 2,060,000 and the p-value was 0.007 while for a SDR of 7 % the mean NPV was $ 1,530,000 and the p-value was 0.015. Based on this, one can conclude that the SDR does not affect the outcome of the CBA for any of the the scenarios.

For the results from scenario 3, both the SDR of 3 % and 7 % had a large NPV standard deviation which reflects a large amount of variation in the NPV data. The p-value of

0.007 and 0.015 indicates for the 100,000 times the analysis ran, the NPV was less than zero in 0.7 % and 1.5 % of the cases for a SDR of 3 % and 7 %, respectively.

The break-even test showed that the break-even number is n=8 and n=9 for a SDR of 3 % and 7 %, respectively. This indicates that only a few number of annual new bladder cancer cases need to be avoided to make the implementation of the sensors worth the cost.

Although the NPV for scenario 1 is negative, the only cost considered in this CBA is the medical cost associated with bladder cancer, which is a lower-bound estimate. In reality, the real cost of bladder cancer is much higher than this lower-bound estimate. In addition, other health effects from DBP exposure such as colorectal cancer, stillbirth, miscarriages and other chronic illnesses are not considered in this CBA. Thus, the real society cost of DBP exposure is much greater than what is assumed in this CBA.

From conducting the sensitivity analysis, it is clear that the number of new annual cancer cases avoided (n) and the cost of cancer treatment (cc) are the two variables that affect the outcome of the NPV. These are also the two most uncertain assumptions in the CBA due to lack of research and data. However, based on the assumptions made in the CBA and the sensitivity analysis, it is clear that alternative a), implementing the online monitoring sensors in the distribution system, should be chosen.

5.4 Overall Considerations of DBP Monitoring

This section addresses the third and fifth main objective for the thesis, the selection of optimal locations for online monitoring sensors in the distribution system and the ascertain of practical efforts needed for a paradigm shift from a post-factum reactive DBP monitoring to a new proactive DBP monitoring. The subsections discuss implementation of online monitoring sensors, risk minimization versus DBP regulation and, DBP monitoring using online monitoring sensors and predictive DBP models.

5.4.1 Implementation of online monitoring sensors

In the current practice, the SPU notes the DBP concentrations at certain sampling points in the distribution system every 90 days. This information is not enough to create a full picture of the DBP formation in the distribution system and its influencing factors.

From analyzing the Seattle Water System and conducting a CBA, it is recommended for SPU to implement spectroscopic UV absorbance sensors at the DWTP and in the distribution system. By using DAS as the surrogate parameter, the utility could gain a real-time overall picture of the DBP formation. Section 4.2 in the results chapter provides a description of the implementation of the online monitoring sensors and can be used as a template for other utilities as well.

The greatest value of the spectroscopic UV absorbance sensors is the information they provide. By being notified of a potential increase in DBP concentration timely, the utilities can take early action and prevent a high DBP spike. That being said, it is not given that implementing the sensors will reduce the overall DBP concentration for every case. The effect of the sensors depends on the season and water supply and demand as the prevention actions are not feasible to carry out all year round.

Facing climate change and frequent DBP spikes in the future, it will be come even more important to gain a complete picture of the DBP concentration and other water quality parameters with time. Online monitoring sensors will play an essential role for water utilities to obtain a overall picture at both the DWTP and in the distribution system.

The online monitoring sensors at Landsburg Diversion and Treatment and Cedar DWTP, discussed in the methods chapter, are only used to get credit for the UV disinfection at Cedar DWTP. These are not to be confused with the spectroscopic UV absorbance sensors discussed in this subsection.

5.4.2 Risk minimization versus DBP regulation

Presently, DBP concentrations in drinking water are controlled worldwide by setting regulatory guidelines for a specific compound. These guidelines are based on identification of former compounds and available toxicological data. Unfortunately, for most DBPs, this information is not available leading to extrapolation of potential health impacts.

The low levels of DBP data combined with expensive sampling procedures mean that in practice, only a handful of DBP are regularly monitored. There is a need to conduct multidisciplinary research to map out all the existing DBPs, and their impact on human health.

An article by Drikas and Fabris, 2018, published in the Australian *Water E-journal*, points out that the current regulations limiting specific DBP compounds are not able to adequately account for the potential health impacts of DBPs. Introduction to addi-

tional DBP guidelines may not be the necessarily the best approach to encourage water utilities to run a more proactive and effective water treatment. The article suggests a more effective approach would be to establish regulations that encourage change in the operational practice to reduce the overall DBP risk.

Hereunder, the article mentions monitoring absorbance change, DAS, as an alternative to monitor and control DBP formation. This can be done by using spectroscopic UV absorbance or fluorescence sensors, which has shown significant potential to assist DBP management in the future.

In summary, online monitoring sensors are a provident and suitable approach to address a more comprehensive measure of DBP formation. The sensors are a great tool for utilities to prevent DBP formation by earlier start regulation for greater removal of DBP precursors such as NOM.

5.4.3 DBP monitoring using online monitoring sensors

The concept of real time DBP formation monitoring is ideal for water quality managers. Using UV spectrometers to monitor DBP formation is an efficient tool, especially for water systems with historically high DBP levels. Installing online monitoring sensors makes the utility aware of the DBP concentration at all time and by that improve the operational factors at the DWTP. Studies show better control of operational factors may contribute to a reduction of DBPs (Sadiq and Rodriguez, 2004).

One key point using online monitoring sensors is the importance of cross-checking the online monitoring data with actual laboratory analysis. The purpose is to validate the online data both for stable water conditions and during times of water quality changes.

With regards to practical efforts for a substantial shift to proactive DBP monitoring, several barriers preventing water utilities to install online monitoring systems need to be broken. The primary barrier is the utilities' experience of issues with the online monitoring instruments. Early experience of unstable sensors when the online sensors first were introduced to the commercial market made the utilities lose confidence in the product. Fouling is a big issue with the sensors and at present time there are still no good cleaning techniques available for the sensors.

In addition to maintenance difficulties, the sensors are a big investment. In most cases, the utility has to take the initiative to make a purchase by itself and get approval from the city. It is therefore important for the water utilities to be motivated to make

proactive changes to gain an overall water quality picture.

The third barrier is the regulation of manual routine monitoring requiring utilities to take quarterly samples regardless of data obtained from the online sensors. Due to this, utilities do not find it necessary to implement the online monitoring instruments. Even if utilities choose to implement online monitoring sensors, they are still required to do the routine grab samples in the distribution system.

Even with these barriers, the overall picture in the water quality industry is a rapid expansion in continuous monitoring (Callaghan et al., 2019). In the future, there are expected to be more stringent regulations pushing towards online monitoring in distribution systems. With development of more technology advanced sensors, there is expected to be a paradigm shift from reactive DBP monitoring to proactive DBP monitoring.

5.4.4 DBP monitoring using predictive models

The results from Unscrambler and ANN presented in subsection 4.1.4 and 4.1.5, show that one can predict the DBP formation with access to basic water quality parameters like pH, turbidity, temperature and color.

Some of the results from the Unscrambler and ANN were inconclusive due to the lack of data in the distribution system, with access only to the inlet and outlet data at the DWTP. Nonetheless, the results show that one can easily predict DBP concentration by taking regular grab samples at the DWTP and in the distribution system.

This is useful in particular for developing countries who wish to track the DBP concentration in the drinking water. For many developing countries, the drinking water is heavily chlorinated without considering the consequences of high DBP concentration. To prevent the DBP concentration to exceed the WHO guidelines, grab samples in combination with DBP predictive models is a powerful and effective method to predict and prevent high DBP concentration in drinking water.

In the future, with more sophisticated wireless communication and affordability of remote power system, online monitoring sensors can be a solution to track DBP formation for developing countries as well as for industrialized countries.

6

Conclusions

In this thesis, a series of possible concepts to monitor DBPs in a drinking water distribution system have been presented. From the analytical research in this thesis, it can be concluded that it is possible to make DBP predictions from basic water quality parameters. In a global context, this a great tool to improve the public health and makes it possible for developing countries to track DBP formation in the distribution system by using simple sampling procedures and DBP models.

From processing the multi-year DBP data, the "hot spots" of DBP formation was found to be in the extremities of the distribution system. NOM was found to be the most important influence factor influencing the occurrence of high DBP values. Other key DBP influencing factors are detention time, pipe material, chlorine reaction time, temperature and pH. Many of these factors change with season, causing most DBP spikes to occur during seasonality changes.

Based on the data analysis, the optimal locations for the online monitoring sensors are at the DWTP (at the inlet of the DWTP, post ozonation and in the clearwells post chlorination), the nearest site sampling point to the DWTP and in the extremities of the distribution system.

From the CBA, it is proven to be beneficial for the City of Seattle to implement online monitoring sensors to prevent future DBP spikes and lower the overall DBP concentration. From the assumptions made in the CBA, this will eventually result in a decrease in new bladder cancer cases. The break-even number for the lowest amount of new bladder cancer cases to be avoided was found to be nine for a SDR of 7 %, for the NPV to be positive and thus, implementation to be successful.

Practical efforts for a paradigm shift towards proactive DBP monitoring include more stringent DBP regulations, utilities being motivated to make monitor changes, and more accurate, robust and inexpensive online monitoring sensors.

6.1 Future Recommendations

The documented research on DBP formation in a real time distribution system is limited. To make progress in this field, there is a need to develop a more suitable, collective sampling procedure. It also requires an improved dialogue between research institutions and water utilities. Without a more frequent data sampling from locations in the distribution system and DBP data, it is difficult for researchers to make any analytical predictions.

Future recommendation on how to better monitor and map DBP formation based on the research in this thesis:

1. For water utilities to measure water quality parameters not only at the inlet and outlet of the DWTP, but also at the sampling sites in the distribution system.

2. For water utilities to create a water quality database to track the development of DBP formation in the system over time.

3. For urban areas, it is an advantage to install online monitoring sensors at the DWTP and in the distribution system, to continuously monitoring the DBP concentration.

4. To better understand the correlation between DBP formation and water quality parameters, there is a need for a more frequent DBP sampling procedure than every three months. This is specifically important during acute events causing DBP spikes.

5. At last, more comprehensive research on DBP species and their impact on human health is needed. In the future, it is important to focus on the operational, epidemiological and regulatory purposes by conducting multidisciplinary research to map out the real health effects of DBPs.

References

American Cancer Society (2019). *Cancer Statistics Center, Urinary bladder*. URL: https://cancerstatisticscenter.cancer.org/%7B%5C#%7D!/data-analysis/NewCaseEstimates (visited on 07/15/2019).

Boardman, A. E., Greenberg, D. H., Vining, A. R., and Weimer, D. L. (2006). *Cost-Benefit Analysis*.

Bureau of Labor Statistics (2015). Table 24. Historical Consumer Price Index for All Urban Consumers (CPI-U): U. S. city average, all items. *CPI Detailed Report Data for December 2015*: 31–34. URL: http://www.bls.gov/cpi/cpid1512.pdf.

Calderon, R. (2000). The epidemiology of chemical contaminants of drinking water. *Food and Chemical Toxicology* 38: S13–S20. DOI: 10.1016/S0278-6915(99)00133-7.

Callaghan, P. O., Carpentier, C., and Ward, C. (2019). Insight Report Online water and wastewater sensors and analyzers : 2019 update.

Chan, S., Pullerits, K., Keucken, A., Persson, K. M., Paul, C. J., and Rådström, P. (2019). Bacterial release from pipe biofilm in a full-scale drinking water distribution system. *npj Biofilms and Microbiomes* 5 (1): 3–10. DOI: 10.1038/s41522-019-0082-9.

Chow, C., Fabris, R., and Dixon, M. (2013). Case Studies Using S::CAN On-line Monitoring System: 1–5.

Chowdhury, S., Rodriguez, M. J., and Sadiq, R. (2011). Disinfection byproducts in Canadian provinces: Associated cancer risks and medical expenses. *Journal of Hazardous Materials* 187 (1-3): 574–584. DOI: 10.1016/j.jhazmat.2011.01.085.

Chui, J. (2011). *An overview of electromagnetic radiation absorption*. URL: https://commons.wikimedia.org/wiki/File:Spectroscopy%7B%5C_%7Doverview.svg%7B%5C#%7Dglobalusage (visited on 07/08/2019).

Dodds, L., King, W., Allen, A., Armson, B., Fell, D., and Nimrod, C. (2004). Trihalomethanes in public water supplies and risk of stillbirth. *Epidemiology 15*.

Drikas, M. and Fabris, R. (2018). Are Current Guidelines Best Practice for Disinfection By-Product Control? *Water e-Journal* 3 (2): 1–8. DOI: 10.21139/wej.2018.017.

ECHA (2017). *Guidance on the Biocidal Products Regulation: Volume II Parts B+C*. Vol. V2.1. March: 1–105. DOI: 10.2823/31176.

Eikebrokk, B., Haaland, S., Jarvis, P., Riise, G., Vogt, R. D., and Zahlsen, K. (2018). *NOMiNOR: Natural Organic Matter in drinking waters within the Nordic Region*.

Ellington, J. J., Crumley, F. G., Buettner, K. M., Evans, J. J., Blount, B. C., Silva, L. K., Waite, T. I. M. J., Luther, G. W., Mckague, A. B., Miltner, R. J., Wagner, E. D., and Plewa, M. J. (2008). Occurrence and mammalian cell toxicity of iodinated disinfection. 42 (22): 8330–8338.

EPA, U. (2013). *Water Treatment Manual : Disinfection*: 1–200.

Grellier, J., Rushton, L., Briggs, D. J., and Nieuwenhuijsen, M. J. (2015). Assessing the human health impacts of exposure to disinfection by-products - A critical review of concepts and methods. *Environment International* 78: 61–81. DOI: 10.1016/j.envint.2015.02.003.

Henderson, R. K., Baker, A., Murphy, K. R., Hambly, A., Stuetz, R. M., and Khan, S. J. (2009). Fluorescence as a potential monitoring tool for recycled water systems: A review. *Water Research* 43 (4): 863–881. DOI: 10.1016/j.watres.2008.11.027.

Hung, Y. C., Waters, B. W., Yemmireddy, V. K., and Huang, C. H. (2017). pH effect on the formation of THM and HAA disinfection byproducts and potential control strategies for food processing. *Journal of Integrative Agriculture* 16 (12): 2914–2923. DOI: 10.1016/S2095-3119(17)61798-2.

King, W. D., Marrett, L. D., and Woolcott, C. G. (2000). Case-control study of colon and rectal cancers and chlorination by-products in treated water. *Cancer Epidemiology Biomarkers and Prevention* 9 (8): 813–818.

King, W. D. and Marrett, L. D. (1996). Case-control study treated of bladder chlorination by-products in Treated Water. *Cancer Causes and Control* 7 (6): 596–604.

Korshin, G. V., Benjamin, M. M., Hemingway, O., and Wu, W. W. (2002). *Development of Differential UV Spectroscopy for DBP Monitoring*.

Krasner, S., McQuire, M., Jacangelo, J., Patania, N., Reagan, K., and Aieta, E. (1989). The Occurrence of Disinfection By-products in US Drinking Water.

Lee, J., Kim, E. S., Roh, B. S., Eom, S. W., and Zoh, K. D. (2013). Occurrence of disinfection by-products in tap water distribution systems and their associated health risk. *Environmental Monitoring and Assessment* 185 (9): 7675–7691. DOI: 10.1007/s10661-013-3127-1.

Lenntech (2019). *Ozone reaction mehanisms*. URL: https://www.lenntech.com/library/ozone/reaction/ozone-reaction-mechanisms.htm (visited on 07/21/2019).

Li, W. T., Jin, J., Li, Q., Wu, C. F., Lu, H., Zhou, Q., and Li, A. M. (2016). Developing LED UV fluorescence sensors for online monitoring DOM and predicting DBPs formation potential during water treatment. *Water Research* 93: 1–9. DOI: 10.1016/j.watres.2016.01.005.

Liang, L. and Singer, P. C. (2003). Factors Influencing the Formation and Relative Distribution of Haloacetic Acids and Trihalomethanes in Drinking Water. *Environmental Science & Technology* 37 (13): 2920–2928. DOI: 10.1021/es026230q.

Minakata, D., Hollender, J., Zimmermann, S. G., Koepke, S., Krauss, M., McArdell, C. S., Ort, C., Singer, H., Von Gunten, U., Siegrist, H., Zhu, H., Shen, Z., Tang, Q., Ji, W., Jia, L., Huber, M. M., Canonica, S., Park, G. Y., Von Gunten, U., Kušić, H., Rasulev, B., Leszczynska, D., Leszczynski, J., Koprivanac, N., Jin, X., Peldszus, S., Huck, P. M., Huber, M. M., Wang, X. X., Zhou, B., Yang, H., Wang, X. X., Xie, Y., Sudhakaran, S., Lattemann, S., Amy, G. L., Hovorka, S. W., Schöneich, C., Lei, H., Snyder, S. A., Von Gunten, U., Sudhakaran, S., Calvin, J., Amy, G. L., Castro, G., Casado, J., Rodríguez, I., Ramil, M., Ferradás, A., Cela, R., Lee, Y., Von Gunten, U., Sudhakaran, S., and Amy, G. L. (2012). Ozonation of drinking water: Part I. Oxidation kinetics and product formation. *Water Research* 43 (20): 7862–7869. DOI: 10.1021/es9014629.

Norsk Vann (2009). *Veiledning til bestemmelse av god desinfeksjonspraksis*. Tech. rep.

Office of Pollution Prevention and Toxins (2007). *U.S EPA: Cost of Illness Handbook*. URL: http://nepis.epa.gov/Exe/ZyPDF.cgi/901A0E00.PDF?Dockey=901A0E00.PDF.

Rahman, M. B., Driscoll, T., Cowie, C., and Armstrong, B. K. (2010). Disinfection by-products in drinking water and colorectal cancer: A meta-analysis. *International Journal of Epidemiology* 39 (3): 733–745. DOI: 10.1093/ije/dyp371.

Reckhow, D. A., Linden, K. G., Kim, J., Shemer, H., and Makdissy, G. (2010). Effect of UV treatment on DBP formation. *Journal - American Water Works Association* 102 (6): 100–113. DOI: 10.1002/j.1551-8833.2010.tb10134.x.

Rice, E. W. and Johnson, C. H. (1991). Cholera in Peru. *The Lancet* 338 (8764): 455. DOI: 10.1016/0140-6736(91)91086-A.

Richardson, S. D. (2005). New Disinfection By-Product Issues: Emerging DBPs and Alternative Routes of Exposure. 7 (1): 43–60.

Richardson, S. D., Plewa, M. J., Wagner, E. D., Schoeny, R., and DeMarini, D. M. (2007). Occurrence, genotoxicity, and carcinogenicity of regulated and emerging disinfection by-products in drinking water: A review and roadmap for research. *Mutation Research - Reviews in Mutation Research* 636 (1-3): 178–242. DOI: 10.1016/j.mrrev.2007.09.001.

Roccaro, P., Chang, H. S., Vagliasindi, F. G. A., and Korshin, G. V. (2008). Differential absorbance study of effects of temperature on chlorine consumption and formation of disinfection by-products in chlorinated water. *Water Research*. DOI: 10.1016/j.watres.2007.11.013.

Rook, J. (1974). Formation of haloforms during chlorination of natural waters.

Ryškevič, N., Juršėnas, S., Vitta, P., Bakienė, E., Gaska, R., and Žukauskas, A. (2010). Concept design of a UV light-emitting diode based fluorescence sensor for real-time bioparticle detection. *Sensors and Actuators B: Chemical* 148 (2): 371–378. DOI: 10.1016/j.snb.2010.05.042.

Sadiq, R. and Rodriguez, M. J. (2004). Disinfection by-products (DBPs) in drinking water and predictive models for their occurrence: A review. *Science of the Total Environment* 321 (1-3): 21–46. DOI: 10.1016/j.scitotenv.2003.05.001.

Salvadori, M. I., Sontrop, J. M., Garg, A. X., Moist, L. M., Suri, R. S., and Clark, W. F. (2009). Factors that led to the Walkerton tragedy. *Kidney International* 75 (SUPPL. 112): S33–S34. DOI: 10.1038/ki.2008.616.

S::CAN (2017). *Datasheet Drinking Water*. URL: https://www.s-can.at/products/spectrometer-probes%7B%5C#%7D (visited on 07/08/2019).

Seattle Public Utilites (2014). *Cedar Slideshow*. Tech. rep.: Power point slides 5 and 12.

Seattle Public Utilites (2018). 2019 Water System Plan Volume 2, Part C - Policies, Procedures and Standards. *2019 Water System Plan Volume 2, Part C - Policies, Procedures and Standards* 2 (7).

Seattle Public Utilites (2019a). *SPU 2019 Water System Plan Volume 1*.

Seattle Public Utilites (2019b). *Tolt Slideshow*. Tech. rep.: Power point slides 5 and 8.

Tedetti, M., Joffre, P., and Goutx, M. (2013). Development of a field-portable fluorometer based on deep ultraviolet LEDs for the detection of phenanthrene- and tryptophan-like compounds in natural waters. *Sensors and Actuators B: Chemical* 182: 416–423. DOI: 10.1016/j.snb.2013.03.052.

Thompson, C., Gilliepie, S., and Goslan, E. (2016). *Disinfection By-products in Drinking Water*.

US EPA (2005a). *Appendices to the Economic Analysis for the Final Stage 2 Disinfectants and Disinfection Byproducts Rule Volume I (A-E2)*. Tech. rep.: 198–204.

US EPA (2005b). Economic Analysis for the Final Stage 2 Disinfectants and Disinfection Byproducts Rule. *Economic Analysis*: 187–255.

US EPA (2019). The Fourth Unregulated Contaminant Monitoring Rule (UCMR 4) General Information. (December 2016): 140–141.

USEPA (2009). National Primary Drinking Water Regulations Contaminant MCL or TT. 1. URL: https://www.epa.gov/sites/production/files/2016-06/documents/npwdr%7B%5C_%7Dcomplete%7B%5C_%7Dtable.pdf.

Villanueva, C. M., Cantor, K. P., Cordier, S., Jaakkola, J. J., King, W. D., Lynch, C. F., Porru, S., and Kogevinas, M. (2004). Disinfection byproducts and bladder cancer: A pooled analysis. *Epidemiology* 15 (3): 357–367. DOI: 10.1097/01.ede.0000121380.02594.fc.

Villanueva, C. M., Cantor, K. P., Grimalt, J. O., Malats, N., Silverman, D., Tardon, A., Garcia-Closas, R., Serra, C., Carrato, A., Castaño-Vinyals, G., Marcos, R., Rothman, N., Real, F. X., Dosemeci, M., and Kogevinas, M. (2007). Bladder cancer and exposure to water disinfection by-products through ingestion, bathing, showering, and swimming in pools. *American Journal of Epidemiology* 165 (2): 148–156. DOI: 10.1093/aje/kwj364.

Waller, K., Swan, S. H., DeLorenze, G., and Hopkins, B. (1998). *Trihalomethanes in Drinking Water and Spontaneous Abortion*.

Werler, M. M. (2011). Birth Defects. *Reproductive and Perinatal Epidemiology* 125 (2): 269–277. DOI: 10.1093/acprof:oso/9780195387902.003.0049.

White, G. C. (1986). *The Handbook of Chlorination*.

WHO (2004). CHEMISTRY OF DISINFECTANTS AND DISINFECTANT BY-PRODUCTS Physical and chemical properties of common disinfectants and inorganic disinfectant by-products: 27–109. URL: https://www.who.int/ipcs/publications/ehc/ehc%7B%5C_%7D216/en/.

World Health Organization (2011). Guidelines for Drinking-water Quality 4th ed., WHO, Geneva, p. 340. *World Health Organization*: 427–429. DOI: 10.1016/S1462-0758(00)00006-6.

Ye, T., Xu, B., Lin, Y. L., Hu, C. Y., Lin, L., Zhang, T. Y., and Gao, N. Y. (2013). Formation of iodinated disinfection by-products during oxidation of iodide-containing waters with chlorine dioxide. *Water Research* 47 (9): 3006–3014. DOI: 10.1016/j.watres.2013.03.003.

Zhang, T. Y., Xu, B., Hu, C. Y., Lin, Y. L., Lin, L., Ye, T., and Tian, F. X. (2015). A comparison of iodinated trihalomethane formation from chlorine, chlorine dioxide and potassium permanganate oxidation processes. *Water Research* 68: 394–403. DOI: 10.1016/j.watres.2014.09.040.

A

Sampling and Lab Procedures at SPU

A.1 Sampling Procedures in the Distribution System

The concentration of the DBPs, THM and HAA, are measured from the quarterly water quality samples in the distribution system. The samples are completed the first week of February, May, August and November of every year. The staff collecting the DBP samples in the distribution system follow a strict protocol routine. The THM samples are collected in two 40 mL clear glass vials glass containing sodium thiosulfate preservative. The HAA sample are collected a 125 mL amber glass bottle containing ammonium chloride. The procedure of collection of samples is as following:

1. Keep the samples on chilled ice during the sampling route.

2. Remove the filters attached to the sampling tap.

3. To assure a representative sample, open the tap and let water run about three minutes until it reaches a constant temperature.

4. For the THM sample: fill the vial to slightly just above the rim, without aeration. Make sure there are no bubbles in the sample. Repeat for both clear glasses.

5. For the HAA sample: Fill the amber glass to the rim. No need to care about the bubbles.

6. Label each bottle with temperature and chlorine measurements, in addition to date and site code. Refrigerate the samples and bring it to the lab the same day.

It is essential that the samples are executed according to the standard procedure to ensure correct data from the distribution system. The most important to take notice from this procedure is that the THM sample cannot contain aeration while the HAA sample can.

A.2 Lab Procedures at SPU

It takes about two weeks to process a DBP sample in the lab. The laboratory at Seattle Public Utilities follow the Standard Operating Procedure (SOP) when analyzing the drinking water samples. The SOP for determination of HAA is the EPA method 552.3: *'Determination of HAA in Drinking Water by Liquid-Liquid Extraction, Derivatization and Gas Chromatography with Electron Capture Detection'*. For determination of THM the SOP used is EPA method 524.2 revision 4.1: *'Measurement of Purgeable Organic Compounds in Water by Capillary Column Gas Chromatography/Mass Spectrometry'*. Below are the summaries of the SOPs for HAA and THM.

A.2.1 Lab Procedures for HAA

40 mL volume of sample Methyl-tert-butyl-ether (MTBE) containing an internal standard is adjusted to a pH less than 0.5. The HAAs have been partitioned into organic phase before being converted to their methyl esters by the addition of acidic methanol. Then the sample is heated for two hours. The methylated HAAs (in solvent phase) are separated from the acidic methanol by adding 7 mL of concentrated aqueous solution of sodium sulfate.

The remaining extract is neutralized with a solution of saturated sodium bicarbonate ($NaHCO_3$) and the solvent layer is removed for analysis. The analytes are identified and quantitated by capillary column Gas Chromatography (GS) using an Electron Capture Detector (ECD). Finally, the analytes are quantitated using procedural calibration standards (EPA method 552.3).

A.2.2 Lab Procedures for THM

The volatile organic compounds and the surrogates are extracted from the sample matrix by bubbling an inert gas through the aqueous sample. The extracted samples are trapped in a tube containing suitable sorbent materials. The sorbent tube is then heated and backflushed with helium. This desorbs the trapped sample into a capillary GS column interfaced to a Mass Spectrometer (MS). The analytes are quantitated using procedural standard calibration. This also includes the surrogate analytes, whose concentration are known in every sample (EPA method 524.2 revision 4.1).

B

Graphs from Python

B.1 Online Monitoring UVA Data

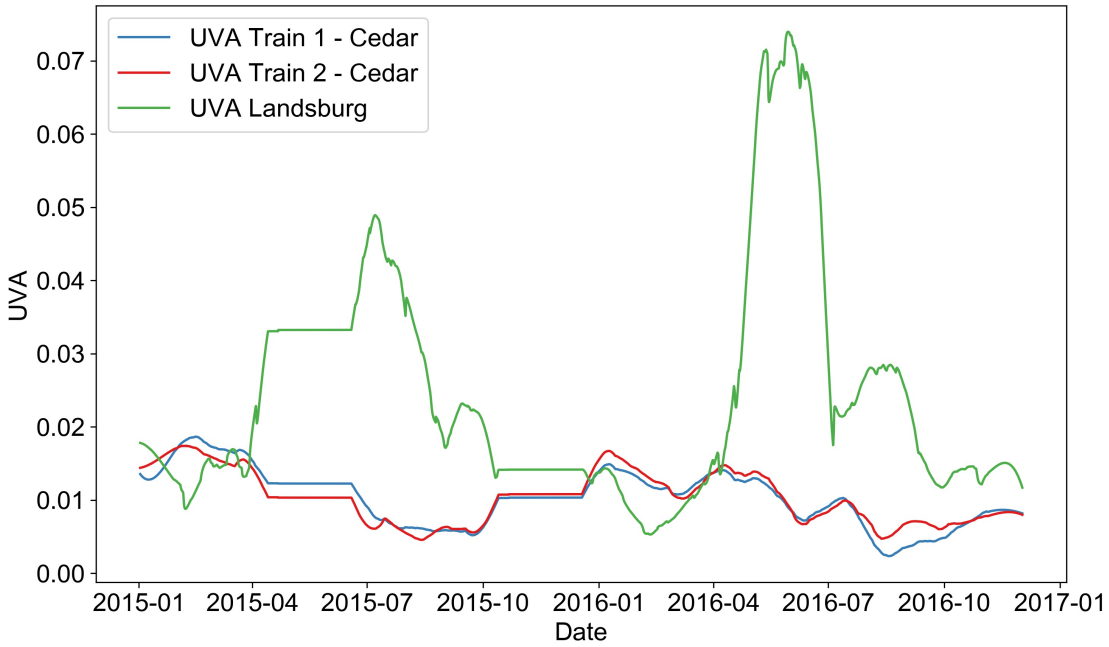

Figure B.1: Online monitoring UVA data from Landsburg, Train 1 and 2 at Cedar DWTP from 2015-2017.

B.2 Scatterplots THM prediction at C-1

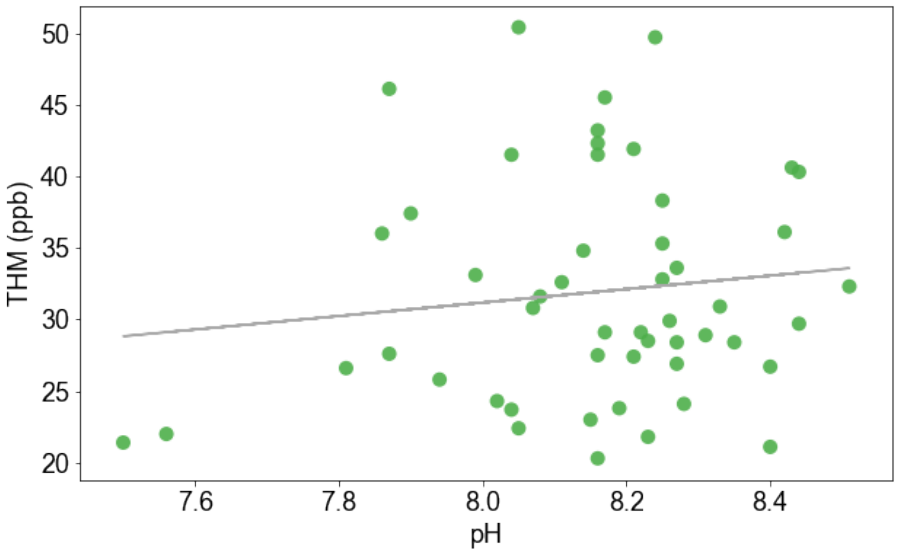

Figure B.2: Scatterplot pH and THM at sampling site C-1 from 2008-2018.

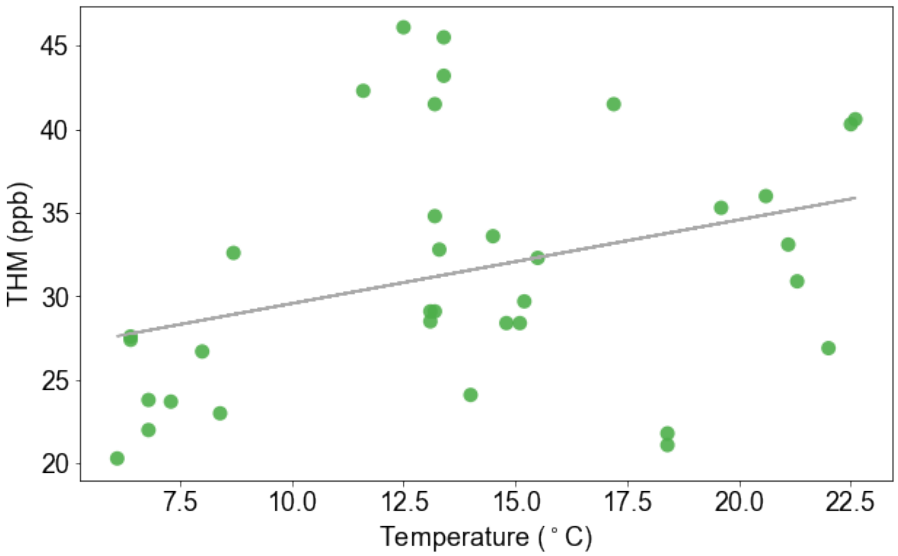

Figure B.3: Scatterplot temperature and THM at sampling site C-1 from 2008-2018.

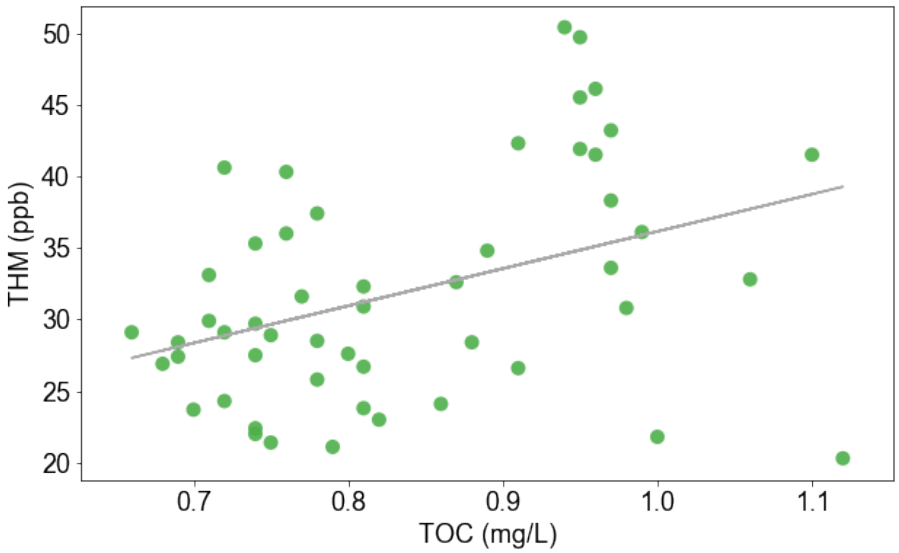

Figure B.4: Scatterplot TOC and THM at sampling site C-1 from 2008-2018.

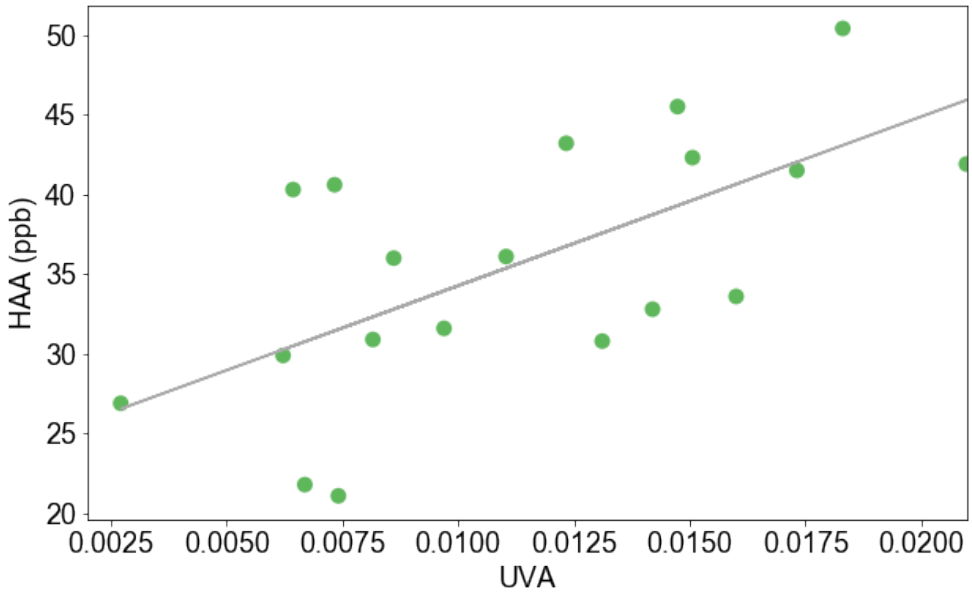

Figure B.5: Scatterplot UVA and THM data for summer months at sampling site C-1 from 2008-2018. For n=4, R^2= 0.51.

B.3 DBP and TOC Scatterplot

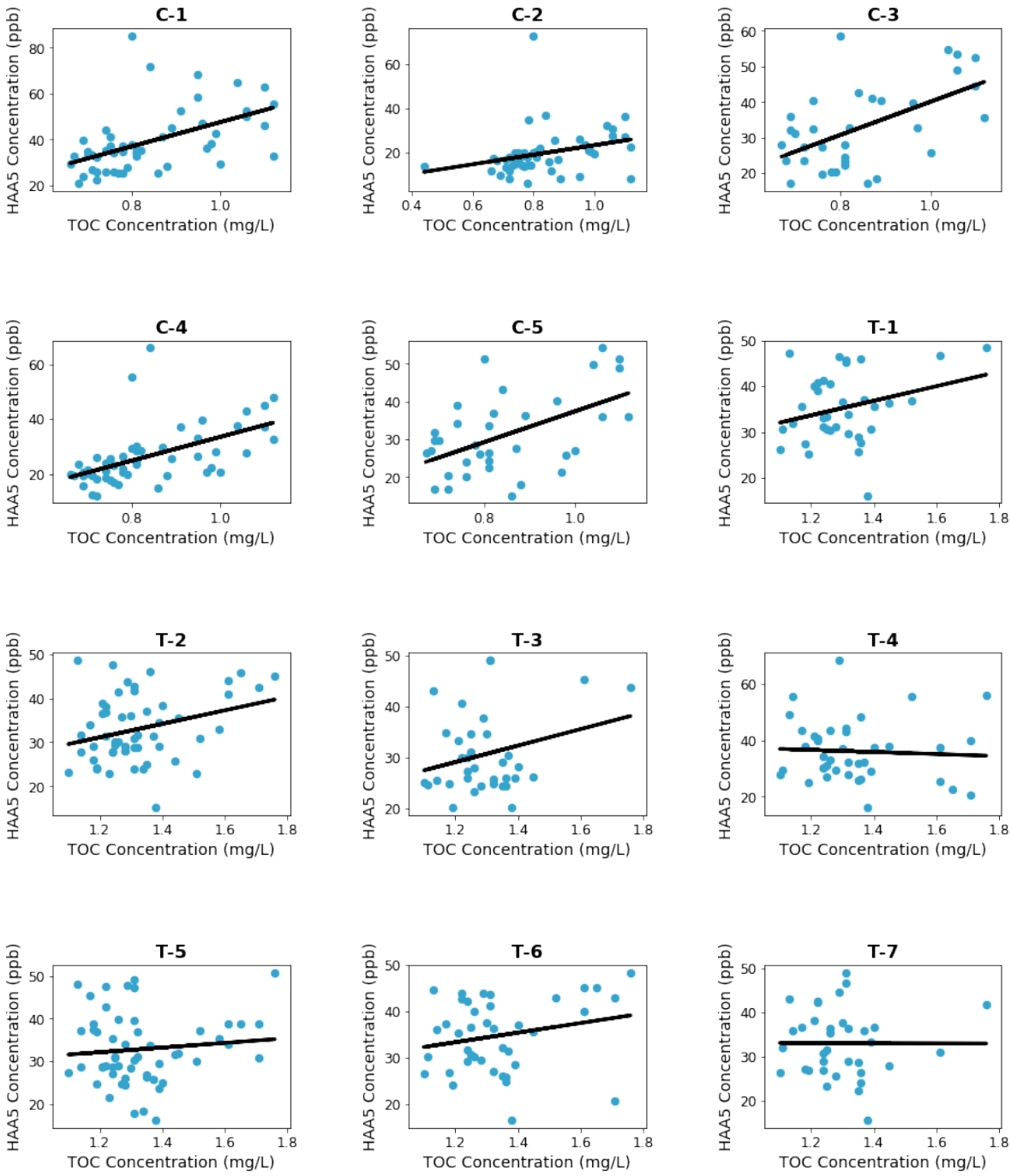

Figure B.6: Scatterplot of TOC and HAA5 concentrations at the sampling sites from 2008-2018.

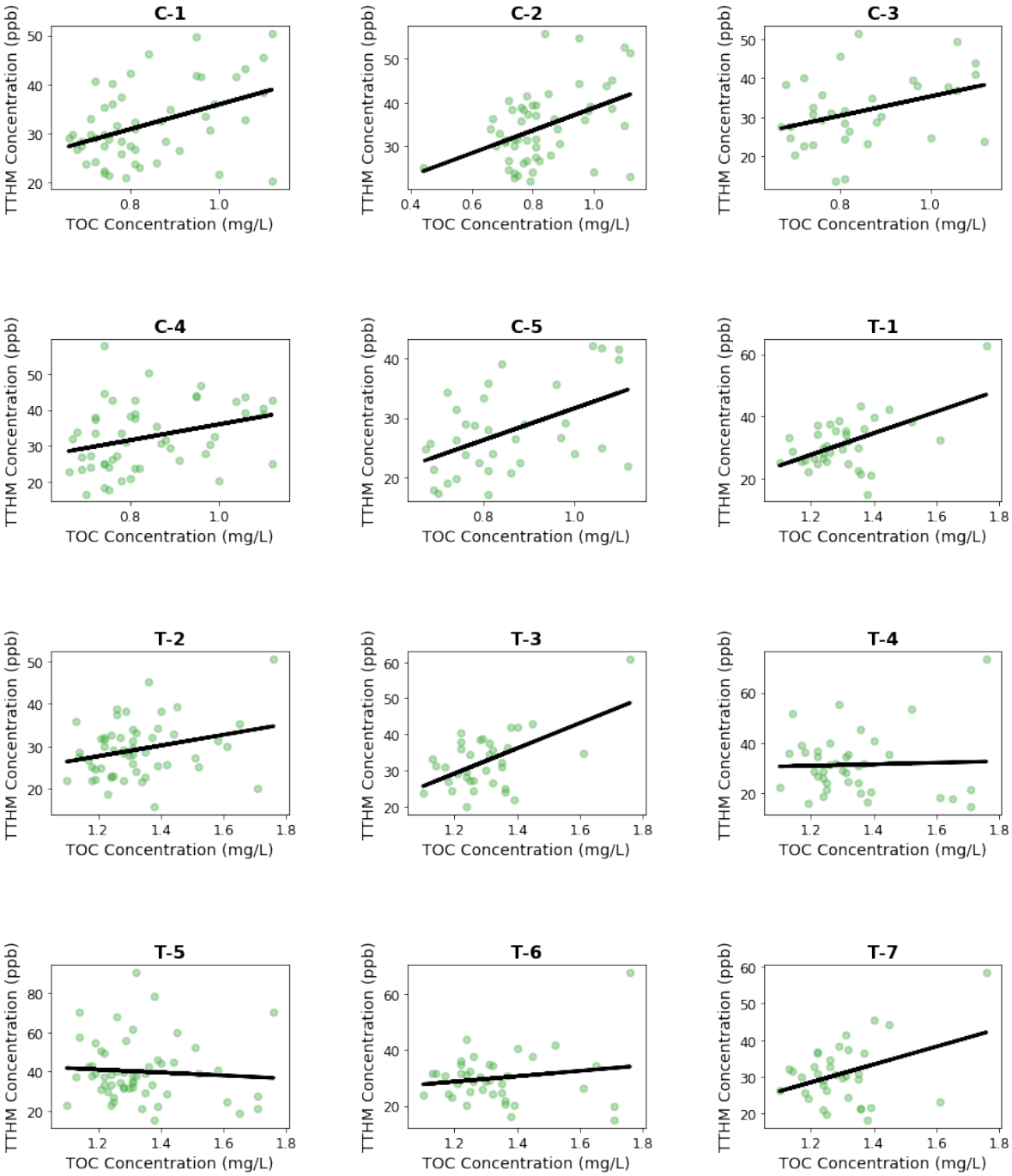

Figure B.7: Scatterplot of TOC and TTHM concentrations at the sampling sites from 2008-2018.

C

Unscrambler

C.1 Graphs from Unscrambler

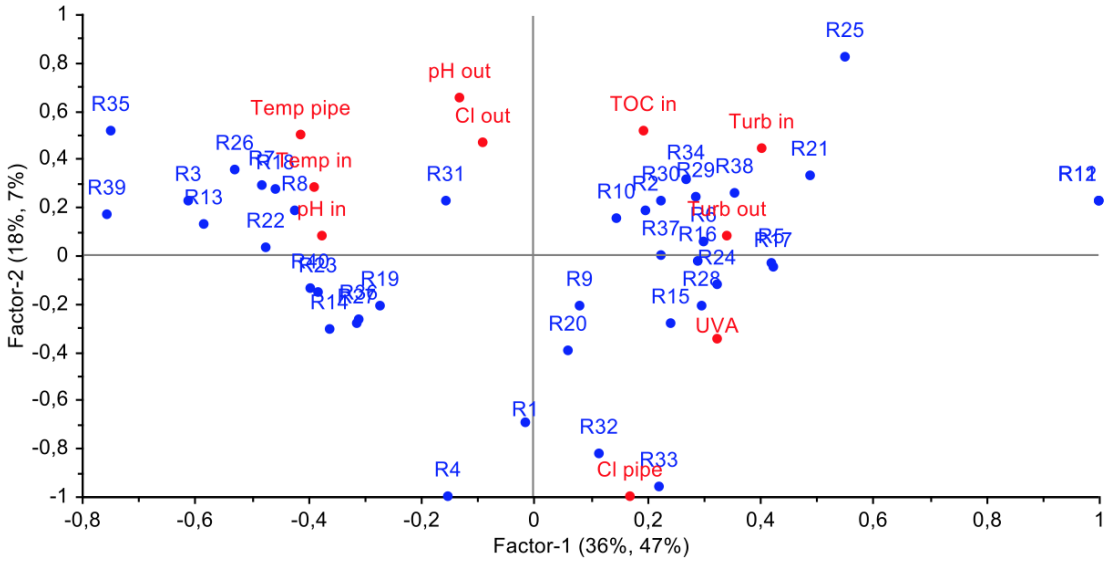

Figure C.1: Bioplot for site C-1 and HAA prediction.

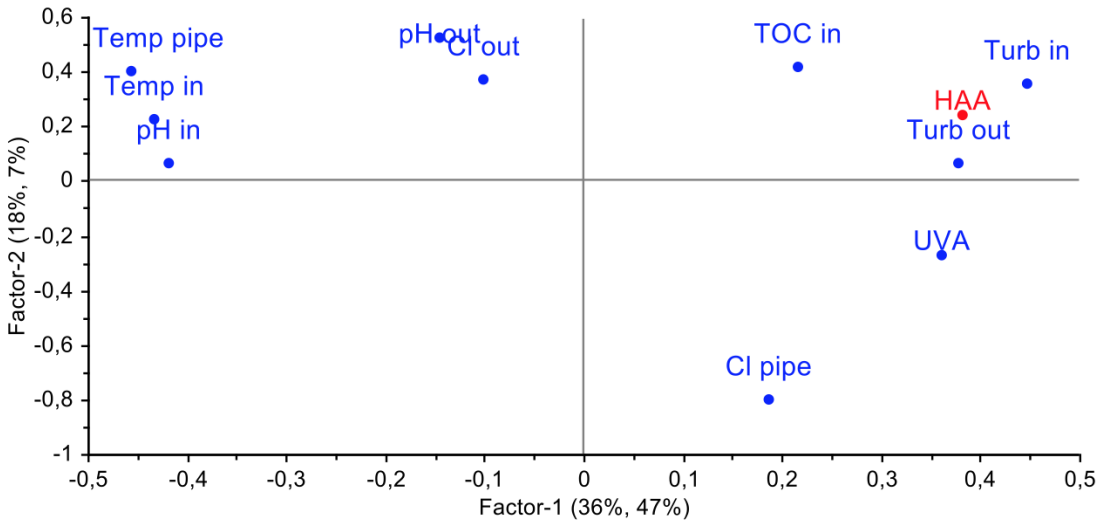

Figure C.2: Loading plot for site C-1 and HAA prediction.

Table C.1: The loadings for PC-1 and PC-2.

Loading	UVA %	TOC in (mg/L)	pH in	Temp in (°C)	Turb in (NTU)	pH out	Turb out (NTU)	Cl out (mg/L)	
PC-1	0.287	0.18	-0.4	-0.4	0.38	-0.15	0.31	-0.13	
PC-2	0.113	-0.27	-0.1	-0.1	-0.14	-0.13	-0.11	-0.06	

	TOC out mg/L	Distance plant-site (km)	Last rechlor-site (km)	Number of reservoirs involved	THM (μg/L)	HAA (μg/L)	Cl pipe (mg/L)	Temp pipe °C
	0.18	-0.0437	-0.0429	0.00388	0.15	0.31	0.15	-0.37
	-0.27	-0.487	-0.492	0.465	-0.03	-0.090	-0.2	-0.16

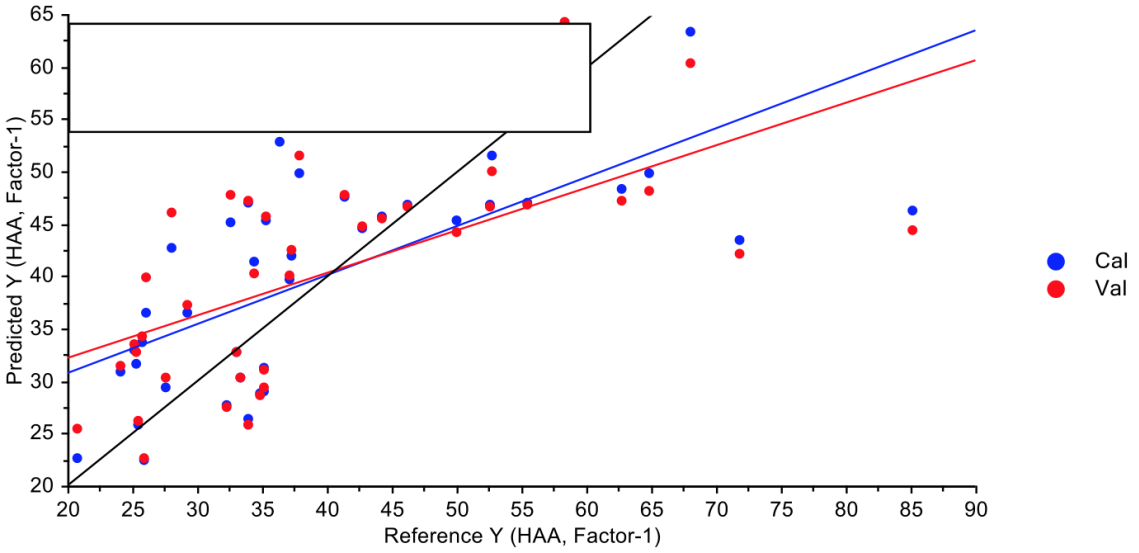

Figure C.3: Prediction vs reference plot for site C-1 and HAA prediction.

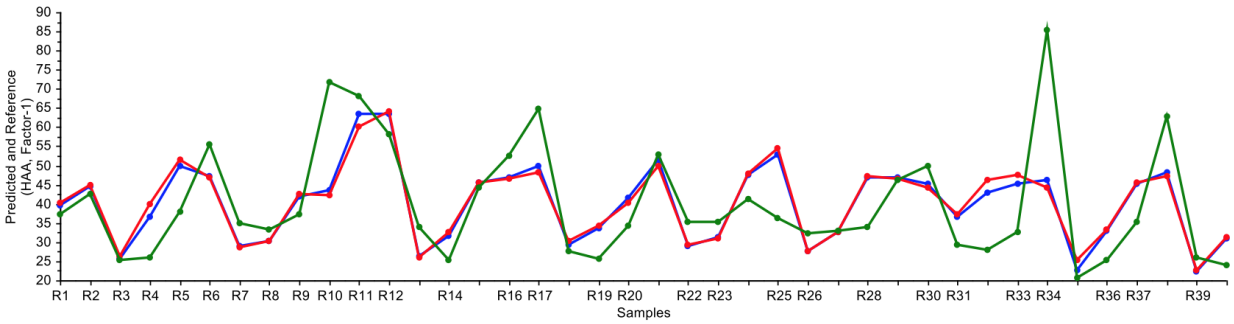

Figure C.4: Prediction vs reference plot by samples for site C-1 and HAA prediction. The blue line is predicted calibration, the red line is cross-validation and the green lines is reference values.

D

ANN Model

D.1 Graphs from ANN Model

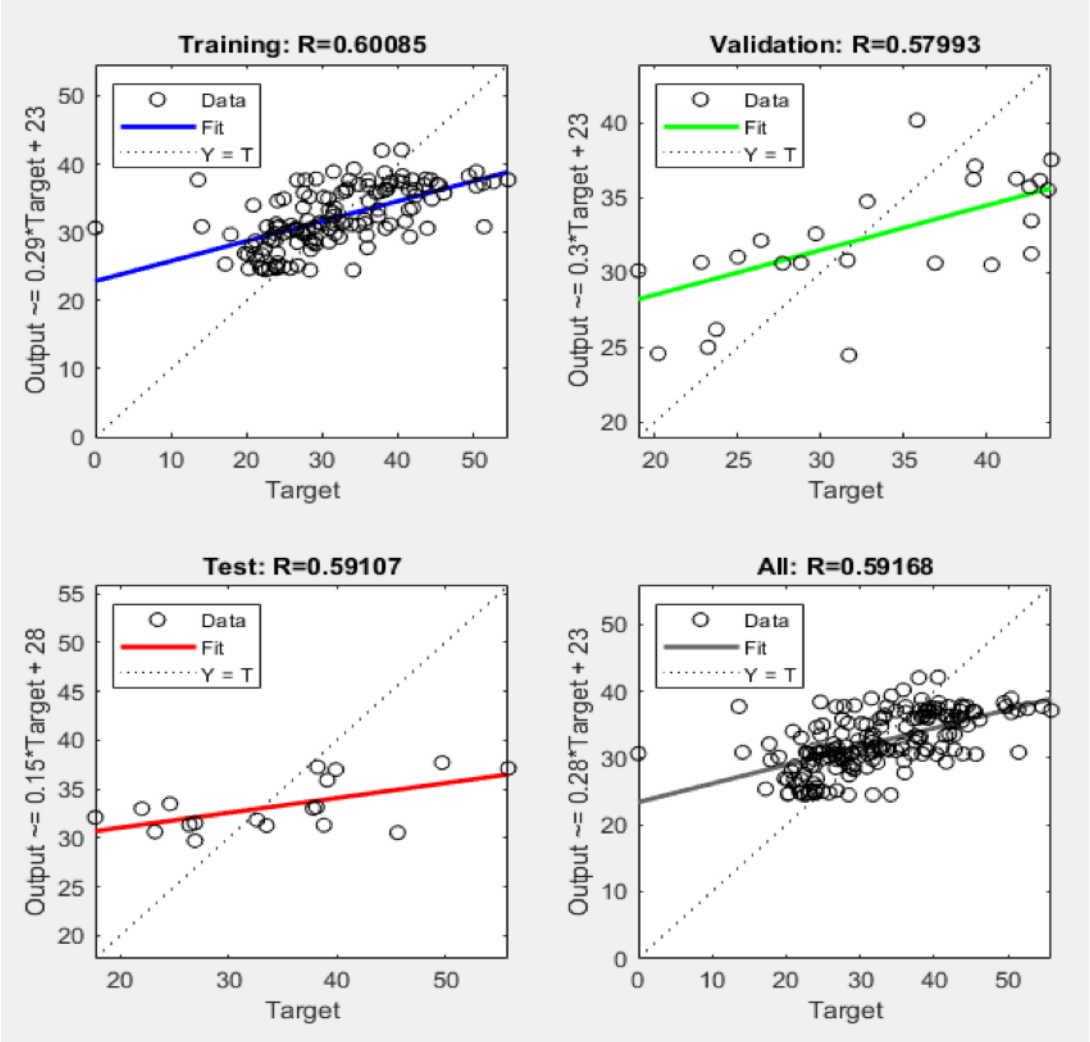

Figure D.1: ANN model for THM with n=2.

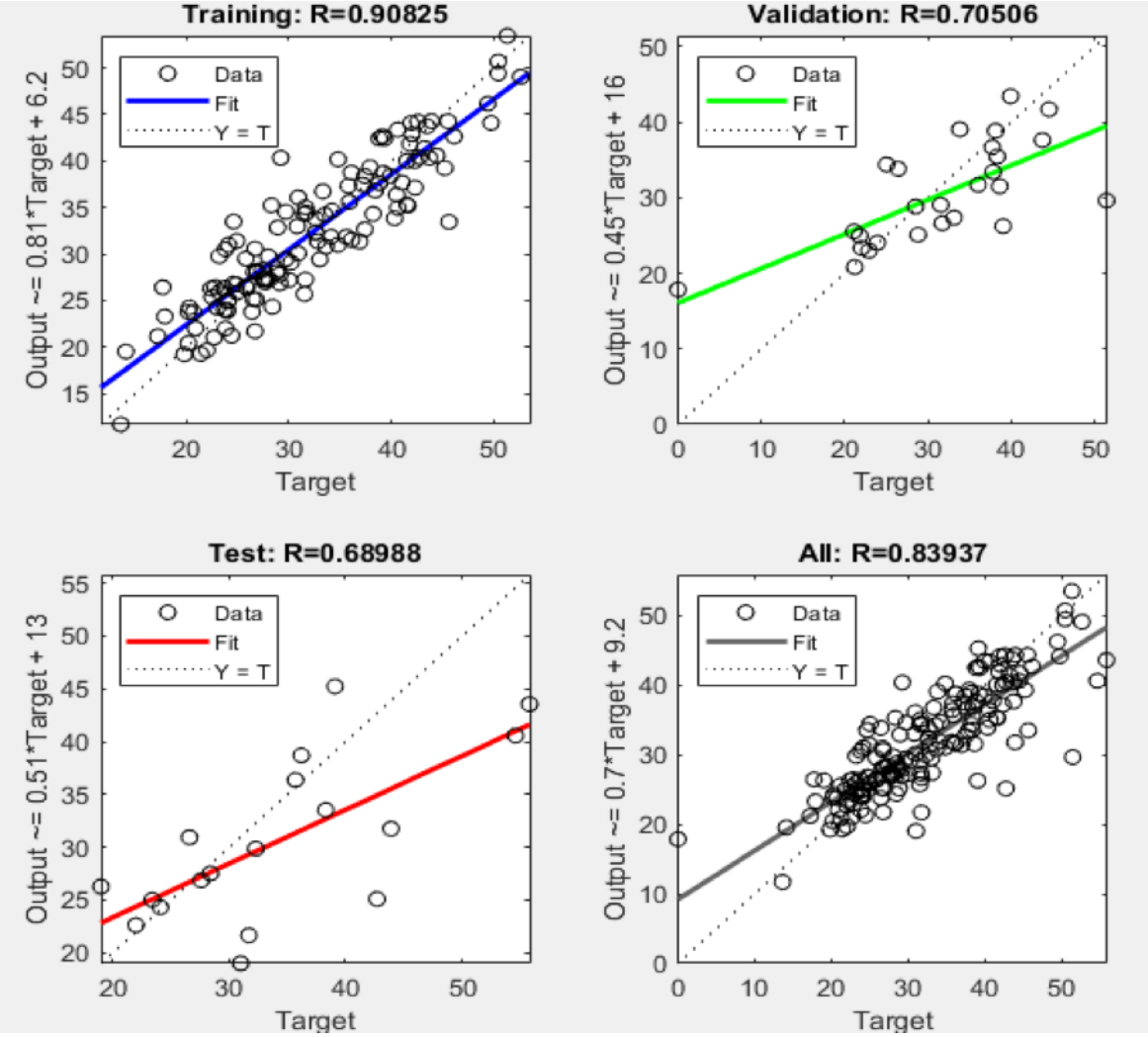

Figure D.2: ANN model for THM with n=6.

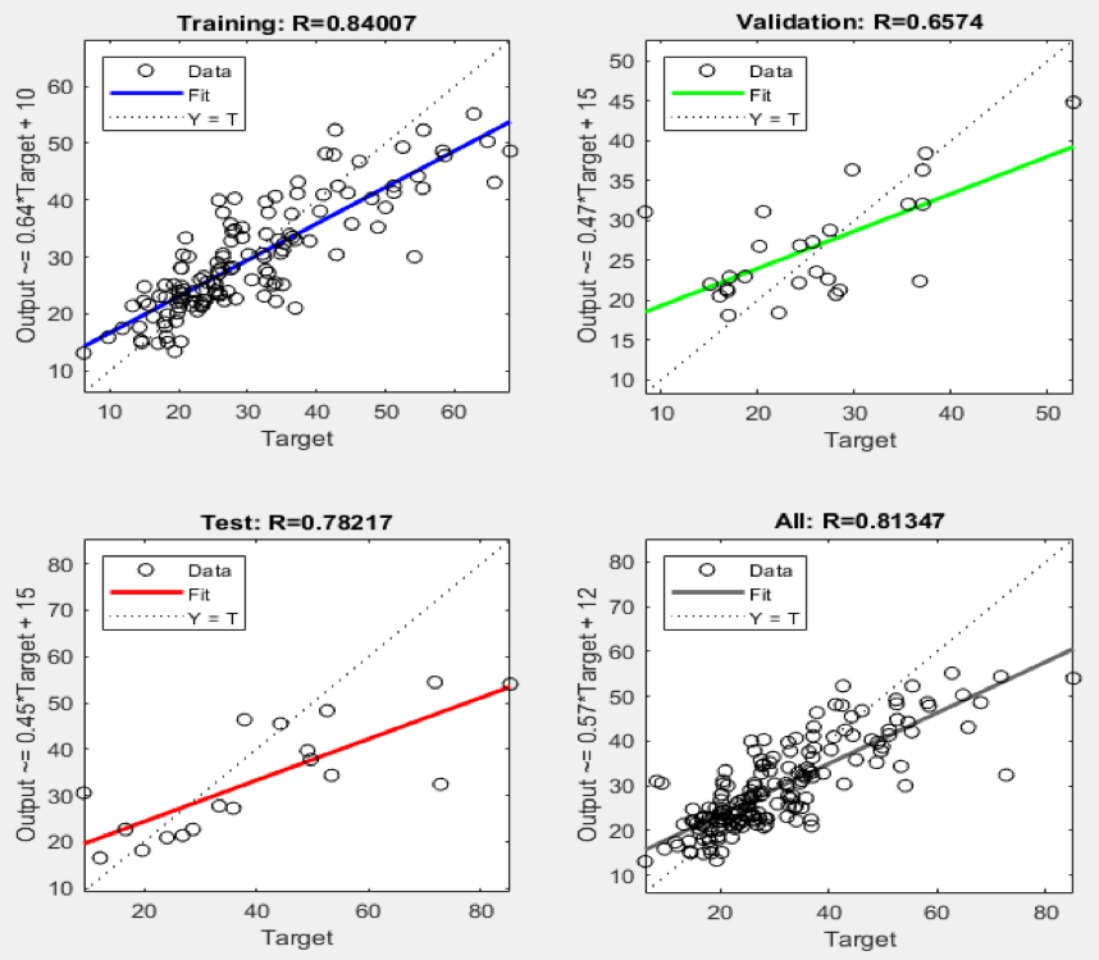

Figure D.3: ANN model for HAA with n=2.

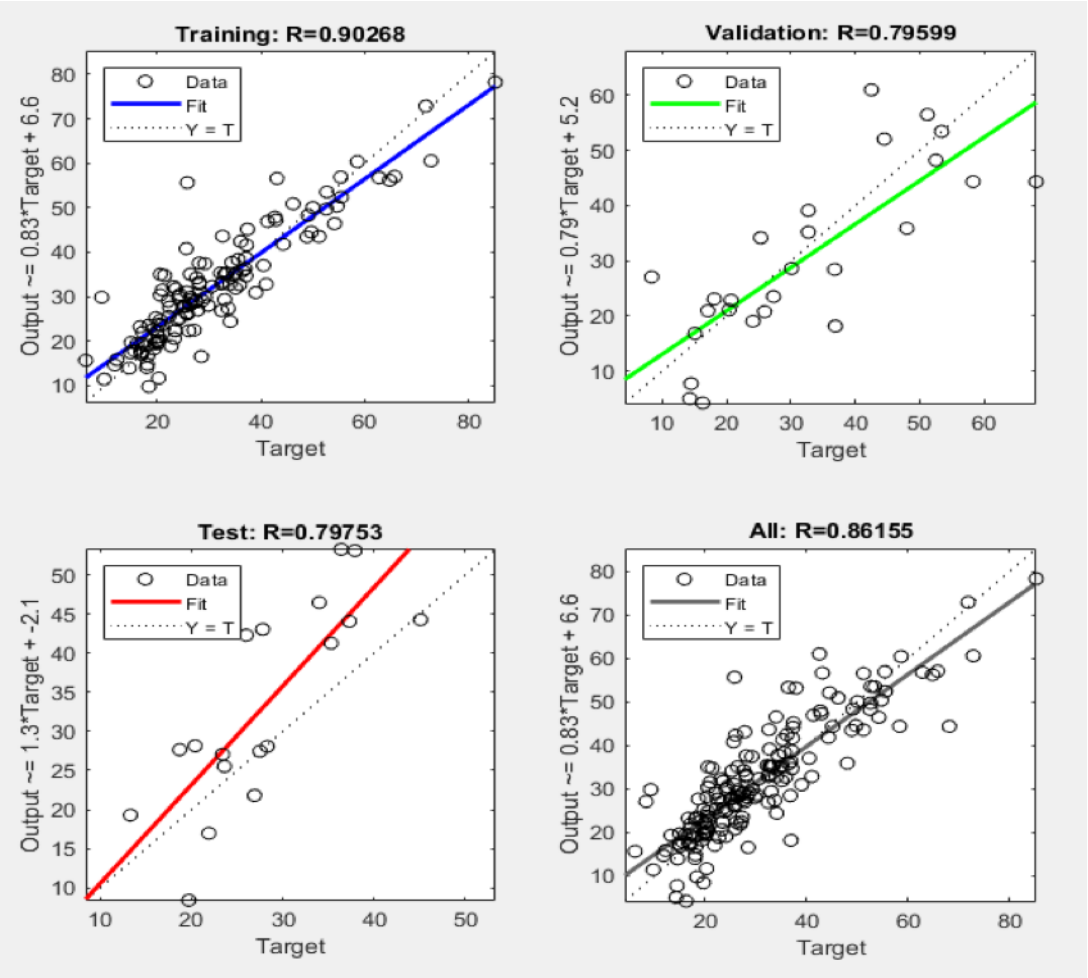

Figure D.4: ANN model for HAA with n=6.

E

CBA Calculations

E.1 Scenario 2 with SDR of 3 %

SDR	3.00 %
METB	$0.17
PV benefits	
Number of bladder cancer cases avoided (n)	12
Average patient lifetime cost bladder cancer (cc	$213 662
PV benefits	$2 563 944
Online monitoring cost	
Number of sensors	12
Number of sensors requiring cabinet installatior	6
Cost per sensor (cs)	$50 000
Cost implementation + IT integration (cii)	$8 000
Cost cabinet installation (cost per sensors) (cci)	$50 000
Cost yearly maintenance (cm)	$24 000

Calculating total PV maintenance

Year	Yearly maintenance	Discounted yearly maintenance
0	$24 000	$24 000
1	$24 000	$23 301
2	$24 000	$22 622
3	$24 000	$21 963
4	$24 000	$21 324
5	$24 000	$20 703
6	$24 000	$20 100
7	$24 000	$19 514
8	$24 000	$18 946
9	$24 000	$18 394
10	$24 000	$17 858
Total PV maintenance		$228 725

PV costs	
Purchase of sensors	$600 000
Implementation + IT integration	$96 000
Cabinet installation	$300 000
Total PV maintenance	$228 725
Total cost project	$1 224 725
Excess burden of taxation	$208 203
PV costs	$1 432 928

NPV calculation	
PV benefits	$2 563 944
PV costs	$1 432 928
Net present value (NPV)	$1 131 016

E.2 Scenario 2 with SDR of 7 %

SDR	7.00 %
METB	$0.17

PV benefits	
Number of bladder cancer cases avoided (n)	12
Average patient lifetime cost bladder cancer (cc)	$175 732
PV benefits	$2 108 783

Online monitoring cost	
Number of sensors	12
Number of sensors requiring cabinet installation	6
Cost per sensor (cs)	$50 000
Cost implementation + IT integration (cii)	$8 000
Cost cabinet installation (cost per sensors) (cci)	$50 000
Cost yearly maintenance (cm)	$24 000

Calculating total PV maintenance

Year	Yearly maintenance	Discounted yearly maintenance
0	$24 000	$24 000
1	$24 000	$22 430
2	$24 000	$20 963
3	$24 000	$19 591
4	$24 000	$18 309
5	$24 000	$17 112
6	$24 000	$15 992
7	$24 000	$14 946
8	$24 000	$13 968
9	$24 000	$13 054
10	$24 000	$12 200
Total PV maintenance		$192 566

PV costs	
Purchase of sensors	$600 000
Implementation + IT integration	$96 000
Cabinet installation	$300 000
Total PV maintenance	$192 566
Total cost project	$1 188 566
Excess burden of taxation	$202 056
PV costs	$1 390 622

NPV calculation	
PV benefits	$2 108 783
PV costs	$1 390 622
Net present value (NPV)	$718 161

E.3 Sensitivity Analysis - Distribution Histograms for Variables

The number of iterations for the variable histograms are 100,000.

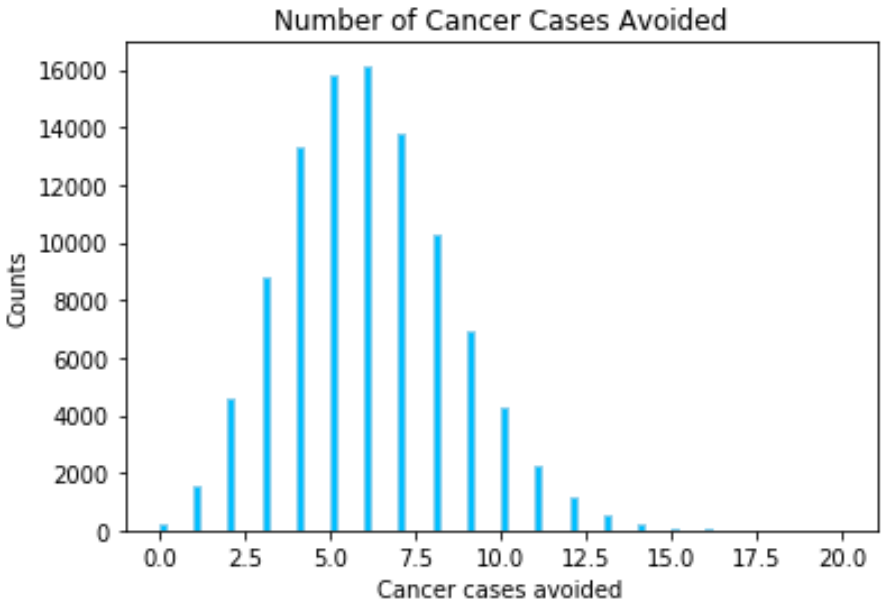

Figure E.1: Poisson distribution for number of new annual cancer cases avoided with a mean of n=6.

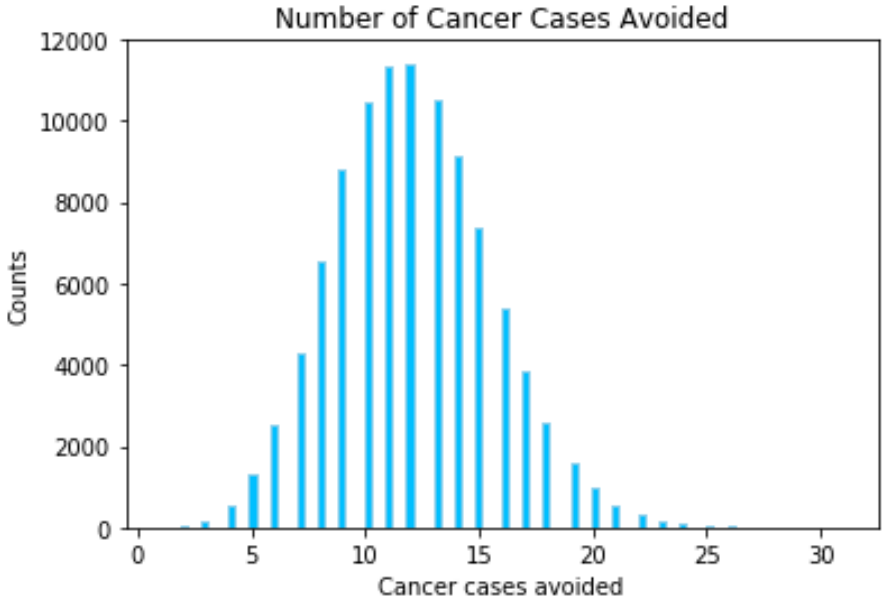

Figure E.2: Poisson distribution for number of new annual cancer cases avoided with a mean of n=12.

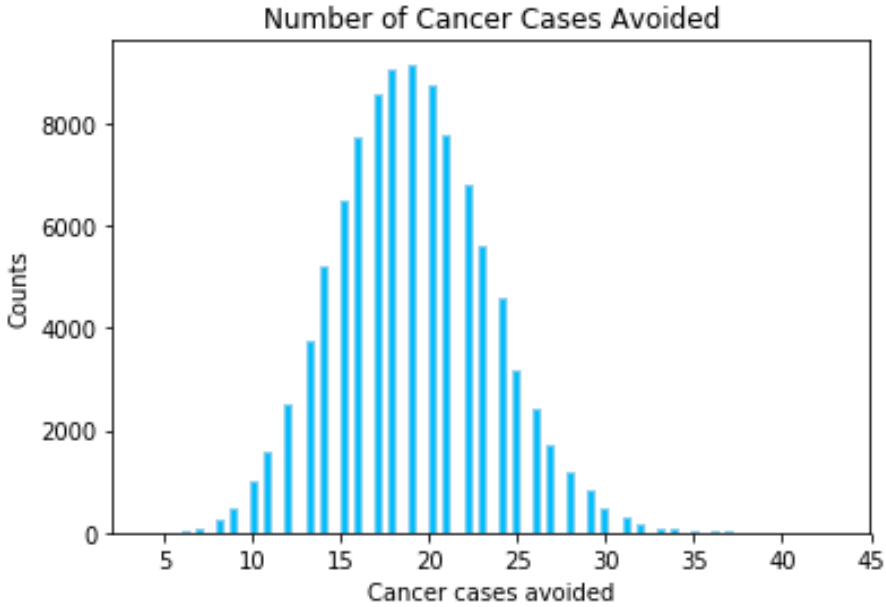

Figure E.3: Poisson distribution for number of new annual cancer cases avoided with a mean of n=19.

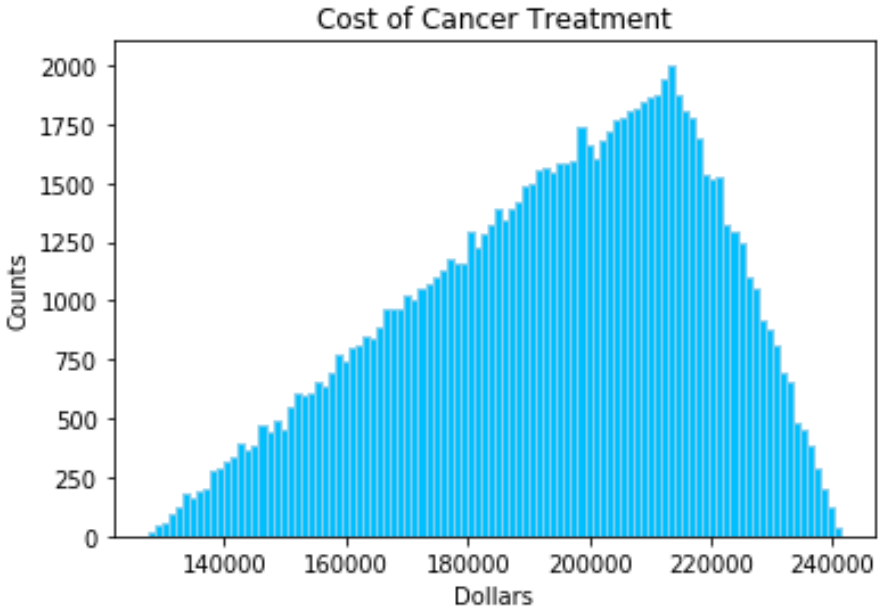

Figure E.4: Triangular distribution for cost of cancer treatment with a SDR of 3 %. The minimum, maximum and average costs for the distribution is from Table 4.6.

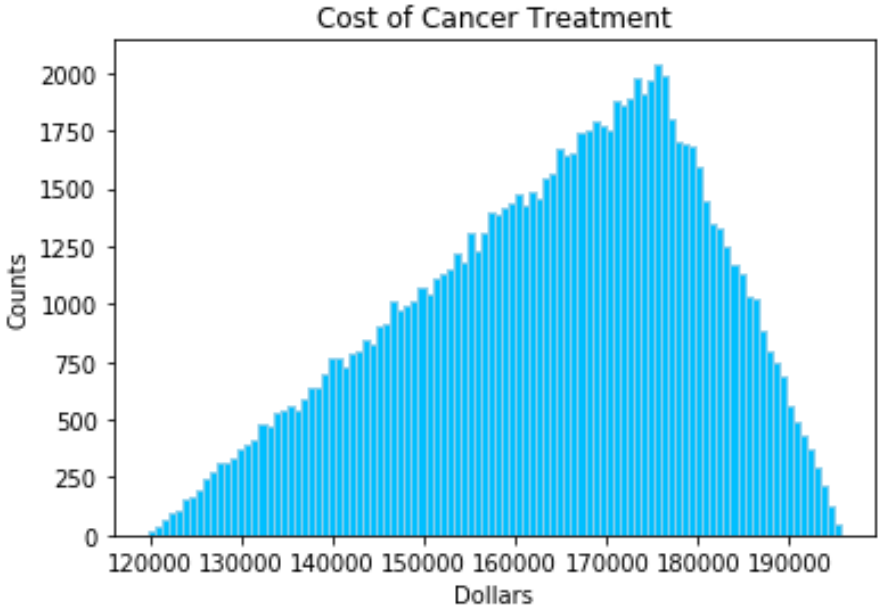

Figure E.5: Triangular distribution for cost of cancer treatment with a SDR of 7 %. The minimum, maximum and average costs for the distribution is from Table 4.6.

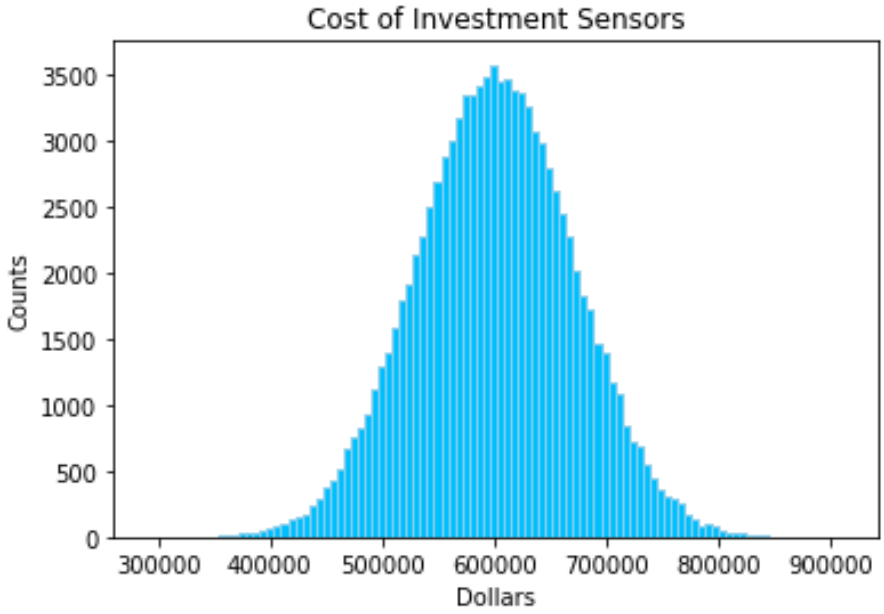

Figure E.6: Normal distribution for cost of sensor investment with a mean of $ 600,000 and standard deviation of $ 70,000.

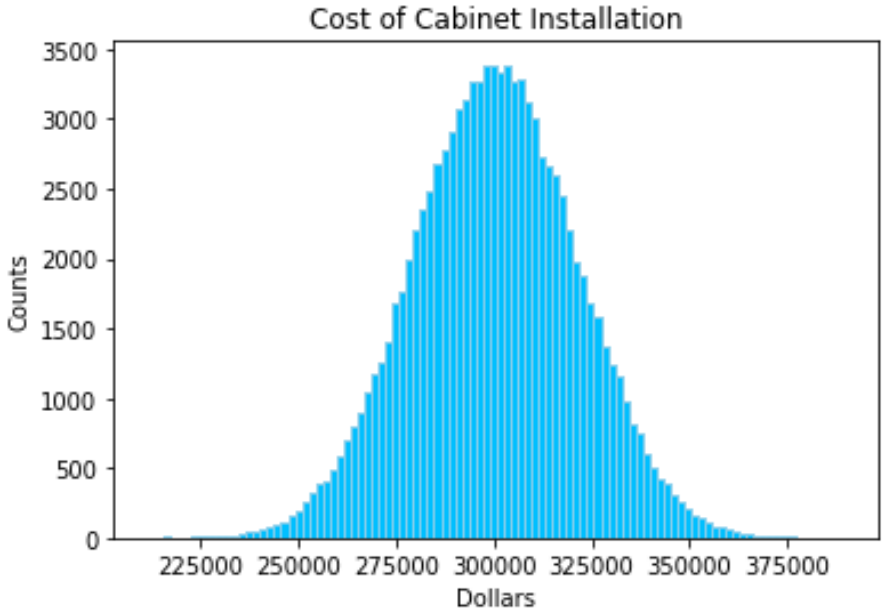

Figure E.7: Normal distribution for cost of cabinet installation with a mean of $ 360,000 and standard deviation of $ 21,000.

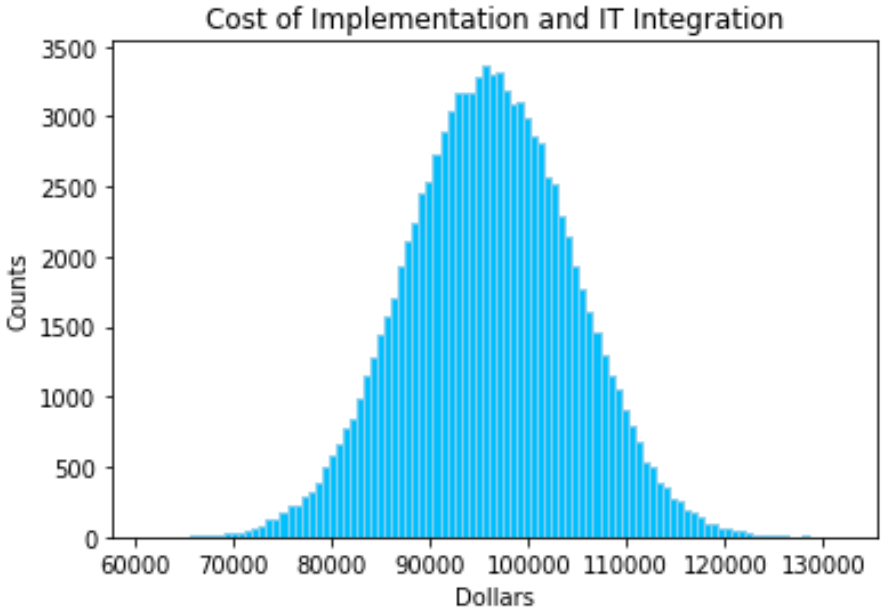

Figure E.8: Normal distribution for cost of implementation and IT integration with a mean of $ 96,000 and standard deviation of $ 8,500.

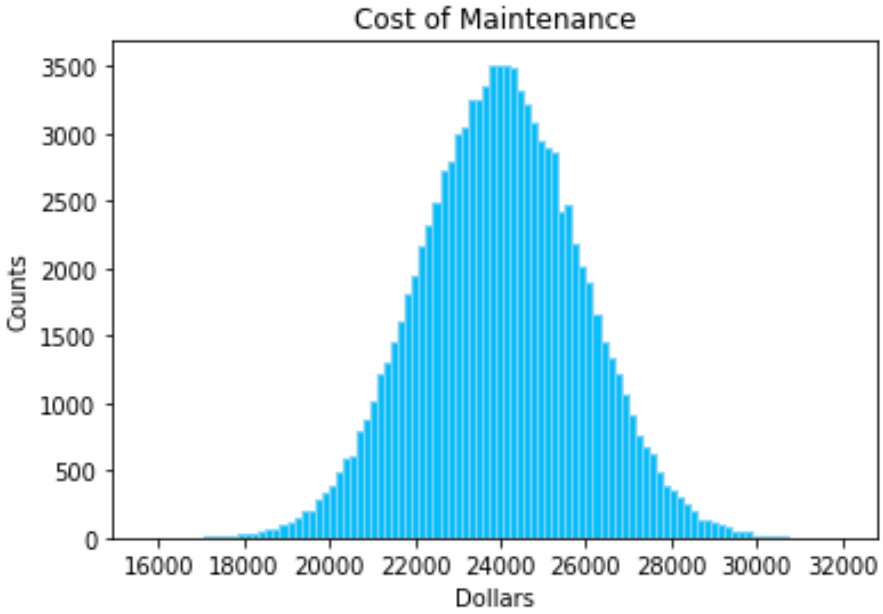

Figure E.9: Normal distribution for yearly cost of maintenance with a mean of $ 24,000 and standard deviation of $ 1,900.

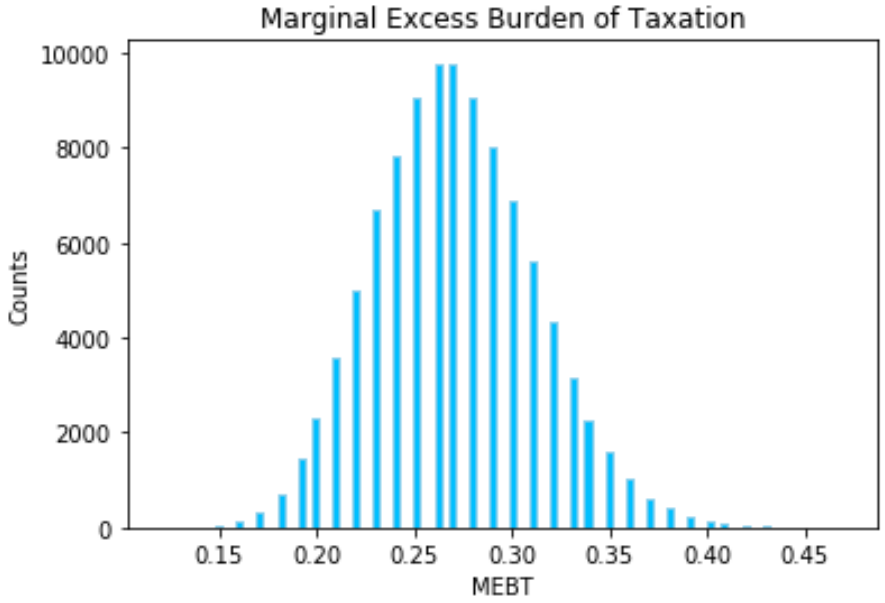

Figure E.10: Poisson distribution for marginal excess burden of taxation with a mean of $ 0.17, minimum of $ 0.10 and maximum of $ 0.40.

E.4 Sensitivity Analysis - Results

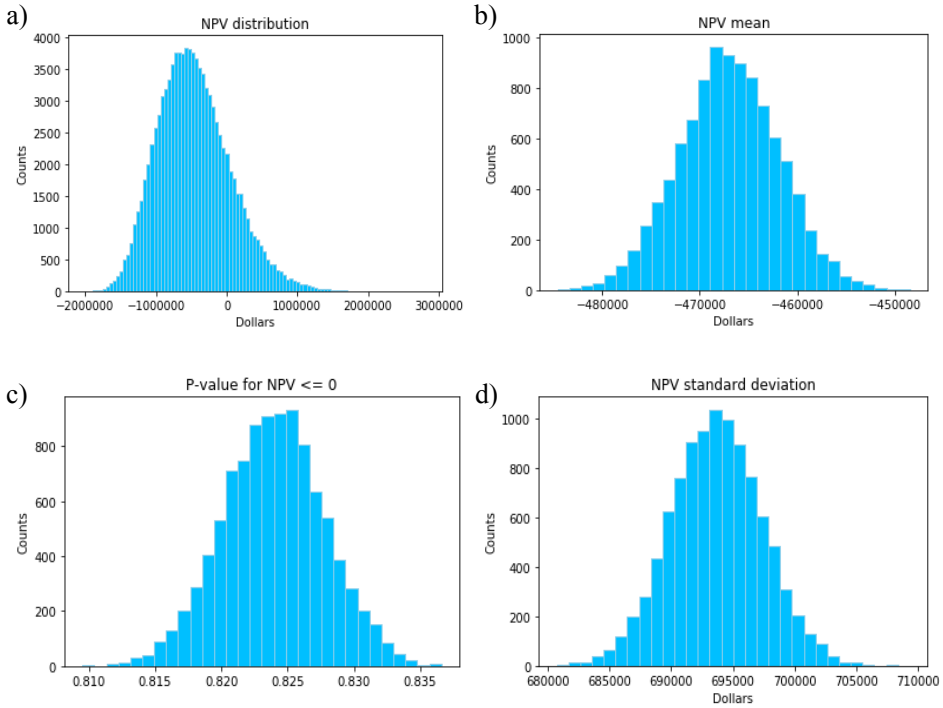

Figure E.11: Results from the sensitivity analysis for scenario 1 with a SDR of 3 %. Histogram a): the NPV distribution, b) the NPV mean, c) the p-value for NPV<=0, d) the standard deviation for NPV.

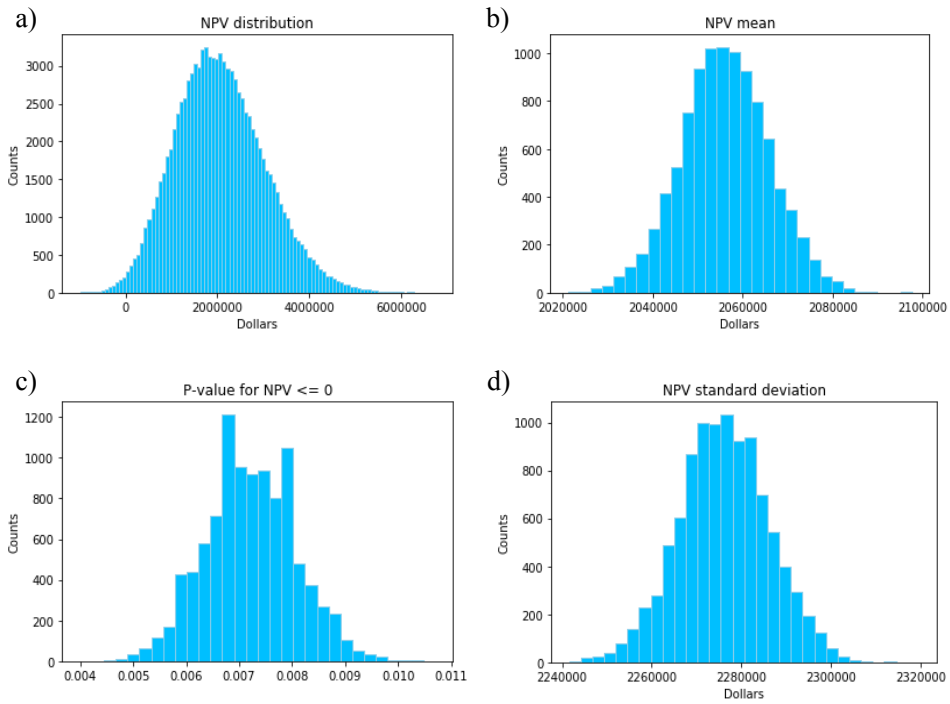

Figure E.12: Results from the sensitivity analysis for scenario 3 with a SDR of 3 %. Histogram a): the NPV distribution, b) the NPV mean, c) the p-value for NPV<=0, d) the standard deviation for NPV.

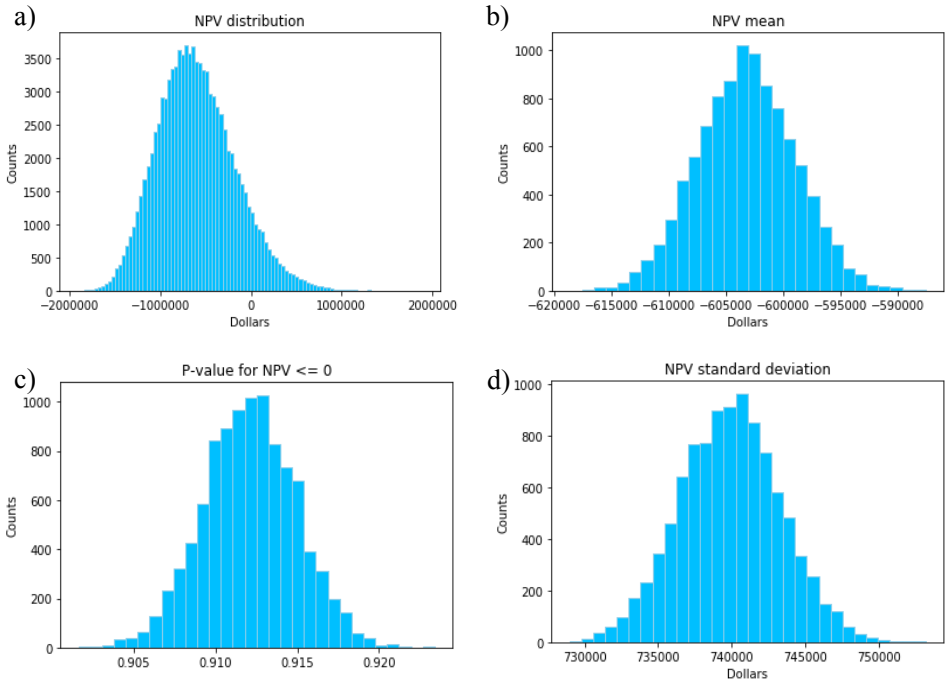

Figure E.13: Results from the sensitivity analysis for scenario 1 with a SDR of 7 %. Histogram a): the NPV distribution, b) the NPV mean, c) the p-value for NPV<=0, d) the standard deviation for NPV.

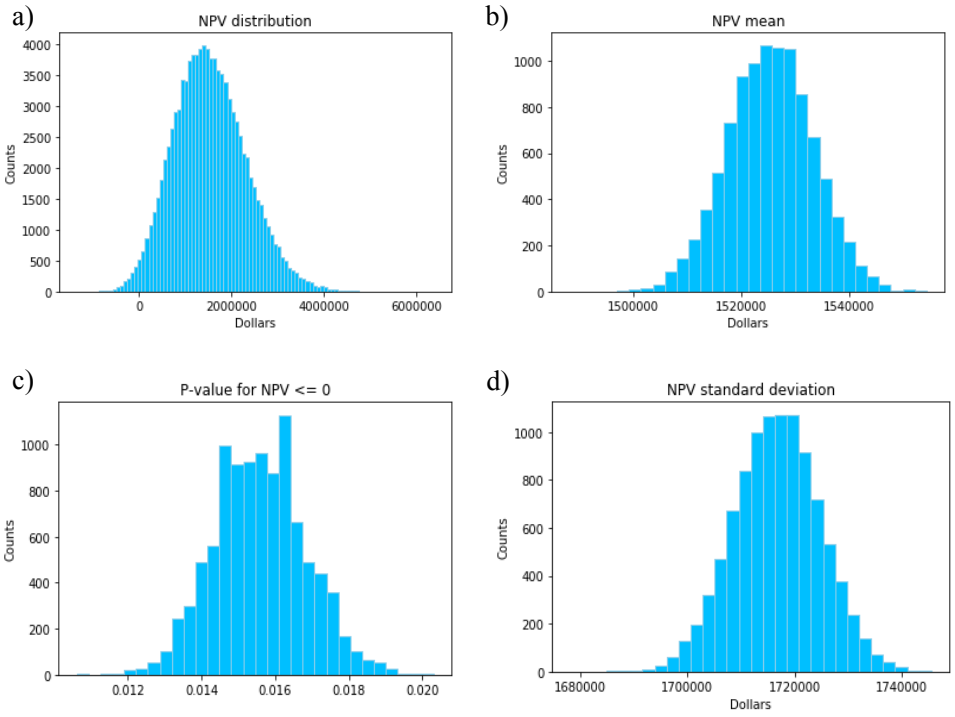

Figure E.14: Results from the sensitivity analysis for scenario 3 with a SDR of 7 %. Histogram a): the NPV distribution, b) the NPV mean, c) the p-value for NPV<=0, d) the standard deviation for NPV.

E.5 Sensitivity Analysis - Break Even Number of New Annual Bladder Cancer Cases Avoided

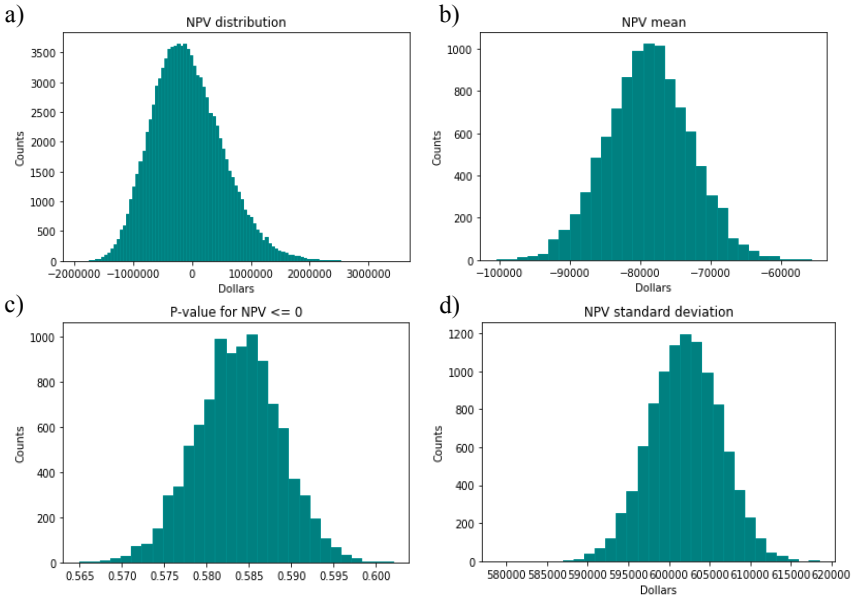

Figure E.15: Break even number (n=8) of annual new bladder cancer cases avoided for a SDR of 3 %. Histogram a): the NPV distribution, b) the NPV mean, c) the p-value for NPV<=0, d) the standard deviation for NPV.

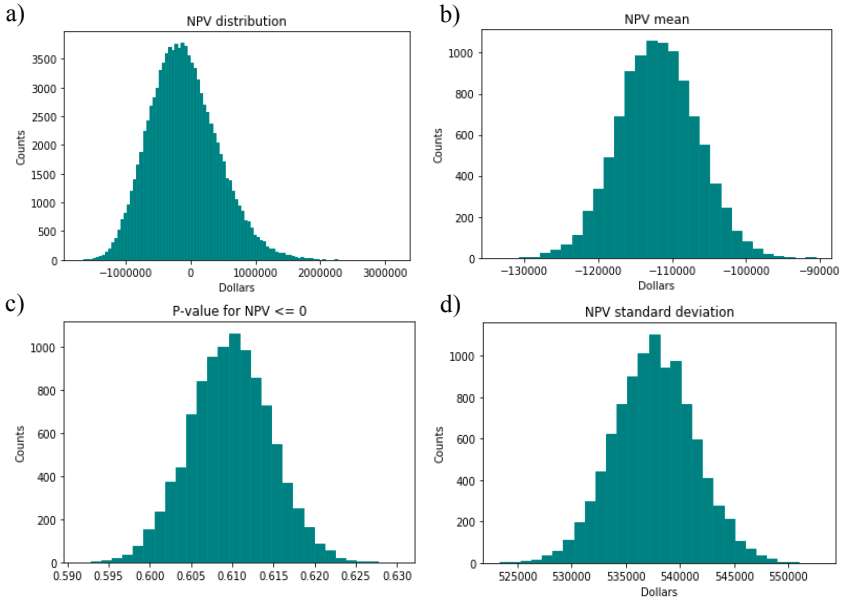

Figure E.16: Break even number (n=9) of annual new bladder cancer cases avoided for a SDR of 7 %. Histogram a): the NPV distribution, b) the NPV mean, c) the p-value for NPV<=0, d) the standard deviation for NPV.

Norges miljø- og biovitenskapelige universitet
Noregs miljø- og biovitskapelege universitet
Norwegian University of Life Sciences

Postboks 5003
NO-1432 Ås
Norway